



UNIL | Université de Lausanne

Unicentre

CH-1015 Lausanne

<http://serval.unil.ch>

Year : 2018

Effect of 16P11.2 copy number variants on cognitive traits and brain structures

Martin-Brevet Sandra

Martin-Brevet Sandra, 2018, Effect of 16P11.2 copy number variants on cognitive traits and brain structures

Originally published at : Thesis, University of Lausanne

Posted at the University of Lausanne Open Archive <http://serval.unil.ch>

Document URN : urn:nbn:ch:serval-BIB_A2EE6B0F30FE1

Droits d'auteur

L'Université de Lausanne attire expressément l'attention des utilisateurs sur le fait que tous les documents publiés dans l'Archive SERVAL sont protégés par le droit d'auteur, conformément à la loi fédérale sur le droit d'auteur et les droits voisins (LDA). A ce titre, il est indispensable d'obtenir le consentement préalable de l'auteur et/ou de l'éditeur avant toute utilisation d'une oeuvre ou d'une partie d'une oeuvre ne relevant pas d'une utilisation à des fins personnelles au sens de la LDA (art. 19, al. 1 lettre a). A défaut, tout contrevenant s'expose aux sanctions prévues par cette loi. Nous déclinons toute responsabilité en la matière.

Copyright

The University of Lausanne expressly draws the attention of users to the fact that all documents published in the SERVAL Archive are protected by copyright in accordance with federal law on copyright and similar rights (LDA). Accordingly it is indispensable to obtain prior consent from the author and/or publisher before any use of a work or part of a work for purposes other than personal use within the meaning of LDA (art. 19, para. 1 letter a). Failure to do so will expose offenders to the sanctions laid down by this law. We accept no liability in this respect.



UNIL | Université de Lausanne

Faculté de biologie
et de médecine

Départements de Génétique Médicale et de Neurosciences Cliniques

**EFFECT OF 16P11.2 COPY NUMBER VARIANTS ON COGNITIVE
TRAITS AND BRAIN STRUCTURES**

Thèse de doctorat en Neurosciences

présentée à la

Faculté de Biologie et de Médecine
de l'Université de Lausanne

par

SANDRA MARTIN-BREVET

Neuroscientifique diplômée de l'Université Paris Descartes, France

Jury

Prof. Sven Bergmann, Président
Prof. Bogdan Draganski, Directeur
Prof. Sébastien Jacquemont, Co-Directeur
Prof. Ole Andreassen, Expert
Prof. Martin Debbané, Expert

Thèse n° 227

Lausanne 2018

*Programme doctoral interuniversitaire en Neurosciences
des Universités de Lausanne et Genève*





UNIL | Université de Lausanne



**UNIVERSITÉ
DE GENÈVE**

*Programme doctoral interuniversitaire en Neurosciences
des Universités de Lausanne et Genève*

Imprimatur

Vu le rapport présenté par le jury d'examen, composé de

<i>Président·e</i>	Monsieur Prof. Sven Bergmann
<i>Directeur·trice de thèse</i>	Monsieur Prof. Bogdan Draganski
<i>Co-directeur·trice de thèse</i>	Monsieur Prof. Sébastien Jacquemont
<i>Expert·e·s</i>	Monsieur Prof. Ole Andreassen
	Monsieur Prof. Martin Debbané

le Conseil de Faculté autorise l'impression de la thèse de
Madame Sandra Martin-Brevet

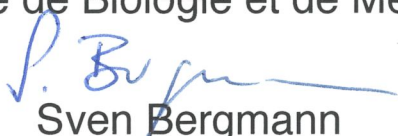
Master en Sciences Cognitives, Ecole Normale Supérieure, Paris

intitulée

**Effect of 16P11.2 copy number variants on cognitive
traits and brain structures**

Lausanne, le 8 juin 2018

pour Le Doyen
de la Faculté de Biologie et de Médecine


Prof. **Sven Bergmann**

ACKNOWLEDGEMENTS

Only a touch of French for the « emotional » part.

Par ces quelques lignes, je remercie toutes les personnes qui ont contribué, d'une façon ou d'une autre, à mon travail.

Tout d'abord, merci au Prof. Sébastien Jacquemont, sans qui mon projet ne se serait réalisé et qui, après un simple rendez-vous Skype (avec quelques problèmes techniques de voix ?!), m'a engagée au sein de son équipe et embarquée avec lui dans ses aventures.

Merci au Prof. Bogdan Draganski d'avoir pris la relève après l'expatriation de Sébastien et de m'avoir ouvert les portes de son laboratoire.

Merci au président du jury, Prof. Sven Bergmann, et aux experts, Prof. Ole Andreassen et Prof. Martin Debbané, d'avoir accepté d'évaluer ma thèse.

Merci à tous mes collègues du service de génétique médicale, pour leurs conseils, avis, aides, expertises, en particulier Aurélie (on refait un petit tour de France ?!), Borja (une liste de questions en attente !!), Claudia (on se prend un petit café ensemble pour parler?), Loyse, Anne, Sonia, Roxane, Inês et Florence (une petite discussion nocturne au Luxembourg ?!). Quelques partages de bureaux peuvent mener à de belles rencontres.

Un merci tout particulier à Jacqui Beckmann pour m'avoir ouvert de nouveaux horizons vers l'étude du microbiome. Merci à Alexandre Reymond, Aurélien Macé et Sébastien Lebon pour le travail partagé.

Merci à tous les étudiants, mes collègues et amis du LREN que j'ai pu côtoyer, avec toutes leurs motivations et leur énergie pour mener à bien leurs projets de recherche. Il y aurait beaucoup de monde à citer... mais je sais que vous vous reconnaitrez !

Merci à Louis Collins de m'avoir reçu au MNI, merci à Alonso pour notre collaboration fructueuse, et plus généralement merci à l'équipe du NIST pour m'avoir accueilli parmi les leurs, en particulier dans notre petit bureau chaleureux face au stade mémorial Percival Molson (full house today ?!). Merci à l'équipe Montréalaise de Sébastien, avec qui j'ai pu partager des moments fort sympathiques (n'oublions pas la « fin du monde », une bien bonne Unibroue un soir de printemps sur une terrasse du CHU Sainte Justine), avec Elise, Abdou, Marie-Pierre, Guillaume, Clara, Catherine, Charles-Olivier, Khadije, Martineau, Antoine, Claudine, Maude, et d'autres PI telle que Sarah.

Merci à toutes les personnes avec qui j'ai pu collaborer à travers le monde, Dr Jared Nielsen et Prof. Randy Buckner à Boston, les collaborateurs de la Simons VIP, l'équipe norvégienne d'Enigma-CNV et en particulier Ida, Dr Evan Elliott en Israël, l'équipe métagénomique à l'INRA-Paris et leurs collaborateurs. Merci à ma mentor, Prof. Francesca Amati, pour son soutien. Merci aux coordinatrices de l'école doctorale. Merci au fonds Jean Falk-Vairant pour avoir participé au financement de séjour à Montréal. Merci à toutes les équipes de génétique médicale à travers notre réseau européen, qui participe au consortium 16p11.2 et en particulier les corps médicaux qui nous ont accueilli dans leurs locaux à travers la France.

Merci à tous les patients et leurs familles qui participent aux projets de recherches et sans qui ce travail n'aurait de sens.

Je n'aurais pas pu accomplir tout cela sans expériences clés dans mon parcours, en particulier mon année au Cogmaster, en passant par l'Ecole Normale Supérieure de la rue d'Ulm, et mon travail avec Prof. Agnès Roby-Brami et ses collègues, envers qui je serai toujours reconnaissante.

Les derniers mais non les moindres... Construire une maison ne peut se faire sans fondation ; et vous représentez mes fondations... Je remercie avec sincérité notre petit groupe de femmes expatriées à Lausanne, et tout particulièrement Moufida, Jérôme et leurs enfants ; mes anciens collègues Pascal et Daphné ; mes amis « par alliance », Line, Vivi et Vir avec leurs familles ; mes amis « parisiens » qui me suivent depuis le début de nos études et auxquels je ne cesse de penser malgré la distance, Séverine, Airelle, Marc, Sylvain, Ida, Shirley, Idan et Béa, Valérie, Marion et leurs familles ; Hélène, Lyne et leurs familles. Merci à ma famille qui peut être septique de me voir encore aux études à mon âge mais ne doute pas de mon succès ; ma belle-famille et mes parents qui sont toujours fiers de moi. Et une phrase spéciale pour mes amours, Johan mon mari qui, malgré les hauts et les bas que peut comporter un PhD, ne m'a jamais demandé d'arrêter, mais au contraire m'a toujours soutenu et encouragé à continuer, jusqu'à me laisser partir 5 mois avec notre petit garçon à Montréal pour que je puisse avancer la thèse; et Noa mon fils, sans aucun doute ma meilleure « production » de ces années de doctorat, qui participait « activement » au lab meeting durant mon congé maternité et m'a toujours soutenu avec ses sourires et sa bonne humeur.

A Ginette, ma maman, qui je suis sûre, aurait été très fière de voir aboutir ce travail et de me soutenir durant la défense de thèse publique.

ABSTRACT

The $\approx 600\text{kb}$ 16p11.2 CNVs (breakpoints 4–5, 29.6–30.2 Mb-Hg19) are among the most frequent genetic risk factors for neurodevelopmental and psychiatric conditions: A 10-fold enrichment of deletions and duplications is observed in autism cohorts and a 10-fold enrichment of duplications in schizophrenia cohorts. Previous studies demonstrated “mirror” effects of both CNVs on body mass index and head circumference (deletion > control > duplication). However, the large global effect of brain size and the sample size of the two previous neuroimaging studies limited the interpretation of the analyses on regional brain structures, any estimate of the effect size, and the generalizability of the results across different ascertainment of the patients.

In the first part of my Ph.D., I analyze structural magnetic resonance imaging (MRI) on 78 deletion carriers, 71 duplication carriers, and 212 controls. I show that both CNVs affect in a “mirror” way the volume and the cortical surface of the insula (Cohen’s $d > 1$), whilst other brain regions are preferentially altered in either the deletion carriers (calcarine cortex and superior, middle, transverse temporal gyri, Cohen’s $d > 1$) or the duplication carriers (caudate and hippocampus, Cohen’s d of 0.5 to 1). Results are generalizable across scanning sites, computational methods, age, sex, ascertainment for psychiatric disorders. They partially overlap with results of meta-analyses performed across psychiatric disorders.

In the second part, I characterize the developmental trajectory of global brain metrics and regional brain structures in the 16p11.2 CNV carriers. I adapt a previously published longitudinal pipeline and normalizing method, derived from 339 typically developing individuals aged from 4.5 to 20 years old. From this population of reference, I Z-score our cross-sectional 16p11.2 dataset and show that all the brain alterations in the 16p11.2 carriers are already present at 4.5 years old and follow parallel trajectories to the controls.

In summary, my results suggest that brain alterations, present in childhood and stable across adolescence and adulthood, are related to the risk conferred by the 16p11.2 CNVs, regardless of the carriers’ symptoms. Additional factors are therefore likely required for the development of psychiatric disorders. I highlight the relevance of studying genetic risk factors and mechanisms as a complement to groups defined by behavioral criteria. Further studies comparing multiple CNVs and monogenic conditions, from the earliest age, are required to understand the onset of neuroanatomical alterations and their overlap between different genetic risk factors for neurodevelopmental disorders.

RÉSUMÉ

Les variations en nombre de copies (CNV), au locus 16p11.2 et d'une taille d' ≈ 600 kb (points de cassure 4–5, 29.6-30.2 Mb-Hg19) représentent un des facteurs de risque génétique les plus fréquents parmi les troubles psychiatriques : 10% d'enrichissement en délétion et duplication pour les troubles du spectre autistique, 10% d'enrichissement en duplication pour la schizophrénie. Les effets « miroirs » des deux CNVs sur l'indice de masse corporelle et le périmètre crânien ont déjà été démontrés (délétion>contrôle>duplication). Cependant, les différences en taille de cerveau et les échantillons des deux précédentes études de neuro-imagerie ont limité les analyses des régions cérébrales, l'estimation de la taille des effets, et la généralisation des résultats selon les modes de recrutement des patients.

Dans cette thèse, j'analyse les images par résonance magnétique (IRM) de 78 porteurs de la délétion, 71 porteurs de la duplication et 212 participants contrôles. Je montre que les deux CNVs sont associées à des différences « en miroir » du volume et de la surface corticale de l'insula (Cohen's $d > 1$), tandis que le cortex calcarin, les gyri temporaux supérieur, moyen et transverse sont préférentiellement altérés par la délétion (Cohen's $d > 1$), les noyaux caudés et l'hippocampe sont préférentiellement altérés par la duplication ($0.5 < \text{Cohen's } d < 1$). Les résultats sont généralisables à travers les différents sites d'IRM, les méthodes d'analyse computationnelle, les âges, les sexes et les divers diagnostics psychiatriques des patients. Les résultats chevauchent partiellement ceux d'une méta-analyse sur plusieurs diagnostics psychiatriques. Dans un second temps, je caractérise la trajectoire développementale de ces différences cérébrales. J'adapte un pipeline longitudinal et une méthode de normalisation déjà publiés, construits à partir de 339 participants contrôles de 4.5 à 20 ans. Je calcule des Z-scores pour nos données transversales et montre que les différences cérébrales liées aux CNVs sont déjà présentes à 4.5 ans, avec les mêmes tailles d'effet et une trajectoire parallèle aux contrôles. En résumé, mes résultats suggèrent que les différences cérébrales, présentes dans la jeune enfance et stables à l'adolescence et l'âge adulte, sont liées au risque conféré par les CNVs en 16p11.2, quelque soient les symptômes. Des facteurs additionnels sont probablement nécessaires pour le développement de maladies psychiatriques. Je montre la pertinence d'étudier les facteurs de risque génétiques en complément des groupes de patients définis sur des critères comportementaux. Des études comparant diverses conditions génétiques, dès la naissance, sont nécessaires pour comprendre le début et le chevauchement des différences neuro-anatomiques observées pour différents facteurs de risque génétiques.

LIST OF ABBREVIATIONS

CNV	copy number variant
ASD	autism spectrum disorder
SCZ	schizophrenia
NDD	neurodevelopmental disorder
ID	intellectual disability
DSM-5	diagnostic and statistical manual of mental disorder, 5 th version
Simons VIP	Simons variation in individuals project
BMI	body mass index
HC	head circumference
FSIQ	full scale intelligence quotient
VIQ	verbal intelligence quotient
NVIQ	non-verbal intelligence quotient
MRI	magnetic resonance imaging
TIV	total intracranial volume
GM	grey matter
WM	white matter

TABLE OF CONTENTS

1. INTRODUCTION	12
1.1 Copy Number Variants and psychiatric disorders	12
1.1.1 Definition of copy number variants	12
1.1.2 Psychiatric diagnoses	13
1.1.3 The contribution of copy number variants to psychiatric disorders	13
1.2 The 16p11.2 Copy Number Variants	16
1.2.1 Psychiatric and medical features	16
1.2.2 Anthropometric measurements	18
1.2.3 Neuropsychological profile and developmental trajectory	19
1.2.4 Variance in phenotypes and additional factors	20
1.3 Contribution of neuroimaging to psychiatric and genetic disorders	21
1.3.1 Neuroimaging techniques	21
1.3.2 Neuroanatomical alterations in psychiatry disorders	23
1.3.3 Previous MRI studies on carriers of a 16p11.2 copy number variant	28
1.4 Goal of the thesis	29
2. RESULTS	31
2.1 Quantifying the effects of 16p11.2 copy number variants on brain structure: A multi-site ‘genetic-first’ study	31
2.2 Developmental trajectories of neuroanatomical alterations associated with the 16p11.2 Copy Number Variations	33
2.2.1 Introduction	33
2.2.1.1 <i>16p11.2 Copy Number Variants (CNVs)</i>	33
2.2.1.2 <i>Z-scoring and developmental trajectory</i>	33
2.2.1.3 <i>Goal</i>	34
2.2.2 Methods	35
2.2.2.1 <i>Participants</i>	35
2.2.2.2 <i>MRI protocol</i>	36
2.2.2.3 <i>Image processing</i>	37
2.2.2.4 <i>Data analyses</i>	37
2.2.3 Results	39
2.2.3.1 <i>Differences between 16p11.2 controls and NIHPD controls</i>	39
2.2.3.2 <i>Developmental trajectory of the global volumes of each genetic group</i>	40
2.2.3.3 <i>Developmental trajectory for regional alterations</i>	43
2.2.4 Discussion	49
2.2.4.1 <i>Effect size and brain alterations on DEL and DUP</i>	49
2.2.4.2 <i>Continuous model of normative developmental trajectory</i>	50
2.2.4.3 <i>Comparison with developmental trajectories in neurodevelopmental disorders and genetic risk factors</i>	51

2.2.5 Conclusion	51
3. DISCUSSION OF THE THESIS	53
3.1 Global and regional differences on the 16p11.2 reciprocal CNVs	53
3.1.1 Regional volumetric and surface differences beyond the effect on the global brain metrics	53
3.1.2 Relationship between the 16p11.2 pattern of brain structures differences and the behavior	55
3.1.3 Additional factors to the rare CNVs in psychiatric disorders	57
3.1.4 The broad age range of the dataset	58
3.2 Normative data and developmental trajectory of brain structures across the development of the 16p11.2 carriers	58
3.2.1 Effect size in neuro-imaging genetic	59
3.2.2 Normalization	60
3.2.3 Developmental trajectories in neuro-imaging of psychiatric disorders	60
3.3 The study of intermediate phenotypes in 16p11.2 cohorts	62
3.3.1 Tissue properties underlying the 16p11.2 associated-volumetric alterations	62
3.3.2 White matter microstructure and brain connectivity	63
3.3.3 Study of microbiota in the 16p11.2 CNV carriers	64
3.4 Neuroanatomy and CNVs in psychiatric disorders	65
3.4.1. Neuroanatomy across CNVs associated with neurodevelopmental disorders	65
3.4.2. Neuroimaging analysis of psychiatric diagnoses	67
3.4.3 Relationship between genes within CNVs and brain alterations	67
3.4.4 Study of CNVs associated with psychiatric conditions	68
4. GENERAL CONCLUSIONS	70
5. REFERENCES	71
6. ARTICLE	84
Quantifying the effects of 16p11.2 copy number variants on brain structure: A multi-site ‘genetic-first’ study	

1. INTRODUCTION

1.1 Copy Number Variants and psychiatric disorders

1.1.1 Definition of copy number variants

Copy number variants (CNVs) are variations of chromosomal structure, widespread in the human genome (>1000 CNVs), including deletion, duplication, inversion and translocation (Malhotra & Sebat 2012). Thanks to the recent key evolution of technologies (as the chromosomal microarray analysis, and most recently the whole-genome sequencing) and the clinical application of these genomic arrays, we begin to understand their essential contribution to inter-individual genetic and phenotypic variations. Many CNVs are probably benign, underlying common normal traits, and some of them are associated with common Mendelian conditions, such as colorblindness, Charcot–Marie–tooth disease type 1A, etc. Some variations can influence susceptibility to complex diseases such as Alzheimer’s disease, Crohn’s disease, and to infection such as the Human Immunodeficiency Virus (Lupski 2007). Therefore, they are thought to play a major role in the etiology of common disorders and complex multifactorial traits, and they could explain the variable penetrance of inherited diseases (Beckmann et al. 2007).

In this thesis, I focus on the deletion and duplication of a recurrent CNV, identified as risk factors for intellectual disabilities (ID), autism spectrum disorders (ASD) and schizophrenia (SCZ). The recurrence is based on the consistent breakpoints of the CNVs among individuals, and they occur in specific locations in the genome, at the level of segmental duplications, also called low-copy repeat-LCR sequences (large stretches of DNA with similar sequences). If these LCR are misaligned during meiosis, this leads to a crossing over between two chromosomal sites and products a recurrent CNV: this process is called nonallelic homologous recombination (Moreno-De-Luca & Cubells 2011). Recurrent reciprocal CNVs allow studying the effect of gene dosage in individuals carrying 1, 2 or 3 copies of a genomic region. The deletion (1 copy of the genomic segment) and the duplication (3 copies) can disrupt a variable number of genes. Aberrations in the number of copies, haplo-insufficiency and over-expression of the genes, represent unique paradigms to identify pathways sensitive to gene dosage in humans. They open a new way for the study of diseases mechanisms and some new approaches to potential treatments, in which the goal is not to correct abnormal or mutant proteins but to modify their abnormal dosage.

1.1.2 Psychiatric diagnoses

Psychiatric disorders are diagnosed based on clinical criteria from the 5th version of diagnostic and statistical manual of mental disorder (DSM-5, American Psychiatric Association) or from the 10th revision of the international classification of diseases (ICD-10, World Health Organisation).

According to DSM-5, neurodevelopmental disorders (NDDs) are a group of conditions with an onset early in development. They are characterized by a series of developmental deficits, producing impairments of social, academic and/or occupational functioning: they include ID (prevalence of about 1%) and ASD. Three criteria must be met to fill in the diagnostic of ID: 1- deficits in intellectual functions, 2-deficits in everyday adaptive functioning to reach personal independence and social responsibility, 3-onset during the developmental period. ASD diagnosis is based on characteristic deficits in social communication and social interaction across multiple context, as well as an excess of repetitive behaviours and restricted interests. ASD frequently co-occur with ID and language impairment. The prevalence is estimated to affect up to than 1 in 68 children (Christensen et al. 2012) and males have a >3-fold higher risk for ASD than females (Volkmar et al. 2004).

SCZ belongs to the “Schizophrenia spectrum and other psychotic disorders” conditions. SCZ involves a large range of cognitive, behavioural and emotional dysfunctions. Individuals meet at least two of these active-phase symptoms during 1 month: first delusions, hallucinations, disorganized speech, and also disorganized or catatonic behaviour, negative symptoms affecting emotional expression or volition. These symptoms affect every day functioning and the disturbance, including prodromal or residual symptoms, has to persist for at least 6 months.

1.1.3 The contribution of copy number variants to psychiatric disorders

The psychiatric disorders present an important heterogeneity and a complexity of the symptoms in clinics. Instead of considering this heterogeneity as noise, it represents a challenge: understanding them is a mandatory step to classify the diagnostic criteria in biologically relevant categories and to advance our understanding of underlying mechanisms. The genetic architecture of these conditions has proven to be complex. In the example of ASD, twin and family studies report up to 90% of heritability, although there is a broad variance according to the studies and the contribution of shared environmental factors could be higher

than previously estimated. Despite this high heritability, a genetic cause can be identified in maximum 25% of cases, such as the presence of chromosomal rearrangements, rare and de novo CNVs or coding-sequence mutations (Huguet et al. 2013). The rare variants bring a new understanding of the diseases and an entry point for investigations into the mechanisms of brain function and dysfunction. They offer an opportunity to study their effects separate from that of manifest phenotypic traits. However, even when ASD is associated with a genetic mutation, expressivity of this mutation is often variable and not totally penetrant. Most of the NDDs are thought to be polygenic or multifactorial, influenced by genetic and environmental factors (Torres et al. 2016).

A growing number of studies demonstrates the association of deletions and duplications with NDDs (Merikangas et al. 2009). “Pathogenic” CNVs, that are rare and large CNVs contributing significantly to diseases (>250 Kb with a frequency <0.1%), are identified in 10 to 15 % of children referred for NDDs (Miller et al. 2010; Battaglia et al. 2013). Such alleles arise by de novo mutation in the individual or the recent ancestry. Sanders et al. (2011) estimate the presence of 130-234 distinct ASD-related CNVs across the genome, Levy’s estimate (Levy et al. 2011) goes up to 250-300 target loci. Large de novo CNVs carry substantial risk, and the same CNVs can increase the risk for multiple cognitive and psychiatric disorders. Recent genome-wide association studies show enrichment of CNV burden in SCZ (odds ratio of 1.11), especially for genes associated with synaptic function and neurobehavioral phenotypes in mice (Marshall et al. 2016).

In table 1, we present the largest and most pathogenic risks alleles, associated with ID, SCZ and ASD (Malhotra & Sebat 2012). These genomic hotspots are important candidate loci in genetic studies of psychiatric disorders, even if they probably represent a minority of risk variants. Beyond their association with a broad range of NDDs, we have only a few pieces of knowledge on the effect of these CNVs on neurodevelopmental mechanisms.

CNV locus	Position (Mb)	Disease category	Odds Ratio [95% CI]
1q21.1 deletion	145.0–146.3	ID SCZ	12.6 [7.4–21.3] 8.1 [4.3–15.6]
1q21.1 duplication	145.0–146.3	ID ASD SCZ	4.4 [2.6–7.4] 8.0 [3.5–18.4] 4.2 [2.1–8.6]
3q29 deletion	197.2–198.4	ID SCZ	41.8 [5.6–311.6] 63.0 [8.1–491.7]
7q11.23 Williams-Beuren syndrome deletion	72.4–73.8	ID	Frequency: 0.27%
7q11.23 Williams-Beuren syndrome duplication	72.4–73.8	ID ASD	16.5 [2.2–124.5] 30.7 [3.4–275.1]
VIPR2 (7q36.3) duplication	158.4–158.8	SCZ	3.2 [1.5–7.1]
15q11.2 deletion	20.3–20.6	ID SCZ	1.9 [1.6–2.3] 2.1 [1.6–2.8]
15q11.2-13.1 duplication including Prader Willy syndrome critical region	20.8–26.2	ID ASD SCZ	18.5 [7.1–47.9] 42.6 [15.7–115.5] 5.1 [1.4–19.1]
15q13.3 deletion	28.7–30.2	ID ASD SCZ	15.1 [8.4–27.4] 10.8 [3.5–33.1] 10.7 [5.4–21.3]
16p13.11 duplication	15.4–16.2	ID SCZ	2.4 [1.8–3.2] 2.0 [1.1–3.5]
16p11.2 deletion	29.5–30.2	ID ASD	9.2 [5.8–14.7] 9.5 [5.2–17.4]
16p11.2 duplication	29.5–30.2	ID ASD SCZ	3.4 [1.8–6.5] 11.8 [6.1–22.7] 9.4 [5.3–16.6]
17p12/HNPP deletion	14–15.4	SCZ	5.7 [2.4–13.7]
17q12 deletion	31.9–33.2	ID ASD SCZ	17.3 [6.1–49.0] 16.0 [2.9–87.9] 9.5 [2.4–38.2]
22q11.21 deletion	17.1–18.7	ID ASD SCZ	Frequency: 0.61% Frequency: 0.07% Frequency: 0.3%
22q11.2 duplication	17.1–18.7	ID ASD	3.7 [2.3–6.1] 3.3 [1.6–6.6]

Table 1: Eleven pathogenic CNV loci across multiple diagnostic categories: intellectual ability (ID), autism spectrum disorders (ASD), schizophrenia (SCZ). In case odds ratio were not available, the frequency of each CNV is reported. Only significant scores are shown in the table. Adapted from Malhotra and Sebat. (Malhotra & Sebat 2012).

Among the 11 pathogenic CNV loci in table 1, the 16p11.2 CNVs are among the most frequent hotspots for recurrent rearrangements in association with ID, ASD and SCZ (Weiss et al. 2008). They are also associated with a range of phenotypic variability and severity. In this thesis, I

investigate intermediate phenotypes in carriers of the 16p11.2 reciprocal CNVs, ascertained through large clinical cohorts.

1.2 The 16p11.2 Copy Number Variants

The 16p11.2 locus encompasses several distinct structural variants, as shown in Figure 1.A. Here, I focus on the most frequent ones, the proximal 600 kb recurrent CNVs, defined by breakpoints 4 and 5 (BP4-5), at genome sequence coordinates of 29.6-30.2 Mb according to the human genome build GRCh37/hg19 (Figure 1.B). These reciprocal CNVs contain 29 genes and present either a deletion or a duplication. They have a prevalence of 1 over 1000 (1 over 2000 for the deletion and 1 over 2000 for the duplication). About 60% percent of cases of deletion occur de novo, the other 40% are inherited, whereas we can estimate more than 60% percent of duplications inherited (D'Angelo et al. 2016).

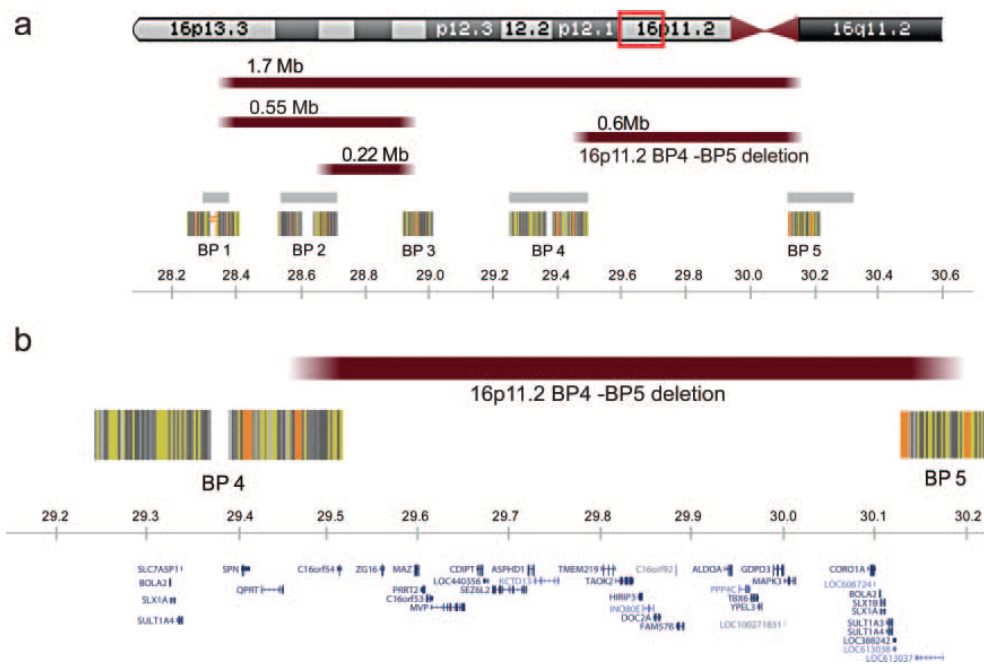


Figure 1: The 16p11.2 locus, A. Four existing rearrangements within the 16p11.2 chromosomal bands, described from telomere to centromere as breakpoints BP1 to BP5; **B.** Twenty-nine genes encompassing the BP4-BP5 genomic region. This figure is from Zufferey et al. (2012), which described the 600 kb deletion syndrome, same rearrangements and breakpoints apply to the reciprocal duplication.

1.2.1 Psychiatric and medical features

The deletion and duplication carriers present a high frequency of psychiatric and developmental disorders (.90% for deletion (Hanson et al. 2015)). Both show about 10-fold

enrichment to develop ASD, duplication shows 10-fold enrichment for SCZ and 4-fold enrichment for bipolar disorder and recurrent depression (Sebat et al. 2007; Weiss et al. 2008). The duplication is associated with multiple psychiatric phenotypes, whereas the reciprocal deletion is more specifically associated with developmental delay (McCarthy et al. 2009). 1 in 100 people diagnosed with ASD has a 16p11.2 deletion or duplication, which make the 16p11.2 CNVs ones of the most common genetic risk factors for autism. Sixteen percent of deletion probands and 20% of duplication probands met diagnostic criteria for ASD (D'Angelo et al. 2016), comparing to only 2.2% of the carrier relatives of duplication probands. Of note, probands are the CNV carriers in a family first referred in clinics, so probably the most affected and symptomatic carrier, compared to relative carriers that are not medically ascertained and diagnosed following familial genetic testing. Even the individuals with the 16p11.2 deletion or duplication not meeting criteria for ASD have a significantly higher prevalence of autism-related characteristics compared with the familial noncarrier control group (Moreno-De-Luca et al. 2015; Green Snyder et al. 2016).

Other psychiatric diagnoses are reported in 59% of deletion probands and 50% of duplication probands, including significant psychiatric comorbidity. Psychiatric conditions are also diagnosed in about 44% of their carrier relatives without a diagnosis of ASD. In the deletion carriers, the diagnosed conditions are developmental coordination disorders, phonologic processing disorders, expressive and receptive language disorders (Hanson et al. 2015): the uniqueness of the articulation, the language, and motor impairments are apparent. Eighty-three percent of 16p11.2 carriers have a history of speech therapy. In the duplication carriers, the phenotype presents a wide variability (from asymptomatic presentation to significant disability), wider than the reciprocal deletion. The diagnosed conditions are ID (inclusive of borderline intellectual functioning), developmental coordination and articulation disorders, attention deficit hyperactivity disorders in children; anxiety, obsessive-compulsive and mood disorders in adults (Green Snyder et al. 2016).

We observe a broad spectrum of malformations and medical issues in both CNVs carriers (Zufferey et al. 2012; D'Angelo et al. 2016). Twenty percent of carriers of the deletion have vertebral and spinal related anomalies and 46% facial dysmorphism. Both CNVs carriers show a variety of neurologic abnormalities, with some shared and some distinct neurologic features. That could reflect some opposite neurobiological mechanisms in the deletion and duplication, resulting in the hypo- vs hyper-reflexia and functional motor impairments. Similar frequency

of epilepsy is observed in deletion and duplication proband carriers, 24% and 19,4% respectively, with broad clinical spectrum and predominance of generalized seizures. In deletion, the mean age of walking, at 20,5 months (standard deviation=8,6), is significantly delayed and gross motor delay is observed in 37,6% of the patients. The median age at first walking is also delayed in duplication proband carriers, with an increased proportion of very late onset walking (>24 months) compared to the deletion proband carriers. The most frequent findings at the MRI level are the cerebral white matter/corpus callosum abnormalities, cerebellar hypoplasia and ventricular enlargement for the duplication carriers; the Chiari I malformations/cerebellar tonsillar ectopia and posterior fossa abnormalities for the deletion carriers (Steinman et al. 2016).

1.2.2 Anthropometric measurements

The dosage effects of the genes regulate in an opposite way the anthropometric measurements (“mirrored” phenotype): mean body mass index (BMI) is significantly higher in the deletion carriers and lower in the duplication carriers than BMI in the familial controls, +0.7 Z-score and -0.6 Z-score respectively (Jacquemont et al. 2011; D’Angelo et al. 2016). Deletion is associated with a high penetrance of obesity (43-fold increased risk of developing morbid obesity), with an increase of BMI with age: birth weight is below average (Z-score=-0.61), then it increases and becomes significantly higher by the age of 3.5 (Z-score=1.01). By the age of 7 years, obesity (BMI \geq 30) is present in more than 50% of the carriers, and the penetrance is up to 70% for the adult carriers (Zufferey et al. 2012). Deletion is also linked to a lack of satiety, from early childhood and even before the beginning of obesity (Maillard et al. 2015). On the contrary, 16p11.2 deletion mice tend to be smaller and leaner than wild-type mice (Portmann et al. 2014). This age-related effect is not observed in duplication carriers, for who the BMI remains relatively stable from 0 to -1 Z-score.

We observe the same inverse and significant gene dosage effect for head circumference (HC) (Jacquemont et al. 2011; D’Angelo et al. 2016): mean HC is significantly higher in the deletion carriers (+0.5 Z-score) and lower in the duplication carriers (-1.1 Z-score) than HC in the familial controls. 17% of deletion carriers and 22,3% of duplication carriers are macrocephalic and microcephalic, respectively (HC Z-score $>$ |2|). HC Z-scores decrease significantly during the first 2 years of life in duplication carriers, mirroring the early increase growth during the same period observed in deletion carriers. The HC correlates positively with the BMI, the early

increase in HC for deletion carriers precedes the onset of obesity. The animal models support this gene dosage effect: brain volume size is affected reciprocally in deletion and duplication mice, in the same direction than human subjects (Horev et al. 2011). KCTD13, a gene in the 16p11.2 interval, seems to be associated with the regulation of brain size in zebrafish: overexpression of this homolog gene causes a significant decrease in brain size in zebrafish embryos whereas inhibition leads to an increase in brain size (Golzio et al. 2012). A recent study on mice show that underexpression of KCTD13 leads to increased levels of Ras homolog gene family, member A (RhoA), that reduce synaptic transmission (Escamilla et al. 2017). Although KCTD13 is implicated in the regulation of neuronal function relevant for neuropsychiatric disorders, it does not seem to alter brain size or neural progenitor cell proliferation in mammals.

1.2.3 Neuropsychological profile and developmental trajectory

Several studies, including ours, demonstrated altered global cognition in 16p11.2 deletion and duplication carriers (Zufferey et al. 2012; D'Angelo et al. 2016; Hippolyte et al. 2016; Hanson et al. 2015; Green Snyder et al. 2016). Full-scale intelligence quotient (FSIQ) decreases by an average of 22 points in the deletion and by an average of 18 points in the duplication carriers, compared with the familial controls (significantly similar mean decreases). In deletion carriers, FSIQ variance is the same than in the general population, verbal IQ (VIQ) is significantly lower than non-verbal IQ (NVIQ), and 20% of the carriers meet criteria for ID. On the contrary, we show in a study I contributed at the beginning of my Ph.D., that the 16p11.2 duplication phenotype is characterized by wider variability than the reciprocal deletion. We observe a higher proportion of very low IQ (30,5% of duplication carriers meet criteria for ID), lower NVIQ and higher rates of additional CNVs, likely reflecting contributions of additional risk factors (D'Angelo et al. 2016).

The number of 16p11.2 genomic copies may also modulate specific cognitive skills: the language domain (phonology, written language, vocabulary), the memory processes (short- and long-term memory) and the verbal and motor inhibition skills (Hippolyte et al. 2016). When neuropsychological scores are adjusted for IQ levels, the deletion carriers show specific impairments in phonology and vocabulary (-1.3 Z-score in a task of non-word repetition and -0.7 Z-score in a task of word definition); as well as an impairment in verbal inhibition (-0.8 Z-score in a task of Stroop). Neuroimaging analyses reveal that the verbal inhibition error rate

may covary with the gray matter (GM) volume of deletion carriers in the bilateral insula and transverse temporal gyri. On the contrary, duplication carriers do not show a specific impairment relative to their global functioning, but they have preserved or even enhanced verbal long-term memory skills (+1.1 Z-score). Some other domains, such as visuospatial and working memory, are unaffected by the 16p11.2 locus, beyond the effect of decreased IQ.

Both CNV carriers show distinct cognitive profiles, highlighting their heterogeneity. The cognitive performances may covary with molecular mechanisms, and the mouse models have enhanced memory skills on a recognition task in duplicated mice compared to wild-type animals (Arbogast et al. 2017). MAPK3 is a good candidate gene mediating the correlation between the 16p11.2 CNV and memory performances (Golzio et al. 2015). This is reminiscent of special isolated skills that can be observed in ASD.

A longitudinal study between the ages of 6 months and 8 years highlights the developmental trajectories for young deletion and duplication carriers: the first ones show VIQ gains early in development but a decline in motor and social abilities, the last ones show VIQ gains and steady trajectories for the other social and motor domains. They also point out the distinct trajectories in the sub-group of 16p11.2 CNV carriers who are ultimately diagnosed with ID, ASD or developmental coordination disorder, compared to the carriers who will not meet the criteria for these psychiatric conditions (Bernier et al. 2017). It is crucial to take into account and continue to study this variability during early development, to better adapt therapies.

1.2.4 Variance in phenotypes and additional factors

Most of the disorders caused by CNVs display a significant clinical variability. Other factors may modulate this variable phenotypic expression of rare highly penetrant variants, such as genetic factors, from rare to common polygenic variation, epigenetic regulation, environmental sources.

Regarding the 16p11.2 CNVs, even if the average effects of the duplication and the deletion on cognition are similar, they have different profiles. The average effect of the deletion is identical for proband and non-proband carriers, suggesting that 'asymptomatic' carriers are uncommon. The variance of FSIQ was also similar among carriers of the deletion and control population: the factors determining the variability of FSIQ may be identical to those at play in the general population and unrelated to the 16p11.2 locus. However, Duyzend et al. (2016) find a strong maternal bias for the origin of the *de novo* deletions and they identify the

presence of rare, not clinically diagnosed, additional CNVs in 69% of the probands, suggesting that genetic background plays a role in the observed phenotypes.

We demonstrate that the duplication is associated with an average decrease of 26.3 points in FSIQ between proband carriers and non-carrier family members. However, there is a smaller decrease (16.2 to 11.4 points) between non-proband carriers and non-carriers (D'Angelo et al. 2016). The distribution of FSIQ in duplication carriers shows a very broad variance, with a 2.0-fold increase in an "above average" group (FSIQ>100) and a 19.4-fold increase in low functioning (FSIQ<40) carriers, compared to the deletion group ($p<0.001$) (D'Angelo et al. 2016). Parental FSIQ predicts part of this variation (~36.0% in inherited probands, compared to 11% for deletion carriers). FSIQ is also significantly lower in the duplication probands with ASD than those without an ASD diagnosis (mean FSIQ, 52.8 vs. 75.4). Additional deleterious CNVs were 2.5-fold higher in duplication compared with deletion probands ($p=0.006$). Duyzend et al. (2016) also observe a modest negative correlation between the number of additional CNVs and FSIQ in 16p11.2 CNV carriers. Other traits, as neurological features, present a broader phenotypic variability among duplication carriers than deletion carriers (Steinman et al. 2016). All these results converge towards additional genetic and familial factors contributing to the phenotype variability: the duplication may require additional factors to reach the threshold for clinical evaluation compared with the deletion.

The 16p11.2 deletion is also reported in apparently unaffected control participants from the general population. However, although these CNV carriers do not reach the current clinical diagnosis thresholds, they exhibit a variety of cognitive deficits (Männik et al. 2015). The same phenomenon is observed in the carriers of 15q11.2 BP1-BP2 deletion from an apparently healthy cohort: they have a history of dyslexia and dyscalculia, even when controlling for IQ, and the brain structures of these CNV carriers exhibit a pattern consistent with structural correlates of dyslexia (Stefansson et al. 2014). More generally, Männik et al. (2015) show that recurrent large pathogenic CNVs, as well as rare intermediate-size (non recurrent) CNVs are negatively associated with educational attainment in general population.

1.3 Contribution of neuroimaging to neuropsychiatric and genetic disorders

1.3.1 Neuroimaging techniques

During the last decades, many neuroimaging studies were published in patients with psychiatric disorders, with the hope that neuroimaging would represent a useful intermediate

phenotype to understand psychiatric conditions better. Even if this field of research is still in its infancy, we have a range of methods to study the structure and function of the brain, with increasing spatial resolution for Magnetic Resonance Imaging (MRI); or better temporal resolution for the electro-encephalography (EEG). In this thesis, I focus on structural MRI, with T1-weighted images, to characterize the brain anatomy of the individuals carrying a 16p11.2 CNV.

The MR signal comes from the application of external magnetic fields on the subject. It aligns hydrogen nuclei along the direction of the applied field. Then, applying a pulse of electromagnetic energy at a specific radiofrequency, the nuclei rotate away from the axes of the magnetic field. It takes time for the nuclei to return, in an exponential way, to their original position, pointing along the magnetic field. T1 represents the time to “relax” back, it depends on the local structural patterns. These local differences in relaxation times are reflected in the contrast of structural MRI (Paus et al. 2001). Based on these image contrasts, different measurements have been developed over time, from volumetric features to surface-based measurements. They are more and more specific regarding the underlying mechanisms: Figure 2 represents the evolution of structural MRI measurements as applied to research on ASD (Ecker et al. 2015). Multiple other types of images can be acquired through the MRI techniques, from which measurements as the white matter (WM) integrity or connectivity, can be quantified.

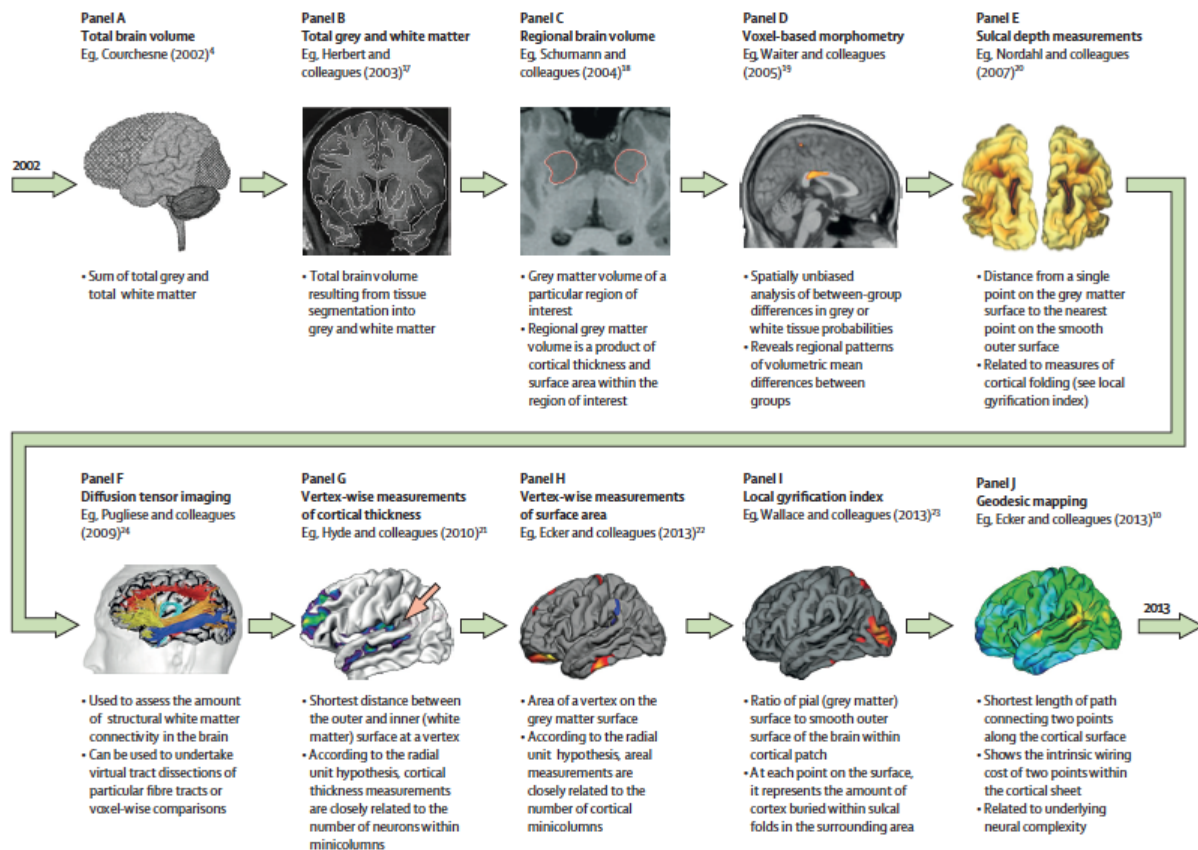


Figure 2, from Ecker et al. (2015): Evolution of structural MRI measurements over time in ASD research. Panel A reproduced from Courchesne (2002); Panel B reproduced from Herbert et al. (2003); Panel C reproduced from Schumann et al. (2004); Panel D reproduced from Waiter et al. (2005); Panel E reproduced from Nordahl et al. (2007); Panel F reproduced from Pugliese et al. (2009); Panel G reproduced from Hyde et al. (2010); Panel H reproduced from Ecker et al. (2013); Panel I reproduced from Wallace et al. (2013); Panel J reproduced from Ecker et al. (2013).

1.3.2 Neuroanatomical alterations in psychiatric disorders

Early brain overgrowth is probably the most replicated finding in people diagnosed with ASD (Anagnostou & Taylor 2011): this accelerated brain volume growth in early childhood corresponds about at a 10% increase in brain volume. Some region-specific differences, such as volumetric alterations of parieto-temporal and frontal lobes, the cerebellar cortex, the hypothalamus, and the striatum are described (Stanfield et al. 2008; Kurth et al. 2011). A decreased volume of the cingulate is associated with reduced metabolic activity (Haznedar et al. 2006), and an increased volume of the caudate is correlated with the severity of repetitive behaviors (Langen et al. 2007; Hollander et al. 2005). A decreased volume of the corpus callosum is also reported, suggesting a reduced interhemispheric connectivity (Hardan et al. 2009; Stanfield et al. 2008). The spread of these findings indicates that ASD is a widely distributed disorder affecting both GM and WM. However, there is little consistency between

studies. Distinct brain patterns can be observed in two groups of children diagnosed with ASD. For example, Hazlett et al. (2009) find a robust enlargement of the caudate nucleus in the brains of the fragile X children with ASD compared to controls, whereas children with idiopathic autism have an enlargement of the amygdala and a modest enlargement of the caudate. Lefebvre et al. (2015) do not observe a significant decreased volume of the corpus callosum in a large cohort of patients diagnosed with autism. Adopting another approach, Ellegood et al. (2014) cluster anatomical regions of 26 different mouse models of autism. The clustering reveals three neuroanatomical patterns, including the key main regions associated with autism in human: group 1 is a cortex to basal ganglia loop (associated with repetitive behaviors, executive function, and communication), group 2 represents more dispersed brain regions involved in social recognition and autonomic regulation, group 3 is localized in the cerebellum. These clusters also distinguish the directionality of the anatomical changes: for example, the cerebellar cortex is oppositely affected in Group 1 compared to Group 3 and not altered in Group 2. Group 1 is associated with an increase and Group 2 with a decrease in similar WM structures.

The volume abnormalities are also associated with atypical functional and structural connectivity in the brain. Many studies provide evidence for decreased cortical-cortical connectivity, with possibly increased connectivity between subcortical regions and cortex, and within primary sensory areas such as the visual cortex. That supports the idea of poor long-distance connectivity in ASD. Intrinsic functional connectivity studies suggest abnormal patterns of network activation in the default mode network (DMN) at rest in ASD (Pua et al. 2017).

Age is an important factor, but fewer studies examine changes in the developmental trajectory associated with autism (Dennis & Thompson 2013). At birth, the brain of ASD individuals seems to be either at the same size or smaller than typically developing controls. During the first 2 years of life, individuals with autism demonstrate a precocious brain growth which exceeds that of the controls (Anagnostou & Taylor 2011). But this peak around 2-4 years of age is probably followed by a plateau. The controls catch up and, at adolescence, there is no statistical difference in brain size between individuals with ASD and age-matched controls. Moreover, a recent developmental study on siblings at risk for ASD shows that very early, post-natal hyper-expansion of cortical surface areas would precede brain volume overgrowth, which is temporally linked to the emergence and severity of autistic social deficits. Early brain

changes would occur during the period in which autistic behaviors are first emerging (Hazlett et al. 2017). The altered neurodevelopmental trajectory seems to vary across the lifespan and different brain regions (Pua et al. 2017). For example, Hardan et al. (2009) examine longitudinal changes in cortical thickness in autistic boys and find a higher decrease with age in cortical thickness in the autistic boys than in the controls.

Regarding SCZ, a decrease of global GM volume and ventricular enlargement are ones of the most consistent findings (Brugger & Howes 2017). Studies show also decreased volume in frontal, temporal (Hulshoff Pol & Kahn 2007; Honea et al. 2005; Shepherd et al. 2012; Fornito et al. 2009), medial temporal regions, including insula and anterior cingulate cortex (Ellison-Wright et al. 2008; Glahn et al. 2008; Shepherd et al. 2012). These volume differences are mainly driven by reduction in cortical thickness, and some reduction of surface area (Rimol et al. 2012). A recent meta-analysis exhibits subcortical brain differences in one of the largest sample size to date (2028 individuals with SCZ and 2540 controls). It ranks them according to their effect size (van Erp et al. 2015): hippocampus (Cohen's $d=-0.46$), amygdala (Cohen's $d=-0.31$), thalamus (Cohen's $d=-0.31$), accumbens (Cohen's $d=-0.25$) and intracranial volumes (Cohen's $d=-0.12$) are reduced in SCZ compared to controls. On the contrary, volumes of pallidum (Cohen's $d=0.21$) and lateral ventricle (Cohen's $d=0.37$) are increased. The GM volume of the total cerebellum is robustly reduced (Cohen's $d=-0.35$), this structure is probably a key node of the network underlying the SCZ (Moberget et al. 2017). Brugger & Howes (2017) show that there is a lower variability of the results in the anterior cingulate, compared to the variability found in other regions implicated in SCZ (temporal cortex, thalamus, putamen and third ventricle volumes). Given this greater homogeneity, they suggest that anterior cingulate cortex volume is a core region in SCZ, shared across subtypes of the disorder. Morphometric abnormalities in this region are also seen across several psychiatric disorders (Crossley et al. 2014; Cauda et al. 2017). Of note, widespread reductions in WM, especially fractional anisotropy, is observed in SCZ, with the largest effect sizes around $d=0.4$ (Kelly et al. 2017).

More generally, Goodkind et al. (2015) identify GM loss in the anterior insula and the dorsal anterior cingulate as a common neural signature across 6 diverse psychiatric diagnoses (SCZ, bipolar disorder, depression, addiction, obsessive-compulsive disorder, and anxiety, with the largest effect size in SCZ). These shared neural substrates may relate to executive function deficits observed across these psychiatric diagnoses. The authors show few diagnosis-specific

effects. (figure 3). This transdiagnostic perspective is coherent with the National Institute of Mental Health’s Research Domain Criteria Project, a dimensional and organizing model of psychiatric disorders, that highlight the importance of shared intermediate phenotypes (Cuthbert & Insel 2013).

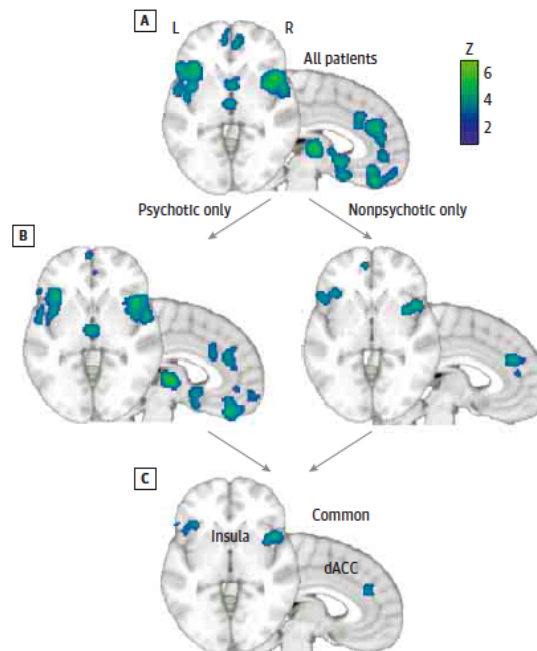


Figure 3, from Goodkind et al. (2015): Shared patterns of decreased gray matter volumes from voxel-based morphometry meta-analysis of 193 studies comprising 15892 individuals (estimation of gray matter loss in z-scores). A, comparison between patients and controls from studies pooled across all diagnoses. The results show a loss of GM volume in anterior insula, dorsal anterior cingulate cortex, prefrontal cortex, thalamus, amygdala, hippocampus, superior temporal gyrus; B, comparison between patients and controls separately by psychotic or nonpsychotic diagnosis studies; C, results from a conjunction across the psychotic and nonpsychotic groups maps in panel B.

In another meta-analysis of 25 voxel-based studies comprising 308 ASD and 352 first-episode SCZ participants, as well as 801 controls, Cheung et al. (2010) show that a decrease of GM volume overlaps in ASD and SCZ within limbic-striato-thalamic circuitry, suggesting a neuro-anatomical proof of shared etiological mechanisms. Some other regions are specific to each disorder (Figure 4).

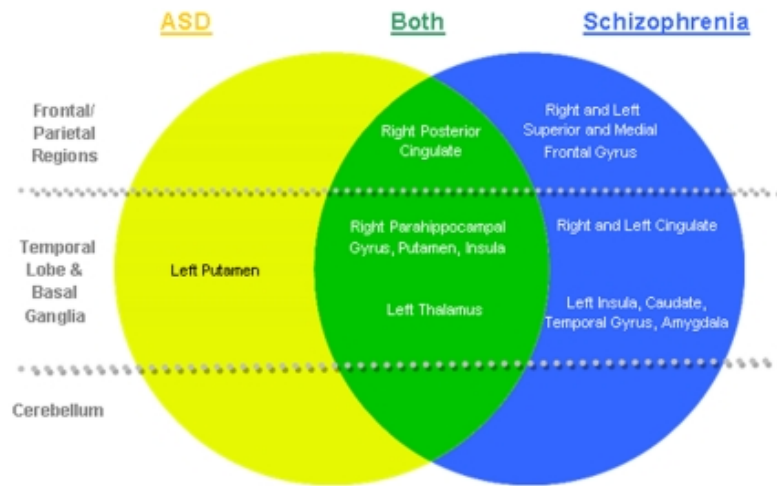


Figure 4, from Cheung C. et al. (2010): Distinct and overlapping regions of decreased gray matter volumes in ASD and SCZ.

Some international consortia aim to target the issue of heterogeneity in psychiatric neuroimaging results, with powerful enough datasets to avoid type I and type II statistical errors and precise estimates of effect sizes (Carter et al. 2017). For example, the Autism Brain Imaging Data Exchange – ABIDE (http://fcon_1000.projects.nitrc.org/indi/abide/), aggregates and openly shares more than 1000 resting-state functional MRI and phenotypic information from 539 individuals with ASD and 573 age-matched typical controls, from 7 to 64 years. The Enhancing NeuroImaging Genetics through Meta-Analysis (ENIGMA) consortium (<http://enigma.ini.usc.edu>) merges data collected by independent studies to determine how genetic variants influence the brain, and how major psychiatric or neurodegenerative diseases affect the brain worldwide (Thompson et al. 2016). By pooling genomic data and brain imaging of over 30 000 individuals, the datasets are the largest in the World. The analyses are going to make possible replication and reproducible results, generalizable estimates of even small effect sizes (Adhikari 2017), and a distinction of common and unique effects of brain disorders on brain structures (Bearden & Thompson 2017). The goal is also to improve the power to detect genetic variants influencing the brain. Even if many brain measures are significantly highly heritable (about 80%), we still don't know most of the specific variants that contribute to the variability of these measurements. First results identify common variants influencing human hippocampal structures and intracranial volumes (Stein et al. 2012; Thompson et al. 2016).

1.3.3 Previous MRI studies on carriers of a 16p11.2 copy number variant

Neuroimaging studies of a large number of individuals carrying a CNV associated with psychiatric disorders help to understand underlying mechanisms better. Two previous studies explore the brain structures of individuals with a 16p11.2 CNV. Qureshi et al. (2014) analyzed structural MRI data of the Simons variation in individuals project foundation (Simons VIP), on 25 children carrying a deletion and 17 adults carrying a duplication, compared with age-matched controls. On the European side, Maillard et al. (2014) analyze data on 14 deletion carriers, 23 controls, and 17 duplication carriers. Both studies show an inverse gene dosage effect on global brain measurements: total intracranial volume (TIV), GM and WM volumes correlate negatively with the number of genomic copies. Qureshi et al. (2014) also identify an increased and reduced size in deletion and duplication carriers respectively, for the subcortical structures and the cerebellum, with the largest effect on the thalamus. They interpret the results as a pervasive effect of the CNV on the brain. This is reinforced by the gene dosage effect on the global cortical surface area, but not the cortical thickness: this suggests that the differences associated with the CNV appear early in the development. Beyond the differences on the global brain metrics, Maillard et al. (2014) show some specific regional gene-dosage effects of GM and WM in key areas of the reward system, language circuitry, and social cognition. The observed brain anatomy changes spatially overlap with brain changes in ASD and SCZ, and they are explained by mRNA levels of all assessed genes within the 16p11.2 interval. Mouse models also demonstrate the reciprocal effect of regional brain volume changes (Horev et al. 2011). In deletion mice, Portmann et al. (2014) find a relative increase in the size of various regions, especially the basal ganglia circuitry, the hypothalamus, as well as a decrease of the corpus callosum. The neuroanatomical differences may be present from the young age (mice at p7).

Moreover, there is evidence of a specific widespread pattern of WM microstructure alterations, not usually reported in NDDs. Owen et al. (2014) show, in deletion carriers, an increase in axial diffusivity in some major central WM tracts (anterior corpus callosum, internal and external capsules), associated with an increase in fractional anisotropy and mean diffusivity in some of the same tracts. Fiber orientation dispersion seems to be decreased in some of the central tracts. Chang et al. (2016) show the reciprocal pattern for the duplication carriers, especially a decrease of fractional anisotropy and the association of WM changes with general cognitive impairments.

1.4 Goal of the thesis

The genetic-first approach is a powerful approach to gain insight the etiologies and mechanisms of psychiatric and developmental disorders, in the context of a biologically homogenous sample of individuals (The Simons VIP Consortium 2012). Whole genome chromosomal microarray (CMA) is now well established as a first-tier clinical diagnostic test in the developmental pediatric clinic, and CNVs contributing to NDDs and other psychiatric disorders are reported back to patients. However, little is known about their effect on brain development and structure. Neuroimaging studies have been conducted in only a handful of CNVs including 22q11.2, 15q11.2, and Williams syndrome.

My Ph.D. is focused on patients carrying a proximal 600 kb 16p11.2 CNV, their family members, and unrelated controls. The main goal is to understand the effects of 16p11.2 deletion and duplication on neuroanatomical traits.

Our two specific goals are:

1- To investigate the effect of the 16p11.2 deletion and duplication on brain structures.

The two previous neuroimaging studies reported gene-dosage effects on global brain metrics, but the large brain size and the sample size limited the analyses and the interpretation of some regional analyses. Here, we merge multiple datasets to increase the sample size. We aim at quantifying the effect of the global and regional gene dosage effect, as well as the specific contribution of the deletion and the duplication to these 16p11.2-associated brain differences. We examine the generalizability of our results across cohorts, scanning sites, sex and a broad age range. Given the different types of clinical ascertainment across the two cohorts, we also aim at understanding the influence of the ascertainment and the relationship between the brain findings and the clinical phenotypes. Specifically, we ask whether language, social responsiveness, IQ, the presence of psychiatric disorders may impact any of the brain findings; and we overlap our results with the ones from a meta-analysis on psychiatric conditions. We also investigate if the non-carrier familial controls show some brain structural differences, compared to the general population, that would contribute to the patterns observed in the 16p11.2 carriers.

To this end, we perform voxel- and surface-based analyses in parallel on 361 participants, including 307 individuals not previously analyzed at the regional level using whole-brain statistical methods. We use two complementary computational methods, to assess the GM

volume, the cortical thickness, and the surface area differences. This first goal is developed in the first paper, “Quantifying the effects of 16p11.2 copy number variants on brain structure: A multi-site ‘genetic-first’ study”.

2- To characterize the developmental trajectory of 16p11.2-associated brain differences.

Following the description of the alterations from the first study, the next question is “when” these differences appear during brain development. In the second study, we aim at comparing the developmental trajectories of the global and regional volumes of the 16p11.2 CNVs carriers to the typical growth trajectories of children and adolescents controls.

To this end, we use a large normative dataset from National Institute of Health MRI study of healthy brain development (NIHPD) with 339 typically developing individuals aged from 4.5 to 23 years old (<https://pediatricmri.nih.gov/>)(Evans 2006). These data are used to obtain age- and sex-normative brain growth trajectories. We compute Z-scores for our 16p11.2 dataset, using previously published longitudinal pipeline and normalizing method (Aubert-Broche et al. 2013). Trajectories of global and ‘per voxel’ brain measurements of the 16p11.2 carriers are compared to the norm, from 4.5 years to 23 years old, to evaluate when the brain differences appear and their effect size through our age range. The 2nd goal is developed in the second chapter of the results: “Developmental trajectories of neuroanatomical alterations associated with the 16p11.2 Copy Number Variations”.

To establish a well-characterized cohort of families, we acquired and pooled data from the European 16p11.2 consortium with the ones from the Simons VIP (<http://www.simonsvipconnect.org/>) in North America. Individuals were recruited through different ascertainment in both studies: they were referred by a geneticist in Europe and were more broadly recruited in the USA, including referral by clinical genetic centers, web-based networks or active online registration of families. They were ascertained regardless of clinical diagnoses or age. CNV carriers are either probands referred to the genetic clinic for the investigation of neurodevelopmental and psychiatric disorders or their relatives. Familial controls are relatives who do not carry the CNV. Unrelated controls are selected among volunteers from the general population who have neither any major DSM-5 diagnosis nor a relative with a NDD. Focusing on structural brain intermediate phenotypes, we collected T1-weighted anatomical images from 7 scanning sites (5 sites in North America and 2 sites in Europe), with multi-echo or single-echo MPRAGE (magnetization prepared rapid gradient echo) sequences.

2. RESULTS

2.1 Quantifying the effects of 16p11.2 copy number variants on brain structure: A multi-site 'genetic-first' study

Sandra Martin-Brevet, MS*, Borja Rodriguez-Herreros, PhD*, Jared A. Nielsen, PhD*, Clara Moreau, MS, Claudia Modenato, MS, Anne M. Maillard, PhD, Aurélie Pain, MS, Sonia Richetin, MS, Aia E. Jønch, MD, Abid Y. Qureshi, MD, Nicole R. Zürcher, PhD, Philippe Conus, MD, 16p11.2 European Consortium, Simons Variation in Individuals Project (VIP) Consortium, Wendy K. Chung, MD, PhD, Elliott H. Sherr, MD, PhD, John E. Spiro, PhD, Ferath Kherif, PhD, Jacques S. Beckmann, PhD, Nouchine Hadjikhani, MD, PhD, Alexandre Reymond, PhD, Randy L. Buckner, PhD, Bogdan Draganski, MD** and Sébastien Jacquemont, MD**

* shared 1st authorship

** shared senior authorship

Biological Psychiatry, 84(4):253-264.

Contribution: elaborated study design, collected and analyzed data, wrote the paper.

ABSTRACT

BACKGROUND

16p11.2 BP4-BP5 copy number variants (CNVs) increase the risk for developing autism spectrum disorder, schizophrenia, language and cognitive impairment. In this multi-site study, we aimed to quantify the effect of 16p11.2 CNVs on brain structure.

METHODS

Using voxel- and surface-based brain morphometric methods, we analyzed structural magnetic resonance imaging collected at seven sites from 78 individuals with a deletion, 71 individuals with a duplication, and 212 individuals without a CNV.

RESULTS

Beyond the 16p11.2-related mirror effect on global brain morphometry, we observe regional mirror differences in the insula (deletion>control>duplication). Other regions are preferentially affected by either the deletion or the duplication: the calcarine cortex and

transverse temporal gyrus (deletion>control; Cohen's $d > 1$), the superior and middle temporal gyri (deletion<control; Cohen's $d < -1$), as well as the caudate and hippocampus (control>duplication; $-0.5 > \text{Cohen's } d > -1$). Measures of cognition, language, and social responsiveness and the presence of psychiatric diagnoses do not influence these results.

CONCLUSIONS

The global and regional effects on brain morphometry due to 16p11.2 CNVs generalize across site, computational method, age, and sex. Effect sizes on neuroimaging and cognitive traits are comparable. Findings partially overlap with results of meta-analyses performed across psychiatric disorders. However, the lack of correlation between morphometric and clinical measures suggests that CNV-associated brain changes contribute to clinical manifestations but require additional factors for the development of the disorder. These findings highlight the power of genetic risk factors as a complement to studying groups defined by behavioral criteria.

2.2 Developmental trajectories of neuroanatomical alterations associated with the 16p11.2 Copy Number Variations

2.2.1 Introduction

2.2.1.1 16p11.2 Copy Number Variants (CNVs)

Genetic variants associated with psychiatric disorders represent unique opportunities to study the same biological mechanism across neurodevelopment, adolescence, and adulthood. In the absence of longitudinal data, the cross-sectional study of a genetic variant can provide a reasonable approximation of age-related effects because the mutation can be studied in individuals with different ages, genetic backgrounds, as well as carriers with or without clinical manifestations. The ~600kb 16p11.2 BP4-BP5 CNVs (breakpoints 4–5, 29.6-30.2 Mb-Hg19) are strongly associated with neurodevelopmental disorders (Weiss et al. 2008). Deletion and duplication carriers have a 10-fold increased risk of developing autism spectrum disorders (ASD), and duplication carriers (but not deletion), a 10-fold increased risk for schizophrenia (McCarthy et al. 2009).

Deletion and duplication carriers are also associated with differences in brain size and shape. Total gray and white matter volumes correlate negatively with the number of genomic copies (Qureshi et al. 2014; Maillard et al. 2014), with more volume in deletion and less volume in duplication carriers than controls. Robust regional structural alterations have been observed in the insula, calcarine cortex, and superior, middle, transverse temporal gyri in deletion carriers. Alterations in the insula, caudate and hippocampus occur in duplication carriers (Martin-Brevet et al. 2018). These findings are thought to reflect the true effect of the CNVs since they are independent of neuroimaging computational methods, sex, ascertainment as well as presence or absence of a psychiatric diagnosis. Alterations are present in older adults as well as adolescents but in the lack of proper normative data, we have been unable to study younger individuals, and it is unknown when these alterations appear during brain development.

Longitudinal studies point out distinct phenotypic trajectories and early cognitive or social communication abilities for 16p11.2 CNVs carriers who are ultimately diagnosed with intellectual disability (ID) or ASD (Bernier et al. 2017), compared to the 16p11.2 CNVs carriers who will not meet the criteria for these psychiatric conditions. Given that some studies in 16p11.2 mice show structural alterations in cortex and striatum at 7 days (Portmann et al.

2014), we hypothesize that the aforementioned brain differences appear during childhood in humans.

2.2.1.2 Z-scoring and developmental trajectory

Because none of the brain measures show linear changes across childhood and adolescence (Giedd et al. 1999), it is impossible to properly correct for age based on small control samples. Instead, large normative developmental datasets are required to infer these trajectories. Aubert-Broche et al. (2013) previously developed a longitudinal image processing pipeline and z-scoring method to define age- and sex-normative brain growth trajectories from the NIH MRI study of normal brain development (NIHPD) derived from 339 typically developing individuals aged 4.5 to 23 years old (<https://pediatricmri.nih.gov/>) (Evans 2006). This method has successfully been applied to determine the impact on brain growth of pediatric-onset Multiple Sclerosis (Aubert-Broche et al. 2014).

To investigate brain alterations beyond *a priori* specified anatomical regions of interest, Tensor-Based Morphometry (TBM) enables a whole brain voxel-by-voxel statistical analysis while accounting for brain size. This is of particular interest for a population as the 16p11.2 deletion and duplication carriers, which are known to have significantly bigger and lower head circumferences respectively, than control individuals. TBM uses the deformation fields resulting from a non-linear registration to an appropriate template. It can be used to quantify changes in morphology across time (Frackowiak 2004; Lau et al. 2008). It enables estimation of voxel-wise trajectories of normal development when applied to data such as the NIHPD study (Frackowiak 2004; Aubert-Broche et al. 2011).

2.2.1.3 Goal

We aimed to characterize the developmental trajectory of global and regional differences in 16p11.2 CNVs carriers. To this end, we z-scored our cross-sectional 16p11.2 dataset (56 deletion carriers, 19 duplication carriers, 105 control individuals) using our previously published longitudinal pipeline and normalizing methods (Aubert-Broche et al. 2013). Jacobian determinants of the deformation field were used as a surrogate metric of relative local tissue volume for the voxel-based analyses.

2.2.2 Methods

2.2.2.1 Participants

16p11.2 CNVs cohort

Cross-sectional data were acquired in 2 different cohorts (the European -EU 16p11.2 consortium and the Simons VIP -SVIP study in North America) of 180 individuals (The Simons VIP Consortium 2012; Maillard et al. 2014). We included data only from participants between 4 to 23 years of age as they could be normalized with the NIHPD data. This included 56 16p11.2 BP4-5 deletion carriers (DEL, 42 American and 14 European individuals), 19 duplication carriers (DUP, 15 American and 4 European individuals), and 105 controls (CTRL, 75 American and 30 European individuals, 34 familial and 71 unrelated controls). CNV carriers were either probands referred for genetic testing or relatives of probands. The familial controls were recruited among the non-carriers of the same CNV-related families. The unrelated controls were selected among volunteers from the general population who did not have a relative with a neurodevelopmental disorder. The study was approved by the institutional review boards of each consortium and signed informed consents were obtained from the participants or their legal representatives. A full description of demographics is available in **Table 2**.

	DEL	CTRL	DUP
N	56	105	19
Age (years)			
Mean (SD)	11.26 (3.62) *	14.15 (4.24) *	12.29 (4.87)
range (min-max)	6.33-22.33	4.67-22.92	5-20.33
Sex (M/F)	29/27	67/38	13/6
Scan parameter (Multi/Single echo acquisition)	38/18	76/29	12/7

Table 2. Population characteristics of the 16p11.2 dataset

* Deletion carriers significantly younger than control individuals ($t = -4.5272$, $p = 1.347e-05$)
DEL, deletion carriers; CTRL, control individuals; DUP, duplication carriers; N, sample size;
SD, standard deviation; M, male; F, female

General population – NIHPD cohort

As normative data for growth reference, we used the multi-site longitudinal data from Objective 1 of the publicly available NIHPD project (Evans 2006). The normative model (Aubert-Broche et al. 2011) used data from 339 children (179 females and 160 males), scanned serially at 2 or 3-time points, with approximately 24 months between scans, for a total of 874

scans. The age range was from 4.5 to 18 years (initial time-point for enrollment), mean age at first scan was 11.0 years.

2.2.2.2 MRI protocol

The MRI data on 16p11.2 individuals included T1-weighted (T1w) anatomical images acquired at 7 sites using different 3T scanners: Philips Achieva, Siemens Prisma Syngo, and Siemens Tim Trio. The MRI protocol included a whole brain, 3D T1w magnetization prepared rapid Gradient echo sequence (MPRAGE) with 1-mm-thick sagittal slices. Three sites used multi-echo sequences for 126 participants (38 DEL, 12 DUP, 76 CTRL with 5 familial and 71 unrelated CTRL), and 4 sites used single-echo sequences for 54 participants (18 DEL, 7 DUP, and 29 familial CTRL). Details of the scanners and image acquisition sequences can be found in **Table 3**. Extensive analyses on the potential effect of these scanning sites and protocols were performed in a previous study showing that none of the regions associated with the 16p11.2 deletion or duplication could be attributed to artifacts introduced by the multisite analyses (Martin-Brevet et al. 2018).

Scans of the NIHPD controls were obtained at 6 study centers with 1.5 MRI scanners from General Electric or Siemens Medical Systems. The MRI protocol included a whole brain, 3D T1w RF-spoiled gradient echo sequence (1-mm-thick sagittal partitions, TR 22–25 msec, TE 10–11 msec, excitation pulse angle 30°, Field Of View 160–180 mm). Details on acquisition and participants were previously published (Evans 2006).

Cohort	Scanner	Echo sequences	TR	TE	Flip angle	Field Of View
EU	Magnetom TIM Trio (1 site)	ME-MPRAGE	2530 ms	TE1: 1.64 ms TE2: 3.5 ms TE3: 5.36 ms TE4 : 7.22 ms	7°	256
EU	Magnetom Prisma Syngo (1 site)	MPRAGE	2000 ms	2.39 ms	9°	256
SVIP	Magnetom TIM Trio (2 sites)	ME-MPRAGE	2530 ms	1.64 ms	7°	256
SVIP	Philips Achieva (2 sites)	MPRAGE	2300 ms	3 ms	9°	256
SVIP	Magnetom TIM Trio (1 site)	MPRAGE	2300 ms	2.98 ms	9°	256

Table 3. Image acquisition parameters for the 16p11.2 dataset

EU European cohort, SVIP Simons VIP cohort, ME-MPRAGE Multi-Echo Magnetization Prepared RAPid Gradient Echo, MPRAGE Magnetization Prepared RAPid Gradient Echo, TR Repetition Time, TE Echo Time.

2.2.2.3 Image processing

The longitudinal automatic image processing pipeline, developed for NIHPD analysis (Aubert-Broche et al. 2013), was adapted to the scans from the 16p11.2 dataset as described below. The preprocessing steps applied to the native T1w images were (1) denoising, (2) intensity inhomogeneity correction using the N3 algorithm (Sled et al. 1998), and (3) intensity normalization by histogram matching to the ICBM152 template (Fonov et al. 2011; Fonov et al. 2009). A hierarchical 9-parameter linear registration based on an intensity cross-correlation similarity measure was performed between the T1w images and the ICBM152 template to align the images with the stereotaxic population template (Collins et al. 1994). Subsequently, images were non-linearly registered using the Automated Nonlinear Image Matching and Anatomical Labelling (ANIMAL) algorithm (Collins et al. 1995), a hierarchical, multi-scale registration algorithm. Brain extraction was achieved using the BEaST algorithm (Eskildsen et al. 2012), a multi-resolution, nonlocal patch-based segmentation technique. To obtain optimal brain extraction, BEaST was applied iteratively three times, with each subsequent iteration including the best segmented images from the previous iteration as additional priors. Whole brain volumes were segmented, and the right and left volumes were combined for analysis. The non-linear deformation grids for each scan's registration to the ICBM152 template were inverted, effectively yielding a voxel-by-voxel nonlinear mapping from the ICBM152 template reference space to the space of each linearly registered scan. A 3D Gaussian filter with FWHM of 10 mm was applied to the resulting inverted deformation grids. The Jacobian determinant of the deformation field was computed for every voxel, log-transformed and used as a surrogate of the local volume difference between each subject and the ICBM152 template. In general, a log-transformed Jacobian determinant value less than 0 represents shrinking from the template to the native space, a value of 0 indicates that there is no volume change in the voxel and a value of more than 0 indicates enlargement with respect to the template.

2.2.2.4 Data analyses

Z-scoring for the main effect of age and gender for global and voxel-based volumes

To compute z scores that normalize for the effect of growth and sex in a pediatric population, we modeled the effect of those 2 variables in the NIHPD normative dataset. Mixed-effect models were used since it is appropriate to estimate growth in longitudinal studies that take

repeated measures from the same individuals over time. It accounts for the within-participant correlation and varying numbers of measurements for each participant.

As we previously described (Aubert-Broche et al. 2013), individual profiles suggest modeling brain growth as a quadratic function over time: we included both linear and quadratic effects of age in the fixed effects structure. Age was not divided into age bins, but it was considered as a continuous variable and was centered at 13 years old, the mean age of NIHPD cohort. The linear effect of sex was also included in the fixed terms (Aubert-Broche et al. 2013).

The proposed mixed-effects model is:

$$\text{Vol}_i = \beta_0 + \gamma_0 + (\beta_1 + \gamma_1) (\text{Age}_i - 13) + \beta_2 (\text{Age}_i - 13)^2 + \beta_3 \text{Sex}_i + \varepsilon_i$$

where

- Vol_i is the value of the response variable (global brain volume or voxel) for subject i ,
- $\text{Age}_i, \text{Age}_i^2, \text{Sex}_i$ are the fixed and random effect explanatory variables for subject i ,
- β_0, γ_0 are the intercept for the fixed and random terms,
- $\beta_1, \beta_2, \beta_3$ are the fixed effects coefficients and are identical for all subjects,
- γ_1 is a random effect coefficient,
- ε_i is the error in subject i . The errors for subject i are assumed to have mean zero and constant independent variance.

To estimate the standard deviation of the model, we extracted the variance-covariance matrix of the fixed effects along with the residual variance of the random effects. Using the mean and the estimated standard deviation of the model we were able to compute Z-scores for the global volumes of the brain as well as for each voxel independently, for the 16p11.2 participants.

Analyses of Z-scored global brain volumes and voxels in CNV carriers and controls

To identify local acquisition biases, as well as differences in scan parameters between the NIHPD and 16p11.2 cohorts (e.g., 1.5T vs. 3T scans), we first compared the Z-scores from the global volumes and the voxel-wise log-transformed Jacobian determinants of CTRL, to the controls from the NIHPD cohort. Any residual effects were corrected for in the linear model used to compare the DEL and DUP subjects with the CTRL from the 16p11.2 dataset. As we consider this control group as our reference and to have a better visualization of the effect sizes, we re-centered at 0 the predicted Z-score mean and corrected for any age related effect of the control group from all groups for the developmental trajectories.

We extracted the p-values from the linear models: results with a Bonferroni correction for 2 simultaneous comparisons are presented for the global volumes and with a False Discovery Rate FDR correction ($q < 0.05$) for the voxel-wise analysis. Regions with significant differences were anatomically labeled using the neuromorphometric atlas (<http://www.neuromorphometrics.com>).

All analyses were conducted using R 3.4.0 (The R Project for Statistical Computing; <http://www.R-project.org/>). The mixed-effect models were built using the nlme package.

2.2.3 Results

Data were analyzed for 56 DEL, 19 DUP, 105 familial and unrelated CTRL (**Table 2**). Age ranges from 4.5 to 23 years, and the range differs significantly between genetic groups: deletion carriers are younger than control individuals from the 16p11.2 dataset.

2.2.3.1 Differences between 16p11.2 controls and NIHPD controls

The NIHPD and 16p11.2 datasets are acquired at different fields of strength (respectively 1.5 and 3 Tesla). To understand the effects due to these differences in magnet and protocol, we first study and Z-score our intrafamilial controls. There is a linear effect of age on Z-scores in our control group. The intercepts and the slopes are, respectively -0.68 / -0.04 for the total brain volume; -0.11 / -0.1 for the gray matter volume (GM); 0.42 / 0.05 for the white matter volume (WM) and -0.32 / -0.02 for the lateral ventricle (LV). The exact same linear effect of age is observed in the deletion and duplication groups.

Regarding voxel-based mean Z-scores, 16p11.2 CTRL show also some deviations from the baseline of NIHPD controls, in particular in the left putamen and the medial frontal cortex (Z-scores between -0.88 and 1.09) (**Figure 5**).

After adjusting for these monotonous and linear effects due to scanning protocol, the control sample shows a normal distribution with a mean of zero at all ages (**Figures 6 and 8**). We further investigate our control group which is a combination of familial controls (34 first degree relatives who do not carry a 16p11.2 CNV) and 71 unrelated controls. The two control groups show no significant differences at the global or voxel level with an adjusted mean of 0 Z-score. For all future analyses, the same adjustment for magnet and scanning protocol controls are performed for controls and CNV carriers.

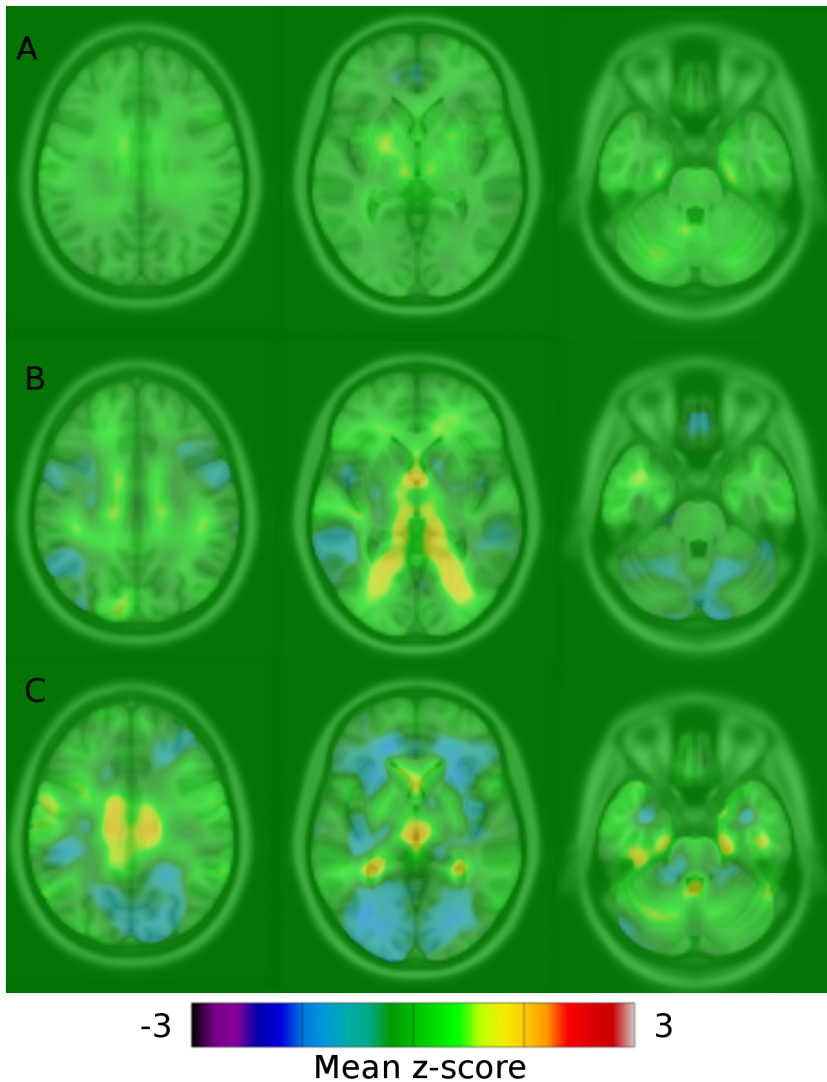


Figure 5. Mean z-scores voxel-based per genetic group

Results of the mean z-scores per genetic groups, on the Jacobian determinants voxel-by-voxel.

A. Mean z-scores for the CTRL; B. Mean z-scores for the DEL; C. Mean z-scores for the DUP.

16p11.2 CTRL show similar profile than the baseline of NIHPD controls, with only some deviations in the left putamen and the medial frontal cortex, whereas DEL and DUP show extensive clusters different from NIHPD controls.

DEL, deletion carriers; CTRL, control individuals; DUP, duplication carriers

2.2.3.2 Developmental trajectory of the global volumes of each genetic group

Deletion carriers have higher volume than controls for total brain volume (mean Z-score=1.165, p-value<0.0001), grey matter (mean Z-score=0.414, p-value=0.00433) and white matter volume (mean Z-score=0.693, p-value<0.0001) (**Figure 6**). Duplication carriers show the opposite effect, with lower total brain volume (mean Z-score=-1.17, p-value=0.0001), grey matter volume (mean Z-score=-0.631, p-value=0.00272) and white matter volume (mean Z-score=-0.53, p-value=0.0018) compared to controls. However, duplication carriers have a higher volume than CTRL for the lateral ventricle, with mean Z-score of 1.629 (p-value<0.0001).

We do not observe any age effects on the age- and sex-normalized z-score global volumes that are specific to one of the three genetic groups (**Figure 6**). As age was centered at 13 years old (mean age for the reference NIHPD cohort) for all analyses, we tested other centering, at

6, 8, 10, 16, 18 years old, and they don't reveal any interaction between genetic groups and age either.

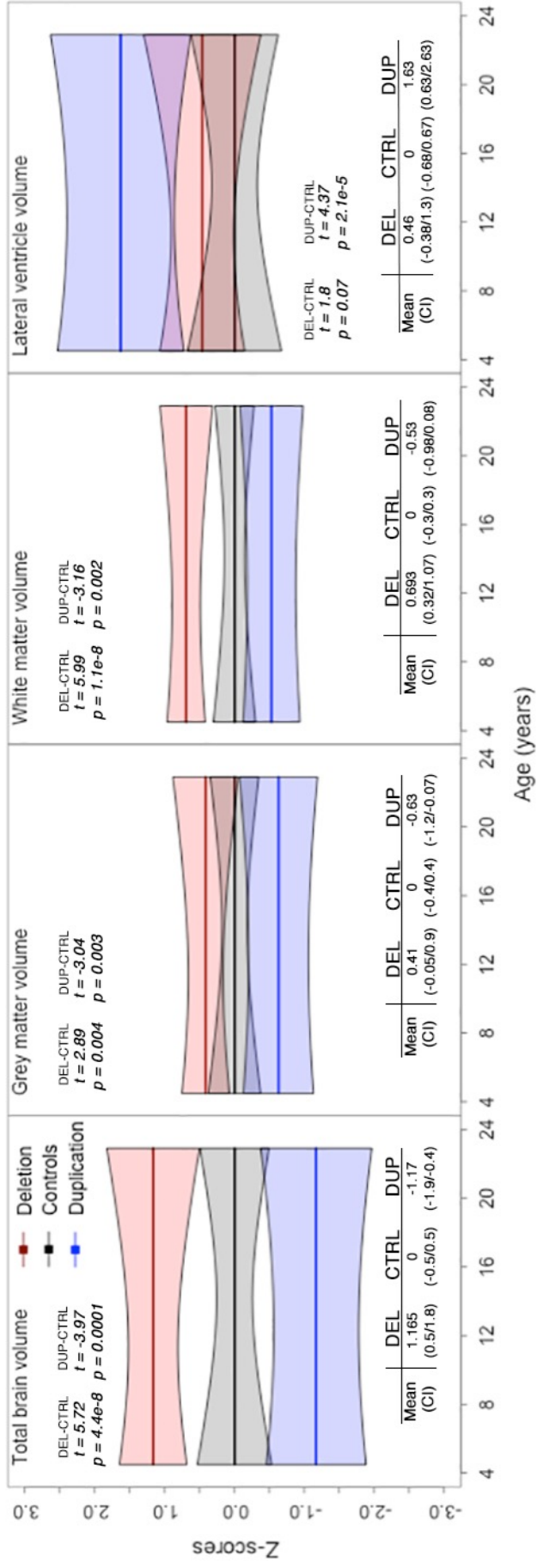


Figure 6. Developmental trajectory of global metrics

Trajectory of the global brain metrics for the 3 genetic groups show an inverse gene dosage, the differences between groups are already present at 4.5 years and identical through the development until 23 years of age.

Raw values of each metric are corrected for age and number of echo (i.e. single echo vs multi echo scans) through a linear model, then values from control individuals are centered to 0 for visualization purposes. For each genetic group, fitted lines represent the predicted mean computed per age range of 2.4 months, polygons represent the confidence interval at each age. Mean (minimum/maximum of the confidence interval) are presented in the table. P-values are corrected with Bonferroni correction for 2 simultaneous comparisons. *DEL: deletion carriers; CTRL: control individuals; DUP: duplication carriers.*

2.2.3.3 Developmental trajectory for regional alterations

The TBM analysis identifies several brain regions associated with an inverse gene dosage effect. Deletion carriers have significantly higher Jacobian determinants values than controls, and duplication have significantly lower values (i.e., DEL>CTRL>DUP) in the following regions: bilateral calcarine cortex, insula, left transverse temporal gyrus, planum temporale, and parietal operculum. Reciprocal inverse gene dosage effects are also present in the frontal and occipital white matter (**Figure 7, Table 4**).

Differences predominantly or specifically associated with the deletion include increased Jacobian determinants values in the cuneus, anterior cingulate, posterior orbital and inferior frontal gyri. Regions predominantly decreased in deletion carriers compared to controls include the bilateral cerebellum, middle cingulate gyrus, pallidum, putamen, precentral and post-central gyri, fusiform gyrus, middle and inferior temporal gyri, supplementary motor cortex, gyrus rectus, left accumbens area and angular gyrus.

The only region predominantly or specifically associated with the duplication is the occipital fusiform gyrus with a decrease in volume compared to controls as well as the lateral ventricles with an increase in volume. Additional regions with smaller significant clusters are described in **Table 4**.

We do not identify any effect of age for any of the clusters described above. **Figure 8** shows this complete lack of age-related effects for the top 8 regional differences with the largest effect sizes. Whatever the age, the DEL have Z-scores of 0.7 and 1 for the anterior insula and the calcarine cortex respectively, and the DUP have Z-scores of -0.9 and -1.2 on the same structures. DEL have Z-scores of 0.9 and 0.7 for the posterior orbital and anterior cingulate gyri respectively; they have the most negative Z-scores, -1.6 and -1.1, for the cerebellum exterior and the fusiform gyrus. DUP have also high Z-scores for the lateral ventricle and inferior temporal gyrus, 1.6 and 0.9 respectively. We observe the same lack of interaction between the genetic groups and age when, in the linear model, we center the age at different values (6, 8, 10, 16 or 18 years).

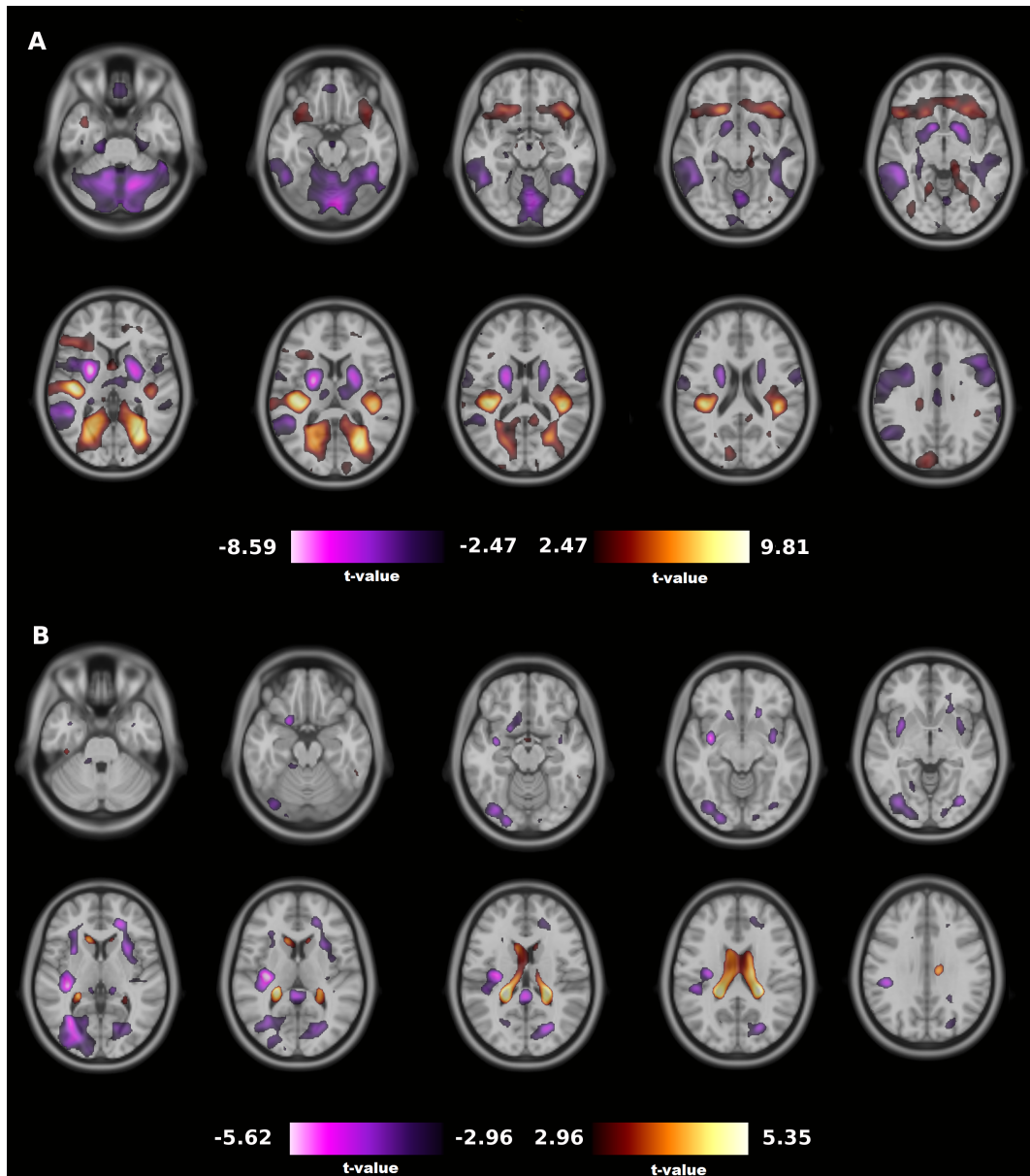


Figure 7. Effect of genetic status on brain structures for voxel-based analyses

Significant differences on Jacobian determinants highlight the inverse gene dosage effect at the regional level on volumes between DEL>CTRL>DUP, as well as some specific volume differences between DEL>CTRL, CTRL>DUP and DEL<CTRL.

A. DEL versus CTRL, B. DUP versus CTRL. Only regions with a False Discovery Rate FDR correction ($q < 0.05$) are presented. Negative t-values represent, respectively, the contrasts DEL<CTRL and DUP<CTRL, positive t-values represent the contrasts DEL>CTRL and DUP>CTRL.

DEL: deletion carriers; CTRL: control individuals; DUP: duplication carriers.

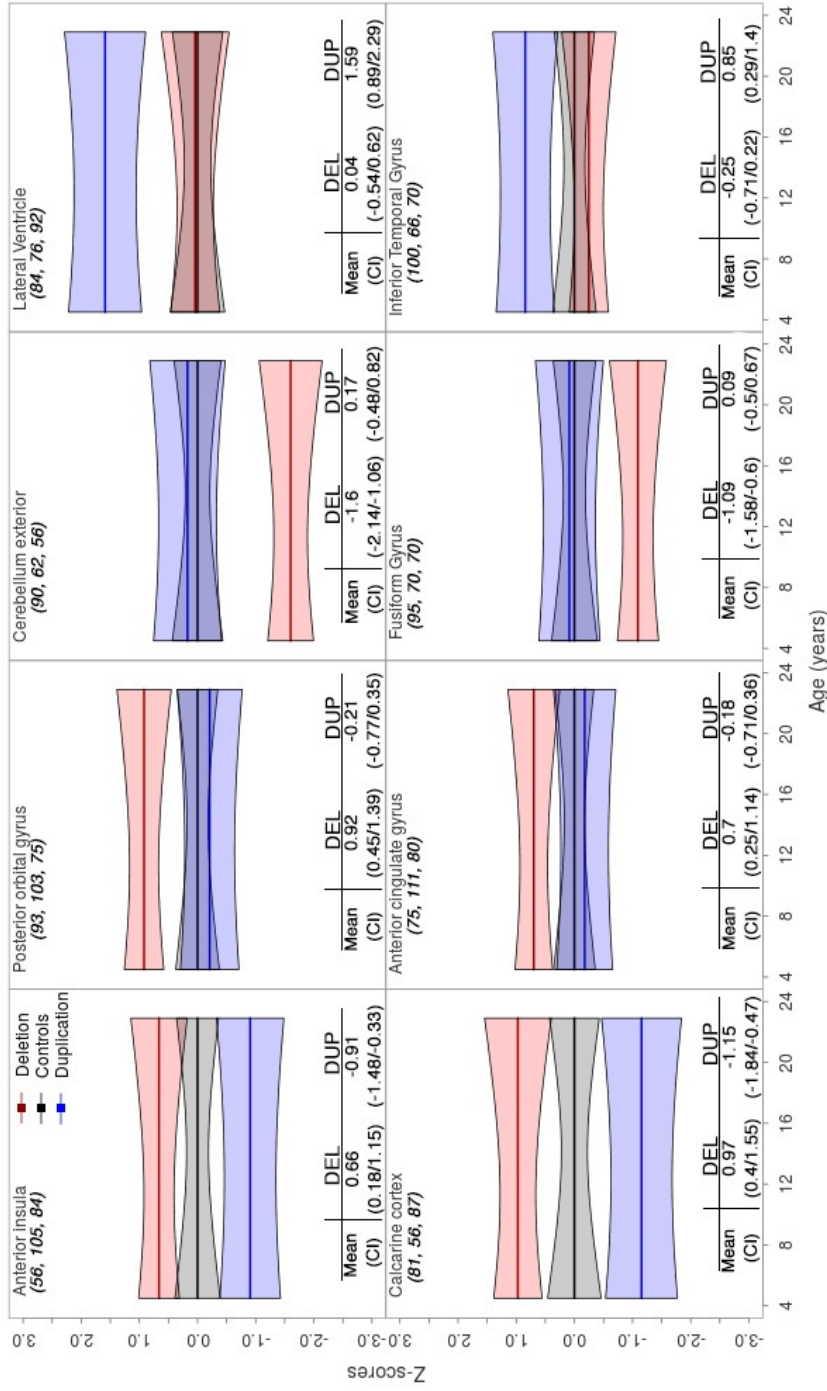


Figure 8. Developmental trajectory from typical voxel showing a difference between genetic groups

Trajectory of the jacobian determinants of 8 representative voxels from regions with significant differences between genetic groups. All of them are from the right hemisphere. Anterior insula and calcarine cortex have some voxels with significantly higher values in deletion and lower values in duplication than control individuals. Posterior orbital gyrus and anterior cingulate gyrus have significantly higher values in deletion carriers compared to controls; on the contrary cerebellum exterior and fusiform gyrus have significantly lower values in deletion carriers than controls. Lateral ventricle and inferior temporal gyrus have significantly higher values in duplication carriers than controls. All these differences are already present at 4.5 years and identical through the development until 23 years of age.

Raw values of each voxel are corrected for age and number of echo (i.e. single echo vs multi echo scans) through a linear model, then values from control individuals are centered to 0 for visualization purposes. For each genetic groups, fitted lines represent the predicted mean computed per age range of 2.4 months, polygons represent the confidence interval at each age. Mean (minimum/maximum of the confidence interval) are presented in the table. DEL: deletion carriers; DUP: duplication carriers. P-values are corrected with a false discovery rate correction, $q < 0.05$.

Table 4. Coordinates of brain regions with significant differences between genetic groups in Jacobian determinant analyses

“**Overlap**” refers to the percentage of significant voxels within each brain region. When some brain regions have more than one cluster that overlaps with them, we reported the bigger one. Only regions with a False Discovery Rate FDR correction ($q < 0.05$) and with size > 30 voxels are presented.

(1) The developmental trajectory of a typical voxel for each of these regions is shown in Figure 8.

A. Deletion > Control	Side	Size	Overlap(%)	Z	Y	X	t-score
CLUSTER 1							
Posterior orbital gyrus (1)	Right	200	62	-14	21	40	5.58
	Left	190	61	-17	23	-31	4.52
Inferior frontal gyrus orbital part	Left	73	49	-8	25	-45	4.39
	Right	64	42	-9	23	41	5.04
Frontal operculum	Left	95	41	-1	27	-43	5.35
Inferior frontal gyrus triangular part	Left	150	35	1	29	-53	4.90
Anterior cingulate gyrus (1)	Right	212	33	-4	37	5	4.44
	Left	142	21	-1	41	-10	3.57
Anterior insula (1)	Left	156	28	3	25	-33	3.88
	Right	148	27	-5	28	29	4.47
Temporal pole	Left	93	8	-26	9	-37	4.80
	Right	61	5	-22	9	39	3.72
CLUSTER 2							
Transverse temporal gyrus	Right	87	60	14	-29	43	7.77
Parietal operculum		174	59	16	-33	41	8.27
Posterior insula		87	31	15	-25	33	5.92
Planum temporale		44	23	13	-33	41	8.17
Posterior cingulate gyrus		134	22	5	-53	21	6.76
Middle occipital gyrus		133	21	6	-81	36	4.76
Calcarine cortex (1)		96	17	7	-68	25	8.75
Lingual gyrus		164	14	3	-58	25	7.94
Ventral DC		92	14	-14	-15	15	3.40
Cuneus		69	11	13	-98	11	5.04
Occipital pole		31	9	11	-103	14	2.82
Central operculum		33	7	14	-19	43	3.88
Precuneus		116	6	7	-60	25	8.16
Lateral ventricle		75	6	6	-54	29	7.58
Inferior occipital gyrus		47	6	4	-83	33	4.07
Thalamus proper		41	3	1	-35	13	4.03
CLUSTER 3							
Calcarine cortex	Left	260	45	5	-67	-25	7.44
Superior occipital gyrus		194	43	30	-88	-12	4.15
Cuneus		241	35	13	-63	-15	4.48
Lingual gyrus		183	15	3	-57	-19	7.04
Posterior cingulate gyrus		95	15	5	-51	-17	6.13
Lateral ventricle		115	9	8	-53	-28	6.25
Inferior occipital gyrus		68	9	3	-83	-33	4.36
Precuneus		140	8	7	-58	-20	6.97
Middle occipital gyrus		30	5	6	-84	-31	3.71
Thalamus proper		35	3	4	-33	-11	3.80
CLUSTER 4							
Transverse temporal gyrus	Left	130	94	7	-21	-41	9.82
Planum temporale		128	59	14	-33	-38	8.11
Parietal operculum		162	59	18	-31	-38	8.35
Posterior insula		99	35	8	-21	-35	7.74
Superior temporal gyrus		124	13	9	-27	-71	4.19

B. Deletion < Control	Side	Size	Overlap(%)	Z	Y	X	t-score
CLUSTER 1							
Pallidum	Right	190	95	4	-1	23	-7.12
	Left	182	89	5	-3	-24	-8.07
Middle cingulate gyrus	Right	543	81	42	9	1	-5.12
	Left	426	61	39	12	-3	-5.30
Putamen	Right	480	77	5	-1	23	-7.20
	Left	454	73	7	-3	-25	-8.60
Accumbens area	Left	34	77	-7	11	-11	-6.04
Cerebellum exterior (1)	Right	6247	70	-53	-61	35	-8.37
	Left	6113	69	-54	-59	-33	-6.89
Precentral gyrus	Left	924	56	61	-13	-30	-5.06
	Right	556	33	27	-1	55	-4.36
Fusiform gyrus (1)	Right	589	54	-26	-45	44	-6.34
	Left	224	20	-21	-50	-47	-4.43
Middle temporal gyrus	Left	1139	51	5	-45	-49	-6.05
	Right	243	12	-5	-29	50	-3.72
Angular gyrus	Left	801	51	47	-65	-50	-5.20
Inferior temporal gyrus	Left	715	40	-17	-51	-51	-5.41
	Right	465	25	-19	-43	47	-5.41
Supplementary motor cortex	Left	258	36	45	11	-3	-4.50
	Right	208	28	45	9	5	-4.20
Postcentral gyrus	Left	434	32	31	-7	-57	-4.03
	Right	167	12	21	-4	57	-3.70
Caudate	Right	116	31	13	10	17	-5.36
	Left	77	21	-5	13	-11	-5.52
Parahippocampal gyrus	Left	90	30	-29	-21	-23	-4.82
	Right	75	27	-30	-20	27	-3.66
Thalamus proper	Right	325	27	9	-15	9	-4.56
Hippocampus	Left	121	25	-2	-37	-27	-4.20
	Right	62	12	-7	-33	33	-3.41
Central operculum	Left	121	24	3	7	-43	-4.90
	Right	106	23	5	-1	47	-3.69
Anterior insula	Left	134	24	4	5	-41	-4.90
	Right	37	7	1	1	45	-3.65
Inferior frontal gyrus opercular part	Right	98	22	29	17	51	-4.61
Superior temporal gyrus	Left	186	20	10	-43	-51	-5.18
	Right	176	20	-5	-25	49	-3.92
Lingual gyrus	Right	237	20	-17	-90	7	-4.99
	Left	208	17	-15	-90	-3	-4.35
Precentral gyrus medial segment	Right	64	18	49	-21	3	-3.58
Brain stem		387	14	-47	-41	-11	-5.78
Temporal pole	Right	136	11	-34	15	23	-3.62
Supramarginal gyrus	Left	146	11	50	-51	-47	-3.27
Middle frontal gyrus	Right	240	8	31	20	49	-5.23
	Left	227	8	31	7	-35	-4.36
Ventral DC	Left	31	5	-9	-25	-25	-3.77
Superior frontal gyrus	Left	84	4	59	-11	-27	-4.47

CLUSTER 2							
Gyrus rectus	Left	182	55	-25	45	-5	-4.68
	Right	149	47	-25	43	1	-4.25
Medial orbital gyrus	Left	102	17	-26	43	-9	-4.36
CLUSTER 3							
Temporal pole	Left	232	19	-37	19	-25	-4.34
CLUSTER 4							
Supramarginal gyrus	Right	137	12	27	-32	70	-3.97
CLUSTER 5							
Superior parietal lobule	Left	153	10	66	-63	-13	-3.71
CLUSTER 6							
Superior parietal lobule	Right	69	5	60	-68	15	-3.22
CLUSTER 7							
Superior frontal gyrus medial segment	Right	41	4	39	49	2	-2.99

C. Duplication > Control	Side	Size	Overlap(%)	Z	Y	X	t-score
CLUSTER 1							
Lateral ventricle (1)	Left	1038	77	14	-37	-23	5.29
	Right	875	67	19	-33	23	5.36
Caudate	Right	66	18	24	-13	17	4.92
	Left	66	18	9	19	-13	3.98
Thalamus Proper	Left	100	8	17	-23	-14	4.43
	Right	70	6	19	-17	15	4.56
CLUSTER 2							
Inferior temporal gyrus (1)	Right	91	5	-24	-53	53	3.56
CLUSTER 3							
Posterior cingulate gyrus	Left	70	11	35	-35	-5	3.76
CLUSTER 4							
fusiform gyrus	Left	41	4	-29	-27	-39	3.67

D. Duplication < Control	Side	Size	Overlap(%)	Z	Y	X	t-score
CLUSTER 1							
Occipital fusiform gyrus	Left	267	60	-13	-91	-25	-4.45
	Right	46	12	-7	-78	31	-4.05
Calcarine cortex (1)	Left	260	45	5	-67	-17	-3.93
	Right	171	30	9	-73	17	-3.94
Inferior occipital gyrus	Left	300	38	2	-85	-29	-4.79
Occipital pole	Left	45	13	3	-101	-11	-3.45
Superior occipital gyrus	Right	58	12	27	-78	28	-3.66
Middle occipital gyurs	Left	62	10	5	-85	-29	-4.72
Cuneus	Right	52	8	19	-71	20	-3.73
Lingual gyrus	Right	65	5	-7	-90	15	-3.48
	Left	43	3	-2	-65	-17	-3.77
Cerebellum exterior	Left	219	2	-21	-81	-37	-3.84
CLUSTER 2							
Anterior insula (1)	Right	187	34	6	15	32	-4.4
Putamen		123	20	3	9	29	-4.34

CLUSTER 3							
Parietal operculum	Left	147	53	25	-33	-45	-4.69
Posterior insula		139	49	8	-19	-35	-5.63
Transverse temporal gyrus		67	49	9	-23	-37	-5.36
Planum temporale		49	23	23	-35	-49	-4.21
Central operculum		37	7	21	-15	-37	-4.1
CLUSTER 4							
Anterior insula	Left	96	17	3	27	-29	-4.08
Putamen		105	17	1	9	-29	-4.65
CLUSTER 5							
Thalamus Proper	Right	88	7	3	-30	15	-4.05
Posterior cingulate gyrus	Left	43	7	15	-43	0	-4.37
CLUSTER 6							
Medial orbital gyrus	Left	54	9	-19	11	-19	-4.62

2.2.4 Discussion

Our study provides a thorough investigation of the effects of the 16p11.2 deletion and duplication on neuroanatomy between the age of 4.5 and 23 years of age. This is to our knowledge, one of the first attempt of tracking changes related to large effect-size genetic variants across a broad period of brain development using a powerful normative sample. We do not observe any age-related effects on global metrics and regional volumes in deletion or duplication carriers. These results are in favor of early brain changes that remain stable across childhood, adolescence and early adulthood. 16p11.2 CNV carriers brain related-differences are already present at 4.5 years of age.

2.2.4.1 Effect size and brain alterations in DEL and DUP

DEL and DUP present similar effect sizes, with a range in absolute values from about 1 to 1.5 Z-scores, for the total brain volumes and the regional brain differences: the highest Z-scores are in the calcarine cortex and the cerebellum; and in the lateral ventricles and the insula for the duplication. These effect size values are 5 to 10 times higher than the ones observed in a recent study on about 1500 ASD individuals (van Rooij et al. 2017), and much closer to the severity of the symptoms. This highlights the important heterogeneity in ASD cohorts and the utility of the genetic-first approach to study biologically homogeneous groups.

Our results also corroborate some global and regional findings from our previous publication: insula is affected in both CNVs in a mirror way, while calcarine cortex, temporal and precentral gyri are altered in DEL. This current paper highlights the importance of the alteration of the cerebellum in the deletion carriers and the alteration of the ventricles in the duplication

carriers. We don't replicate specific alterations of the caudate and the hippocampus in DUP: in our current analyses, the anterior and medial portions of the caudate have higher values in DUP, while the posterior and lateral portions show lower values in DEL. However, the results in the duplication carriers need to be interpreted carefully: the small sample size of this group (N=19) can bias the brain regions involved and over/under-estimate some of the effect sizes for the significant regions (Carter et al. 2017). Moreover, given the large effect in the ventricle, it may cause registration errors which in turn can propagate to the brain segmentation, depending on the different computational methods used in the previous and current publications.

Familial and unrelated controls show homogeneous global and regional values, and so we merged all the control individuals. We don't find the subtle differences between the unrelated controls and the familial controls with a relative carrying the deletion, as suggested in our previous paper, which is probably associated with the very low sample sizes of these sub-groups of controls.

2.2.4.2 Continuous model of normative developmental trajectory

One of the major contributions of our paper is the use of a model to normalize the non-linear effect of age during typical brain development (Giedd et al. 1999; Aubert-Broche et al. 2013). This allows us to reliably study a sample of mutation carriers and controls spanning a broad age range. Papers analyzing developmental trajectories of brain structures have mostly used narrow age bins because the study-specific control groups were too small (less than 100 individuals) to model the effect of age reliably. Here, despite the fact that the NIHPD data have been collected with a 1.5T magnet, the model for the effect of age during typical brain development is robust and applies to data acquired on a 3T after a straightforward adjustment. It is known that images acquired at 3T and 1.5T can differ due to the presence of different artifacts as well as different inhomogeneity field characteristics (Dietrich et al. 2008). Other studies have shown that some differences in signal-to-noise and contrast-to-noise ratios can be found between 3T and 1.5T fields, and are to a certain degree dependent on the specific imaging protocol used (Fushimi et al. 2007; Stanisiz et al. 2005).

Integrating large normative datasets to correct for complex covariates such as age still requires an additional control group scanned with the same protocol as the cases. It may be possible to include in control groups, future normative dataset acquired with 3T scanners.

2.2.4.3 Comparison with developmental trajectories in neurodevelopmental disorders and genetic risk factors

Our results are in line with previous findings in ASD. Early brain differences may be already present during the first 2 years of life on high-risk children who were finally diagnosed with autism at 2 years of age, compared to low-risk children: the significant hyper-expansion in the cortical surface area between 6 and 12 months precedes the brain volume overgrowth between 12 and 24 months (Hazlett et al. 2017), across multiple brain regions. A longitudinal study did not show an increased rate of cortical growth between 2 and 4-5 years old, except an enlargement in WM temporal lobe (Hazlett et al. 2011). Similar parallel trajectories of global brain volume between 2 and 5 years of age were observed between children with fragile X syndrome and controls, even if they show some specific increase in WM temporal lobe, GM cerebellum, caudate nucleus, and smaller amygdala. Recently, the largest ASD neuroimaging study (van Rooij et al. 2017) analyzed individuals between 2 and 64 years old: the authors found differences in subcortical volumes and cortical thickness from the earliest age. Without interaction between age and ASD diagnosis for subcortical volumes, they concluded that ASD and healthy controls follow similar developmental trajectories for these volumes. However, they highlighted an interaction for the cortical thickness with a peak of differences around adolescence. The cortical thickness developmental trajectories of the carriers of a 22q11.2 deletion syndrome are also different than control trajectories for each age bin, with significantly thicker cortex in preadolescents with 22q11DS, and subsequent disappearance of the changes by the end of adolescence (Schaer et al. 2009). This underscores the need to go beyond the effect in volumes and to study other brain measurements.

Our results are in also line with brain alterations in 16p11.2 mice, that are already present at 7 days (equivalent to neonate period in humans). The increase of head circumference for DEL and the decrease for DUP is also before one year of age (D'Angelo et al. 2016). Finally, early brain differences may occur before the clinical phenotypes related to the 16p11.2 CNV.

2.2.5 Conclusion

Neurodevelopmental disorders and genetic-first approach are a unique situation to study alteration of brain growth trajectories. Thanks to a continuous model of normative developmental trajectory per voxel, we show that the 16p11.2 CNV carriers have brain alterations already present at 4.5 years old, with an effect size similar from 4.5 to 23 years old.

The brain differences found in the insula and the calcarine cortex for both CNVs, cerebellum and temporal gyri for the deletion carriers and lateral ventricles for the duplication carriers, replicate the brain differences already known in adults carrying a 16p11.2 CNV. The computational method developed in this paper needs to be applied to normative datasets at younger and older age, to understand when the brain alterations appear during development and whether this CNV has a differential impact on brain structures later in age. Finally, a larger dataset would allow studying how the ultimate cognitive level of the 16p11.2 carriers is associated with the age of onset of the alterations.

3. DISCUSSION OF THE THESIS

3.1 Global and regional differences on the 16p11.2 reciprocal CNVs

The first study replicates the gene dosage effects of the 16p11.2 CNVs on total brain metrics as well as the regional effects for volumetric, surface area and cortical thickness parameters. Beyond the replication, the sample size of this new study allows to decipher the reciprocal and non-reciprocal anatomical effects of the deletion and duplication. We demonstrate a robust reciprocal alteration for the volume and surface of the insula (deletion>control>duplication, Cohen's $d > 1$) and non-reciprocal alterations in the calcarine cortex and transverse temporal gyrus (Cohen's d for deletion > 1), superior and middle temporal gyri (Cohen's d for deletion < -1), caudate and hippocampus (Cohen's d for duplication between -0.5 and -1). These alterations are stable in adults, adolescents and old children, males and females. We do not observe any correlation between these brain regions and measures of general cognition, language scores, or social behavior. However, we find partial overlap with regions altered in a psychiatric cross-disorder meta-analysis. We also highlight some brain differences comparing familial and unrelated controls: controls from deletion families show changes in volume and cortical thickness of the left posterior insula and right lingual gyrus, compared to unrelated controls. We hypothesize that additional factors, potentially visible first degree relative, are required for CNV carriers to develop significant psychiatric symptoms.

3.1.1 Regional volumetric and surface differences beyond the effect of the global brain metrics

The two previous papers analyzing the brain structures of the 16p11.2 carriers differed in their analyses and interpretations. Qureshi et al. (2014) found differences between deletion and duplication carriers, compared to controls, on global brain measurements. At the regional level, only differences in the thalamus survived correction for intracranial volume. The authors concluded on a pervasive effect of the 16p11.2 CNVs on the brain without clear regional brain differences. In particular, the latter could not be interpreted due to the general effects of brain volume and the surface area. Maillard et al. (2014) showed the same differences for global metrics, as well as voxel-wise differences between the deletion and the duplication in the reward system, language, and social cognition circuitry.

The first study was run in parallel in 2 labs pooling all available data and reconciles findings from the two previous papers. It demonstrates that regional differences are associated with deletions and duplications, regardless of the TIV. Moreover, we share some conclusions with Qureshi et al. (2014) as the surface area is mainly impacted in the results, and not the cortical thickness, which is in favor of some early and pervasive effects.

We show consistent results across both cohorts which were ascertained through different methods. Individuals in Europe were directly referred by geneticist, whereas participants were more broadly recruited in the USA, including referral by clinical genetic centers, social media requiring online registration on the part of the families. D'Angelo et al. (2016) showed that the IQ was higher in the American compared to the European cohorts across carriers and controls, and we have the same trend on IQ for the sub-sample that has passed the MRI. The head circumference of CNV carriers and the age range was also different between cohorts. All these differences have challenged the replication of the results.

Replication is one of the major issues in neuroscience. Carter et al. (2017) point out the issue of false-positive results: "only 21% of studies met a previously specified minimum criterion (for an imaging study) of 20 subjects per cell, .90% had flaws in the clinical/genetic design, correction for multiple comparisons was rare, and few true replications were reported (Gurung & Prata 2015)". A reasonable sample size is between 50 and 100 in numbers, to detect effect sizes of 0.5 or greater (as the effect size observed in our dataset). This is exactly what we reach with about 70 carriers in each CNV group and more than 200 control individuals (Carter et al. 2017). Underpowered studies are associated not only with low reproducibility but also with over-estimation of the effect sizes (Button et al. 2013). Moreover, the differences in scanners and acquisition protocols could lead to site-to-site differences in resolution, quality, and temporal signal-to-noise ratio (Adhikari 2017). Our powerful sample size, using T1 MPAGE images (one of the most standardized images in the World), also allows overcoming the effect of the scanners. Of note, it's essential to continue to support the harmonization of scanners and acquisition protocols, as well as shared optimized pipelines, through different types of MRI images.

We also take advantage of several major software programs to analyze the data and combine the results of their main outcomes. Even if a critical debate exists between the use of these various software programs, for example about the linear and non-linear registration process used by the software programs, we still arrive at the same main statistical differences between

the genetic groups. In a large cohort worldwide, Stein et al. (2012) also find consistent results using two widely-used software programs, analyzing human hippocampal and intracranial volumes: they conclude that no single algorithm performs better for measuring these volumes.

Finally, it's important to use different metrics to understand the different process. Cortical GM volume is decomposed into its orthogonal components: surface area and cortical thickness. We show that most of the volumetric differences between the genetic groups overlap with the surface area differences. The cortical thickness differences are lighter. In a biological point of view, cortical thickness and surface area represent different features of the cortical architecture (Ecker et al. 2015). They are believed to arise from different types of progenitor cells. Cortical surface area is associated with the production of radial unit progenitor cells and reflects the number of cortical columns (Pontious et al. 2008; Rakic 1988; Rakic & Lombroso 1998): increase in the division of progenitor cells in the embryological periventricular area is associated with an increased cortical surface area. It seems to be associated with very early brain development. Cortical thickness is related to intermediate progenitor cells (Pontious et al. 2008): it depends on the neuronal output from each radial unit (Rakic 1995) and represents the number of neurons in the column (Rakic 1988; Rakic & Lombroso 1998). It reflects the variations in the dendritic development in GM or myelination at the interface of GM and WM (Huttenlocher 1990; Huttenlocher & de Courten 1987; Sowell et al. 2004). Regional cortical thickness varies during childhood and provides important information on cortical maturation. As the cortical surface is more affected in 16p11.2 CNV carriers than cortical thickness, this is a sign of an early alteration in brain development.

3.1.2 Relationship between the 16p11.2 pattern of brain structures differences and the behavior

Regions impacted by the CNVs are known to affect different cognitive domains. We submitted the results to the Neurosynth platform, to decode the psychological terms most closely associated with the main structural clusters of the findings on the 16p11.2 dataset. As expected, we show that temporal gyri are associated with language, phonology, and auditory terms. These regions are the ones mainly altered in the deletion carriers, and the results are in coherence with the language impairment observed in these patients. In their paper, Blackmon et al. (2017) demonstrate, with a different methodology, that the focal cortical

anomalies in the left temporal and frontal areas (Broca's area) are associated with lower performance on comprehensive language on 16p11.2 deletion carriers. Regarding the top associations of the anterior insula and caudate in the Neurosynth platform, they are associated with terms such as reward, pain and executive function. Reward system and executive functions are two critical domains in psychopathology, in particular in ASD.

Maillard et al. (2014) already reported, qualitatively, the overlap between the structures altered in the 16p11.2 CNV patients, with areas known to be affected in ASD and SCZ. In our paper, we can quantify this overlap with a Dice index, using a large cross-disorder neuroimaging meta-analysis (<http://anima.fz-juelich.de> (Goodkind et al. 2015)). We observe a partial overlap: 33% of overlap in mean for the right and left insula. Insula is an important and « underestimated » brain area in psychopathology (Namkung et al. 2017). At the intersection of three lobes, it has a main role in interoception, in the integration and the homeostasis of the body states. It has a role in the subjective feelings (a basis for the « self ») and in the motivation, to encode incentive values of a stimulus. The dysfunction of the dynamic interactions between feelings, motivation, and cognition is crucial in a lot of psychiatric disorders. This region appears to be categorized as “high cost / high values” hubs in human brain networks and more likely affected in many neurological and psychiatric disorders (Crossley et al. 2014).

In our analyses, the cognitive and behavioral scores (on global cognition, social behavior, and language) do not correlate with the 16p11.2 brain patterns. The limited power may lead to this lack of correlation between the brain measurements and the cognitive data. Other metrics than the typical structural MRI metrics, may be more associated with the phenotype, as diffusion metrics (Alexander et al. 2007; Travers et al. 2012). Looking at a simple correlation and between-group differences in average can also lead to some missing results, and probably other statistical methods and measurements should be explored (Brugger & Howes 2017b). However, in coherence with our results, the intermediate phenotypes are assumed to be closer to the gene effects than the clinical symptoms and psychiatric disorders, that may be influenced by a lot of factors (Hashimoto et al. 2015).

Of note, in the European cohort, few patients carrying the CNV are diagnosed with ASD. But even if they don't have a formal diagnosis, they have differences in scores on some social traits, compared to controls. The CNV is a model to study brain structures, that could overlap with sub-groups of ASD-like patients. We also observe an important co-morbidity in the

diagnoses for the patients. Even if we focus our discussion on the literature on ASD, the 16p11.2 CNV is not only a model for ASD, but more generally for some categories of symptoms that can overlap between different disorders.

3.1.3 Additional factors to the rare CNVs in psychiatric disorders

We also hypothesize an additive model underlying psychiatric disorders (Weiner et al. 2017): CNVs contribute to the psychiatric condition, but additional brain alterations and other factors are required for the onset of the disorder. Combination of common and rare variants also act additively to lead to a diagnosis as ASD or other conditions as bipolar disorders (Weiner et al. 2017; Mellerup et al. 2017). That highlights the importance of familial background when accounting for phenotype variability. It's what we point out when we compare the familial and unrelated controls, and we show that, even at the neuroimaging level, we can see some brain differences between the two types of controls, reinforcing the idea of a familial loading. The discovery of some of these additional risk factors would be decisive for an accurate projection of the various outcomes associated with these pathogenic CNVs. In one of our studies (D'Angelo et al. 2016), we show an enrichment in additional deleterious genetic variants in duplication carriers, some of which are inherited. The duplication carriers can be subdivided into different levels of global cognition, with a specific "low-functioning" group also enriched in ASD diagnosis. This group may be associated with some specific additional deleterious variants. Green Snyder et al. (2016) argue that the phenotypic variability in 16p11.2 duplication carriers could depend on "double hits" with large effect, heritable common variants with small effect, and non-genetic factors.

In a study in progress, we explore the differences between the 16p11.2 carriers who develop ASD and the ones who don't (Maillard et al., May 2017). We identify distinct clinical and neuroanatomical profiles in deletion and duplication carriers that reach the threshold for clinical evaluation. For example, deletion carriers meeting criteria for ASD present larger head size and higher nonverbal skills than carriers without ASD: these effects are already present in their parents (not diagnosed with ASD). In contrast, the duplication carriers with ASD show an additional decrease in IQ compared to the duplication carriers without ASD. Of note, it's not because a proband doesn't reach the arbitrary threshold for a categorical diagnostic that he's not affected (Moreno-De-Luca et al. 2015). Another approach to characterizing additive effects is to compare individuals carrying the CNV and ascertained for a neurodevelopmental

disorder to the ones identified in the general population (Männik et al. 2015; Stefansson et al. 2014).

Finally, our results are a proof that the haplo-insufficiency and over-expression of the same reciprocal CNV may have a different impact on the phenotype observed, and so on the neural mechanisms. The deletion is known to be more deleterious than the duplication. However, we have to take into account that to be included in the study, the participants have to be able to pass a MRI, without too many movements, and this limitation may exclude the “low-functioning” group of duplication carriers.

3.1.4 The broad age range of the dataset on rare CNVs

Another crucial aspect of the paper is the broad age range of the dataset, from 6 to 63 years old. As we work on rare patients, with less than 1 for 2000 per CNV, we have to aggregate data from spread age to have sufficient sample size. Qureshi et al. (2014) tackle this issue by selected only deletion children compared to age-matched controls (most of the deletion carriers are children), and only duplication adults compared to age-matched controls (most of the duplication carriers are adults). We choose another strategy by using the whole dataset and including the linear and quadratic expansion of age as a covariate in the model (the cubic expansion do not show any significant effects and so is not included in the design matrix). We also perform a division of the dataset in 3 age groups (children, adolescents, adults) to consider if the brain differences are already present in children. However, to go further in the analyses and to know the real developmental trajectories of the brain structures, we tackle this issue in the next section, with the second paper.

3.2 Normative data and developmental trajectory of brain structures across the development of the 16p11.2 carriers

Carriers of the 16p11.2 CNV present structural brain differences when compared to control individuals. However, it remains unknown when during development these brain alterations appear. The 2nd objective of my Ph.D. is to characterize the developmental emergence of the structural alterations and to reveal how these genetic risk factors become expressed over time. Z-scores and typical growth curves are computed from a normative dataset of the NIH MRI study of normal brain development (<https://pediatricmri.nih.gov/nihpd/info/index.html>) (Evans 2006): it consists of 339 typically developing children from 4.5 to 23 years old. We find

that the global and regional brain alterations are present at 4.5 years, and the curves for the deletion and duplication brain structures are parallel to the ones of the controls until 23 years. To our knowledge, this is the first time this methodology is used in the field of NDDs. This kind of proof of concept, to adapt this methodology to our dataset, is a first step toward the acquisition and the analysis of a broader age range of normative dataset and a 16p11.2 dataset on younger children.

3.2.1 Effect size in neuro-imaging genetic

Few studies in neuro-imaging directly report the effect sizes. In our results, we find similar effect sizes than the ones we previously published on cognition (D'Angelo et al. 2016), between 1 and 1.5 Z-scores in absolute value. We observe that the effect sizes in the 16p11.2 brain patterns are 5 to 10 times larger than the ones observed in a paper on ASD with a huge sample size (1571 patients diagnosed with ASD and 1651 healthy control subjects) (van Rooij et al. 2017). This Enigma paper highlights some effect sizes between 0.1 and 0.2, which seems low in comparison to the strong alterations in ASD. Enigma consortium analyzes the volume and the cortical thickness per regions of interest, while we analyze the data per voxel: this can be part of the variability between the studies. In our results, they are often only parts of the brain structures that are altered. It's possible that an approach per region of interest underestimates the effect size of the results, or the voxel analyses could also over-estimate the results. However, the differences could be due to the heterogeneity in an ASD cohort: there may be only a small common denominator between individuals with ASD, reflected by low effect sizes; whereas the large effect sizes for a CNV directly reflect the large impact of the genetic variant. The same phenomenon is observed in other psychiatric conditions, such as SCZ: the effect sizes on the volumes of subcortical structures are below 0.5, in absolute value, and most of them are around 0.3 (van Erp et al. 2015). The heterogeneity of the patients diagnosed with SCZ could cancel part or the totality of some effects. On the other side, large effect sizes are observed in a risk factor as the 22q11.2 deletion syndrome carriers (Lin et al. 2017), between -1 and -2 Z-scores for the most important findings. Mechanistically homogenous groups are closer to the effect of the diseases, with Z-scores closer to the ones observed on cognition. Interestingly, the effect sizes are more important in the 22q11.2 deletion than the duplication (between 0.5 and 1 Z-scores for the most significant). This is

coherent with the idea that the duplication CNVs have less deleterious effects than the deletion (Männik et al. 2015).

3.2.2 Normalization

Most of the studies are not able to have large-enough control groups. A real norm and some proper comparisons between healthy individuals and patients cannot be done. This lack of control individuals also contributes to diminishing the power of these studies. We overcome this issue thanks to the NIH MRI normative dataset.

A limitation of our work is the difference between the strength of the magnetic field used in the normative dataset (1.5 Teslas) and the 16p11.2 dataset (3 Teslas). It's known that artifacts can happen in the 3 Teslas acquisition (Dietrich et al. 2008). This effect can be confused with the real effect of age on the data. Hopefully, we manage to add a correction to our linear model to have similar curves for the NIH MRI controls, from the ones for the 16p11.2 controls. Thus the NIH MRI controls are a reliable norm to model our comparison between the genetic groups. For sure, other normative data with 3T and the comparison of normative data between 1.5 and 3 teslas would be beneficial to confirm the results.

Moreover, the model to obtain the norms has been tuned for this particular data and age range. NIH MRI study already acquired in their objective 2, neuroimaging and clinical data on newborns to preschooler's children, from 3 months for the youngest participants to 4.5 years old. The preprocessing pipeline of the data has to be adapted to the specific GM and WM maturation at these crucial early ages, and the trajectory of the data needs to be modeled according to the specific growth curves at this age range. The information on the younger age is still limited in NDDs, in particular in the CNV carriers. The same question can be asked for the adult ranges: what happens to individuals with autism as they age?

The Enigma consortium just initiates a Lifespan working group, to compile charts of regional brain volumes, through life from 3 to 90 years old (Bearden & Thompson 2017). Once again, this type of dataset will be beneficial to draw reference growth curves per regional structures, with the standard variation in the healthy population, to ultimately compare them to patients and better understand the evolution of the brain diseases.

3.2.3 Developmental trajectories in neuro-imaging of psychiatric disorders

In research on ASD, the developmental studies target children at high risk for ASD (i.e., having a sibling with a diagnosis of ASD): they show that at-risk children could be distinguished from

low-risk controls before overt behavioral symptoms appear (Elsabbagh & Johnson 2016). Changes in brain volume and cortical surface may become significant in the second year of life (Courchesne et al. 2011; Ecker et al. 2015; Hazlett et al. 2011; Schumann et al. 2010), with an increase in total brain volume and surface area during development, not observed anymore in adolescents and adults (Hazlett et al. 2011; Schumann et al. 2010). A recent mega-analysis, including participants from 2 to 64 years old, shows, in mean, smaller subcortical volumes in the cognitive and affective parts of the striatum and the amygdala, reduced thickness in the temporal cortex, increased thickness in the frontal cortex, compared to controls (van Rooij et al. 2017): the subcortical volumes don't show any age by diagnosis interaction, but the development of the cortical thickness would differ according to the age of the patients, showing a peak around adolescence (greater thickness in the ASD group in the frontal cortex, and lesser thickness in the temporal areas).

However, given the heterogeneity of the development of this disorder, it's important again to study developmental changes in a mechanistically homogeneous group, as in a 16p11.2 cohort, with clear knowledge of the adolescent/adult clinical and neuroanatomical outcomes (unlikely to ASD patients). Right now, only one paper exists on the developmental trajectories of behavioral phenotypes in young children carrying a 16p11.2 CNV. Some papers exist on the brain developmental trajectories in the 22q11.2 deletion syndrome: the carriers of this CNV would have distinct patterns of cortical thickness alterations, especially around adolescence (Schaer et al. 2009).

Age effects appear to be nonlinear across a wide age range, which may limit the ability to detect interactions across the lifespan. Daan van Rooij et al. (2017) use a fractional polynomial approach to face this issue. Each paper develops its own model or its metrics to characterize the developmental trajectories. On the contrary, our study is based on a modeling with a normative dataset, and could be easily transferred to another genetic risk factor for NDDs or any types of disorders. Tensor-Based Morphometry is a great measure to go over the global metric issue, without GM-WM classification issue, but other measurements should be interested in looking at, as the trajectory of cortical thickness and surface area. In the first study of my thesis, we show some potential interaction between older age and cortical thickness. We model the mean cortical thickness to evaluate the group differences in developmental trajectories. When the age variable is centered one standard deviation above the mean age (39 years), the duplication group shows a significantly thinner cerebral cortex

than the control participants. No differences are found for the deletion group. In brief, it would be good to develop our method on other metrics, tackling differential developmental process.

Finally, we still lack information about individual trajectories, and prediction of some potential different outcomes for the carriers of a 16p11.2 CNV, to better adapt the prevention strategies. In the analyses, we never take into account the form of treatment followed by the participants, as the medication, the behavioral and physical therapies, the particular school-based supports, etc (Bernier et al. 2017).

3.3 The study of intermediate phenotypes in 16p11.2 cohorts

Further steps including some multi-modal approaches, network analyses and some other intermediate phenotypes, may improve our understanding of the 16p11.2-associated differences.

3.3.1 Tissue properties underlying the 16p11.2 associated-volumetric alterations

The study of the histological tissue properties, through a multi-modal approach, could help to understand the pathological processes underlying the GM volume changes (Draganski et al. 2011; Lutti et al. 2014; Weiskopf 2013). Multi-Parameter Mapping –MPM sequences provide a set of quantitative measures to highlight intrinsic characteristics of brain tissue indicative of myelin, iron and tissue water content. The 4 maps are so called proton density map, associated with water content; magnetization transfer map and R1 map, which correlate with myelin content; and R2* map sensitive to iron concentration. I already acquired data on 18 deletion carriers, 31 control individuals and 8 duplication carriers with MPM data. First validation has been done for an increase of the standard isotropic voxel dimension of the usual MPM, from 1 mm³ to 1.5 mm³, to reduce time acquisition. Then, our preliminary analyses on the genetic groups focused on the comparison between deletion carriers and control individuals. Different types of tissue alterations could explain the volumetric differences: anterior insula in the deletion carriers seems to be altered on the proton density maps, calcarine cortex on the R1 maps and some frontal parts and postcentral gyrus on the R2* maps. Additional MPM data and analyses are necessary to replicate and interpret these results.

3.3.2 White matter microstructure and brain connectivity

Heritability of diffusion-weighted measurements are important (Jahanshad et al. 2013). Owen et al. (2014) reported widespread alterations of WM microstructures in children carriers of the deletion. In some current analyses, Moreau et al. (June 2017) emphasize these first results by analyzing subcortical diffusivity in 16p11.2 CNV carriers. Despite the reciprocal effect of the deletion and the duplication on the overall brain volume, both variants seem to be associated with increased mean diffusivity compared to controls, on all subcortical structures examined, except the putamen. More precisely, the caudate, amygdala, thalamus have increased mean diffusivity in the deletion and duplication carriers; the mean diffusivity in nucleus accumbens only increases in deletion carriers; in hippocampus and globus pallidus, it only increases in duplication carriers. These alterations are supported by the results of behavioral analyses, which show differential relationships between mean diffusivity and social responsiveness, as well as FSIQ, in several subcortical structures. Interestingly, caudate and hippocampus are also the regions we highlight in our first study with specifically lower volumes in duplication carriers compared to controls. The opposite direction for diffusion measurement (increase) in sub-cortical structures and brain volume and surface (decrease) worth studying more precisely.

Some other analyses are focusing on measures of the gray-white intensity contrast (Lewis et al., June 2017), a ratio of the intensity of the T1 sampled 1mm inside and 1mm outside the white surface. In the deletion carriers, the contrast is reduced in broad regions of the bilateral insula, temporal lobe and part of the inferior frontal cortex (Broca's area and right hemisphere homolog). In duplication carriers, the contrast is increased in the bilateral central sulcus, medial visual areas and the left primary auditory cortex: this pattern is aligned to localize abnormalities in regions associated with low-level sensory processing. These additional findings related to WM corroborate our results on reciprocal and non-reciprocal effects on volumes in the deletion and the duplication. They could be integrated with our cortical thickness analyses.

Finally, recent results on resting-state functional MRI are showing striato-striatal and striato-cortical over-connectivity in the deletion carriers compared to the individual controls and the duplication carriers (Moreau et al., October 2017). The highest proportion of altered connectivity are among the caudate, putamen and lateral occipito-temporal gyrus. The duplication carriers do not show specific differences in functional connectivity compared to

the control groups, probably due to the low sample size. These results are consistent with previous reports of aberrant functional connectivity in ASD. Given the role of the cortico-striato-thalamo-cortical circuitry in sensory-motor processes and learning, these mechanisms are interesting targets for future analyses in our 16p11.2 dataset. The 16p11.2 functional network could be part of an “autism cluster”, contributing to parse the heterogeneity of ASD. It would also be interesting to examine whether and how structural variations are related to functional variations during some well-known experimental tasks, as the monetary incentive delay task that tackles the reward system or other social tasks already used in the field of ASD. Further investigations of biochemical markers of the integrity of GM and WM, as the magnetic resonance spectroscopy, may help to identify some chemical substrate of aberrant connectivity (Anagnostou & Taylor 2011).

3.3.3 Study of microbiota in the 16p11.2 CNV carriers

The mechanisms underlying the variability of the 16p11.2 cognitive and behavioral phenotypes could also implicate peripheral mechanisms including alterations of the gut microbiota. Amounting evidence suggests a microbiota-gut-brain axis, with bidirectional communication between the central nervous system and the intestinal organs (Foster et al. 2016). That has led researchers to hypothesize that gut microbiota could modulate brain function via immune, neural, and metabolic mechanisms (Stilling et al. 2013).

Obesity is among the most common comorbidity of neurodevelopmental and psychiatric disorders (Chen et al. 2010), and it's especially true for the 16p11.2 CNVs. Obesity is also associated with 'low gene count' reflecting low bacterial richness (Le Chatelier et al. 2013) and only a few bacterial species are needed to differentiate obese from lean people. Contrastingly, energy restriction can increase gut microbiota richness (Cotillard et al. 2013). Genetic factors are important determinants of the microbiota profile in individuals (Stilling et al. 2013). The gut microbiota profile may mediate some of the associations underlying the complex relationship between genes, cognition, and BMI. Dysbiosis of the gastrointestinal tract has been associated with cognitive deficits, in conditions such as neurodegenerative disorders (Scheperjans et al. 2015) and psychiatric diseases (Jiang et al. 2015; Son et al. 2015). Animal models studies corroborate and extend these human findings (Clarke et al. 2012; Neufeld et al. 2011; Bercik et al. 2011). Gene dosage at the 16p11.2 locus may modulate the gut microbiota, which could have an impact on the severity and the nature of the observed

phenotype. In 16p11.2 deletion carriers, 75% of adults develop obesity and among adult obese patients, 45% are morbidly obese (Zufferey et al. 2012). The investigation of the gut microbiota in these CNVs could give considerable insight into changes due to the dysregulation of satiety and could allow identifying gut microbiota changes in individuals at high risk but who do not present an increase in BMI yet.

A study in progress aims at determining the dysregulation of the microbiome in the carriers of the 16p11.2 CNVs, using 16S high-throughput sequencing of stool samples. Specific bacteria seem to be increased in these individuals, especially a few species within the bacterial genus *Lactobacillus*, previously implicated in social behavior. Some of the same species are also dysregulated in the 16p11.2 mouse models: this highlights the role of genetics in establishing the microbiome. It would be interesting to go even further in the analyses of the gut microbiota diversity, to characterize gene presence and abundance. Comparing CNV carriers with an obese reference group could also help to understand the gut microbiota differences related to the host's genetic variation, independent of obesity. If proven correct, modifying the gut microbiota composition could provide new therapeutic leads, such as specific diet, probiotic medication or gut microbiota transplantation for 16p11.2 CNV carriers. Indeed, previous animal studies have shown that improvement in behavior may be achieved by changing gut microbiota composition (Savignac et al. 2015; Hsiao et al. 2013; Bercik et al. 2011), but these observations still need to be replicated in human studies.

3.4 Neuroanatomy and CNVs in psychiatric disorders

3.4.1. Neuroanatomy across CNVs associated with neurodevelopmental disorders

We observe recurrent overlapping brain regions across different genetic risks factors associated with SCZ and ASD. A recent work on the distal interval of the 16p11.2 locus, containing the *SH2B1* gene, find a negative gene dosage effect on intracranial volume and sub-cortical structures (pallidum, accumbens, and caudate, putamen), independently of the neurodevelopmental conditions and ancestry, with effect size around -1 (Sønderby et al., October 2017). As the proximal 16p11.2 CNVs, the distal 16p11.2 CNVs would have some common neuropathological patterns underlying the various clinical symptoms. They would play a role in the development of the basal ganglia structures, essential for core phenotypes of major NDDs. Both distal and proximal 16p11.2 CNVs also are associated with the BMI,

highlighting the role of these brain structures in the predisposition to obesity (Bochukova et al. 2009; Willer et al. 2009).

The 22q11.2 deletion syndrome (22q11.2 DS) is another strong risk factor for SCZ. Most of the protein-coding genes within this deletion are highly expressed in the brain (Guna et al. 2015). Some prior studies report widespread structural cortical changes (Jalbrzikowski et al. 2013; Eisenberg et al. 2010): a reduced cortical volume and surface area in occipito-parietal cortex (Bearden et al. 2006; Gothelf et al. 2007; Kates et al. 2001), temporal cortex (Chow et al. 2011; van Amelsvoort et al. 2004) and anterior cingulate cortex (Dufour et al. 2008; Shashi et al. 2010). Right precentral and middle frontal cortices would also be affected. Debbané et al. (Debbané et al. 2006) observe a significantly reduced volume in the hippocampus, driven by a decrease of the body of the hippocampus. On the contrary, an increased volume is observed in bilateral insula and some frontal regions, driven by increased cortical thickness (Campbell 2006; Simon et al. 2005). Significant age by genetic group interaction is found for cortical thickness in occipital and parietal regions: the typical pattern of decreased thickness with age observed in controls (Tamnes et al. 2009) is not observed in 22q11 DS participants. The cortical maturation of adolescents with 22q11.2 DS would be disrupted, in particular in regions as fusiform gyrus and precuneus. These regions are known to be important for socially relevant processes (Cavanna & Trimble 2006; Schultz et al. 2003). Some of these alterations would be related to the psychotic symptoms (Kates et al. 2011; Dufour et al. 2008).

The 7q11.23 deletion (Williams syndrome), another genetic risk factor associated with NDDs, is associated with reduced total brain volume as well as regional differences compared to controls. Some gyrification abnormalities in the orbital frontal cortex would be linked to their social profile and the same abnormalities in superior parietal regions would be associated to their visuospatial deficits (Eisenberg et al. 2010). Sylvian fissures (located at the insula level) and basal ganglia seem also affected, with variance depending on the size of the deletion. The alterations are consistent in both adults and children cohorts (Fan et al. 2017).

Some of these brain regions affected in the 22q11.2 and/or the 7q11.23 deletions, as the insula, the temporal gyrus, the cingulate cortex and some occipital regions, are similar to the ones altered in the 16p11.2 CNVs carriers. A formal and quantitative comparison between CNVs associated with NDDs is required to understand the common and distinct neural mechanisms between several genetic risk factors, to characterize the probability of overlap between neuroanatomical alterations and to compare the effect size of the global and

regional alterations depending on the size of the mutation.

3.4.2. Neuroimaging analysis of psychiatric diagnoses

A long-term perspective is to perform a multivariate pattern classification of ASD and SCZ neuroanatomical differences and to compare these patterns to the ones related to different genetic loci (common and specific patterns). This would contribute to identify ASD or SCZ subgroups that share alterations in the same pathways than the genetic loci. Advances in statistical methods and modeling will help to understand the complex genetic architecture of these diseases.

On the animal model, Ellegood and al. (2014) adopted an ingenious approach by conducting a genetic-first approach with several genetic risks factors: they implemented structural neuroimaging in 26 mouse models for genes associated with ASD and intellectual disability. Results demonstrate that the 26 genetic models are associated with 3 patterns of neuroanatomical alterations, suggesting that different ASD genetic risk factors may converge on shared brain structures and networks involved in ASD. These results are in favor to implement the same type of design in human studies and to compare the results to mouse models. Although mice and humans are separated by 80 million years of evolution and show divergence in the structure and function of the brain, the general organization of the brain is conserved across mammals. Genes differentially expressed in one brain region in humans are highly likely to be differentially expressed in mice. Some cognitive impairments in mice may be relevant to some aspects of cognitive phenotypes in human (Yang et al. 2015). However, neuroanatomical measurements are more analogous between model organisms and humans (Malhotra & Sebat 2012), and some neuroanatomical alterations seem well conserved across humans and mice with the same genetic variant (Horev et al. 2011; Portmann et al. 2014). On the other hand, neuroimaging alterations showing no concordance across species and different genetic risk factors may also have implications for translational and preclinical studies. Another step is to study the developmental aspect of the abnormalities, to understand at what stages of development multiple-gene effects or genetic interactions occur (Eisenberg et al. 2010).

3.4.3 Relationship between genes within CNVs and brain alterations

The pathways from genes to neural circuits to phenotypes remain elusive. In their paper on neuro-imaging 16p11.2 patterns, Maillard et al. (2014) did some complementary analyses on

peripheral measures of gene expression levels. mRNA levels of most of the genes within the 16p11.2 interval show a negative correlation with global metrics of brain volume. However, only a few papers tried to isolate the relative contribution of genes responsible for the observed phenotypes and influencing the cortical development. Lin et al. (2015) investigated the changes in protein interactions network and identified that the mid-fetal cortical development is critical for the 16p11.2 proteins to connect with proteins from other genes expressed during the human brain development. The dysregulation of the KCTD13-Cul3-RhoA pathway in layer 4 of the inner cortical plate could play a role in the mirror phenotype on brain size and connectivity, although this is still in debate (Golzio et al. 2012; Escamilla et al. 2017). Right now, it seems that none of the genes in the 16p11.2 interval have a major effect. This would be the interaction between all of them and the addition of their small effects that would lead to the large alterations (Huguet et al., 2018). Animal models targeting specific subsets of genes in the 16p11.2 interval are still important tools to associate intermediate phenotypes variability with a temporal/spatial pattern of genes expression and to understand the genotype-phenotype relationship and the neurodevelopmental processes.

3.4.4 Study of CNVs associated with psychiatric conditions

A last point is about our focus on a rare recurrent CNV. Since the implementation of chromosomal microarrays in clinics in 2009, pathogenic CNVs are currently identified in 10 to 15 % of patients referred for NDDs (Battaglia et al. 2013; Miller et al. 2010). However, clinical and general population studies suggest that the majority of CNVs is not recurrent (Miller et al. 2010; Itsara et al. 2009). Association studies show that the non-recurrent CNVs are enriched in the population diagnosed with NDDs (Cooper et al. 2011; Männik et al. 2015). Over 75% of “clinically significant” CNVs are observed only once or a few times in patients: there is still need to characterize and quantify these “non-recurrent” CNVs. To this end, it’s necessary to move from a case-control design to model the effect of mutations on cognitive and neural traits, by developing predictive models, depending on the characteristics of the disrupted genes. It will also be important to integrate the information from de novo, inherited, rare and common variations (Malhotra & Sebat 2012). Right now, despite the high heritability of ASD, a genetic cause is identified in only 25% of cases maximum, with genes implicated in chromatin remodeling, mRNA translation, metabolism, synaptic function. Neuroimaging can

be a tool to help to discover new genetic variants, through genome-wide association studies with brain measurements.

Detailed cataloging of rare and penetrant variants allows making models with strong construct validity. However, common variants also contribute to ASD susceptibility, with much smaller effects for each variant (Huguet et al. 2013; Sullivan et al. 2018). Enigma consortium is initially focus on the discovery of common variants that influence normal brain variation (Bearden & Thompson 2017). Their current studies aim at identifying genetic overlap between multiple brain imaging phenotypes and risks for psychiatric disorders (Lee et al. 2016; Franke et al. 2016; Smeland et al. 2017). Finally, the penetrance and variability of the variants might be influenced by complex interactions between genetic, epigenetic and environmental factors. Trying to unravel some of these factors will hopefully give insights on additional events necessary to push the CNV carriers beyond the threshold of diseases (Pua et al. 2017).

4. GENERAL CONCLUSIONS

Neuroimaging studies of psychiatric disorders such as ASD have produced conflicting results and do not fully contribute to the understanding of the underlying mechanisms. That is likely due, in part, to their heterogeneous and complex genetic architecture. The genetic first approach is a way to tackle this heterogeneity and to define subtypes of such diseases (Stessman et al. 2014).

In my Ph.D., I focused on large recurrent CNVs associated with NDDs, at the 16p11.2 locus. I replicate, in a large dataset, some previous findings and demonstrate the robustness of our results. The reciprocal deletion and duplication are associated with robust reciprocal structural brain differences. The haploinsufficiency and over-expression of the same genes lead also to some distinct neural mechanisms, highlighting by specific cerebral alterations.

We observe that the effect-sizes of this genetic risk factor on neuroanatomy, are consistent with its effect sizes on cognitive and behavioral symptoms. That puts into perspective the much smaller effect-sizes observed in neuroimaging studies performed in groups of ASD patients, for example. This may be the consequence of the presence of multiple neuroanatomical patterns present in such groups.

16p11.2 CNVs seem to have an early impact on the brain, and further studies are required to test whether neuroimaging patterns may appear before the onset of behavioral symptoms. It worths to test if and which additional factors, summed with those of the 16p11.2 CNVs, are required to meet criteria for a psychiatric diagnosis. Understanding the developmental trajectories and the variable phenotypes of 16p11.2 patients will require further studies in very young carriers.

More generally, in the context of ASD, significant progress has been made to improve and systematize behavioral therapies (Amaral 2011), but no biomarkers are available to guide the clinical decisions. Neuroimaging features are potentially important tools to evaluate the effect of treatments, they may improve the predictive value of preclinical studies and, first of all, they may help to the diagnosis. Many genetic and environmental factors modify brain development in ASD. Delineate some specific molecular mechanisms involved in ASD, as investigated in a genetic-first approach, may be a crucial step on the path to precision medicine.

5. REFERENCES

- Adhikari, B.M. et al., 2017. Heritability estimates on resting state fMRI data using ENIGMA analysis pipeline. *Pac symp Biocomput*, 23, pp.307–318.
- Alexander, A.L. et al., 2007. Diffusion tensor imaging of the corpus callosum in Autism. *NeuroImage*, 34(1), pp.61–73.
- Amaral, D.G., 2011. The promise and the pitfalls of autism research: An introductory note for new autism researchers. *Brain Research*, 1380, pp.3–9.
- Anagnostou, E. & Taylor, M.J., 2011. Review of neuroimaging in autism spectrum disorders: what have we learned and where we go from here. *Molecular Autism*, 2(4), pp.1-9.
- Arbogast, T. et al., 2017. Reciprocal Effects on Neurocognitive and Metabolic Phenotypes in Mouse Models of 16p11.2 Deletion and Duplication Syndromes. *PLoS Genetics*, 12(2), pp.e1005709.
- Aubert-Broche, B. et al., 2014. Onset of multiple sclerosis before adulthood leads to failure of age-expected brain growth. *Neurology*, 83, pp.2140–2146.
- Aubert-Broche, B. et al., 2013. A new method for structural volume analysis of longitudinal brain MRI data and its application in studying the growth trajectories of anatomical brain structures in childhood. *NeuroImage*, 82, pp.393–402.
- Aubert-Broche, B. et al., 2011. Regional brain atrophy in children with multiple sclerosis. *NeuroImage*, 58(2), pp.409–415.
- Battaglia, A. et al., 2013. Confirmation of chromosomal microarray as a first- tier clinical diagnostic test for individuals with developmental delay, intellectual disability, autism spectrum disorders and dysmorphic features. *European Journal of Paediatric Neurology*, 17(6), pp.589–599.
- Bearden, C.E. & Thompson, P.M., 2017. Emerging Global Initiatives in Neurogenetics: The Enhancing Neuroimaging Genetics through Meta-analysis (ENIGMA) Consortium. *Neuron*, 94(2), pp.232–236.
- Bearden, C.E. et al., 2006. Mapping Cortical Thickness in Children with 22q11.2 Deletions. *Cerebral Cortex*, 17(8), pp.1889–1898.
- Beckmann, J.S. et al., 2007. Copy number variants and genetic traits: closer to the resolution of phenotypic to genotypic variability. *Nature Reviews Genetics*, 8, pp.639–646.
- Bercik, P. et al., 2011. The anxiolytic effect of Bifidobacterium longum NCC3001 involves vagal pathways for gut–brain communication. *Neurogastroenterology and motility*, 23(12), pp.1132–1139.
- Bercik, P. et al., 2011. The Intestinal Microbiota Affect Central Levels of Brain-Derived Neurotrophic Factor and Behavior in Mice. *Gastroenterology*, 141(2), pp.599–609.

- Bernier, R. et al., 2017. Developmental trajectories for young children with 16p11.2 copy number variation. *American Journal of Medical Genetics Part B: Neuropsychiatric Genetics*, 174(4), pp.367–380.
- Blackmon, K. et al., 2017. Focal Cortical Anomalies and Language Impairment in 16p11.2 Deletion and Duplication Syndrome. *Cerebral Cortex*, pp.1–9.
- Bochukova, E.G. et al., 2009. Large, rare chromosomal deletions associated with severe early-onset obesity. *Nature*, 463(7281), pp.666–670.
- Brugger, S.P. & Howes, O.D., 2017. Heterogeneity and Homogeneity of Regional Brain Structure in Schizophrenia. *JAMA Psychiatry*, 74(11), pp.1104–17.
- Button, K.S. et al., 2013. Power failure: why small sample size undermines the reliability of neuroscience. *Nature Reviews Neurosciences*, 14(5), pp.365–376.
- Campbell, L.E., 2006. Brain and behaviour in children with 22q11.2 deletion syndrome: a volumetric and voxel-based morphometry MRI study. *Brain*, 129(5), pp.1218–1228.
- Carter, C.S. et al., 2017. Enhancing the Informativeness and Replicability of Imaging Genomics Studies. *Biological Psychiatry*, 82(3), pp.157–164.
- Cauda, F. et al., 2017. Are schizophrenia, autistic, and obsessive spectrum disorders dissociable on the basis of neuroimaging morphological findings?: A voxel-based meta-analysis. *Autism research*, 10(6), pp.1079–1095.
- Cavanna, A.E. & Trimble, M.R., 2006. The precuneus: a review of its functional anatomy and behavioural correlates. *Brain*, 129(3), pp.564–583.
- Chang, Y.S. et al., 2016. Reciprocal white matter alterations due to 16p11.2 chromosomal deletions versus duplications. *Human Brain Mapping*, 37(8), pp.2833–2848.
- Chen, A.Y. et al., 2010. Prevalence of obesity among children with chronic conditions. *Obesity*, 18(1), pp.210–213.
- Cheung, C., Yu, K., Fung, G., Leung, M., Wong, C., Li, Q., Sham, P., Chua, S. & McAlonan, G., 2010. Autistic Disorders and Schizophrenia: Related or Remote? An Anatomical Likelihood Estimation. *PLoS ONE*, 5(8), pp.e12233.
- Christensen, D.L. et al., 2016. Prevalence and Characteristics of Autism Spectrum Disorder Among Children Aged 8 Years - Autism and Developmental Disabilities Monitoring Network, 11 Sites, United States, 2012. *MMWR Surveill Summ*, 65, pp.1-23.
- Chow, E.W.C. et al., 2011. Association of Schizophrenia in 22q11.2 Deletion Syndrome and Gray Matter Volumetric Deficits in the Superior Temporal Gyrus. *American Journal of Psychiatry*, 168(5), pp.522–529.
- Clarke, G. et al., 2012. The microbiome-gut-brain axis during early life regulates the hippocampal serotonergic system in a sex-dependent manner. *Molecular Psychiatry*, 18(6), pp.666–673.

- Collins, D.L. et al., 1994. Automatic 3D intersubject registration of MR volumetric data in standardized Talairach space. *Journal of computer assisted tomography*, 18(2), pp.192–205.
- Collins, D.L. et al., 1995. Automatic 3-D model-based neuroanatomical segmentation. *Human Brain Mapping*, 3(3), pp.190–208.
- Cooper, G.M. et al., 2011. A copy number variation morbidity map of developmental delay. *Nature Genetics*, 43(9), pp.838–846.
- Cotillard, A. et al., 2013. Dietary intervention impact on gut microbial gene richness. *Nature*, 500(7464), pp.585–588.
- Courchesne, E., 2002. Abnormal early brain development in autism. *Molecular Psychiatry*, 7 Suppl 2, pp.S21–3.
- Courchesne, E., Campbell, K. & Solso, S., 2011. Brain growth across the life span in autism: Age-specific changes in anatomical pathology. *Brain Research*, 1380, pp.138–145.
- Crossley, N.A. et al., 2014. The hubs of the human connectome are generally implicated in the anatomy of brain disorders. *Brain*, 137(8), pp.2382–2395.
- Cuthbert, B.N. & Insel, T.R., 2013. Toward the future of psychiatric diagnosis: the seven pillars of RDoC. *BMC Medicine*, 11(126), pp.1–8.
- Debbané, M. et al., 2006. Hippocampal volume reduction in 22q11.2 deletion syndrome. *Neuropsychologia*, 44(12), pp.2360–2365.
- Dennis, E.L. & Thompson, P.M., 2013. Typical and atypical brain development: a review of neuroimaging studies *Dialogues in Clinical Neuroscience*, 15(3), pp.359–384.
- Dietrich, O., Reiser, M.F. & Schoenberg, S.O., 2008. Artifacts in 3-T MRI: Physical background and reduction strategies. *European Journal of Radiology*, 65(1), pp.29–35.
- Draganski, B. et al., 2011. Regional specificity of MRI contrast parameter changes in normal ageing revealed by voxel-based quantification (VBQ). *NeuroImage*, 55(4), pp.1423–1434.
- Dufour, F., Schaer, M., Debbané, M., Farhoumand, R., Glaser, B. & Eliez, S., 2008. Cingulate gyral reductions are related to low executive functioning and psychotic symptoms in 22q11.2 deletion syndrome. *Neuropsychologia*, 46(12), pp.2986–2992.
- Duyzend, M.H. et al., 2016. Maternal Modifiers and Parent-of-Origin Bias of the Autism-Associated 16p11.2 CNV. *The American Journal of Human Genetics*, 98(1), pp.45–57.
- D’Angelo, D. et al., 2016. Defining the Effect of the 16p11.2 Duplication on Cognition, Behavior, and Medical Comorbidities. *JAMA Psychiatry*, 73(1), pp.20–30.
- Ecker, C., Bookheimer, S.Y. & Murphy, D.G.M., 2015. Neuroimaging in autism spectrum disorder: brain structure and function across the lifespan. *Lancet Neurol*, 14, pp.1121–34.

- Ecker, C., Ginestet, C., et al., 2013. Brain surface anatomy in adults with autism: the relationship between surface area, cortical thickness, and autistic symptoms. *JAMA Psychiatry*, 70(1), pp.59–70.
- Ecker, C., Ronan, L., et al., 2013. Intrinsic gray-matter connectivity of the brain in adults with autism spectrum disorder. *Proceedings of the National Academy of Sciences of the United States of America*, 110(32), pp.13222–13227.
- Eisenberg, D.P., Jabbi, M. & Berman, K.F., 2010. Bridging the gene–behavior divide through neuroimaging deletion syndromes: Velocardiofacial (22q11.2 Deletion) and Williams (7q11.23 Deletion) syndromes. *NeuroImage*, 53(3), pp.857–869.
- Ellegood, J. et al., 2014. Clustering autism: using neuroanatomical differences in 26 mouse models to gain insight into the heterogeneity. *Molecular Psychiatry*, 20(1), pp.118–125.
- Ellison-Wright, I., M.R.C.P. et al., 2008. The Anatomy of First-Episode and Chronic Schizophrenia: An Anatomical Likelihood Estimation Meta-Analysis. *American Journal of Psychiatry*, 165(8), pp.1015–1023.
- Elsabbagh, M. & Johnson, M.H., 2016. Autism and the Social Brain: The First-Year Puzzle. *Biological Psychiatry*, 80(2), pp.94–99.
- Escamilla, C.O. et al., 2017. Kctd13 deletion reduces synaptic transmission via increased RhoA. *Nature*, 551(7679), pp.227.
- Eskildsen, S.F. et al., 2012. BEaST: Brain extraction based on nonlocal segmentation technique. *NeuroImage*, 59(3), pp.2362–2373.
- Evans, A.C., 2006. The NIH MRI study of normal brain development. *NeuroImage*, 30(1), pp.184–202.
- Fan, C.C. et al., 2017. Williams syndrome-specific neuroanatomical profile and its associations with behavioral features. *NeuroImage: Clinical*, 15, pp.343–347.
- Fonov, V. et al., 2011. Unbiased average age-appropriate atlases for pediatric studies. *NeuroImage*, 54(1), pp.313–327.
- Fonov, V.S. et al., 2009. Unbiased nonlinear average age-appropriate brain templates from birth to adulthood. *NeuroImage*, 47, p.S102.
- Fornito, A. et al., 2009. Mapping grey matter reductions in schizophrenia: an anatomical likelihood estimation analysis of voxel-based morphometry studies. *Schizophrenia Research*, 108(1-3), pp.104–113.
- Foster, J.A. et al., 2016. Gut Microbiota and Brain Function: An Evolving Field in Neuroscience. *International Journal of Neuropsychopharmacology*, 19(5).
- Frackowiak, R.S., 2004. Human brain function (2nd edition). *Elsevier Academic Press*.
- Franke, B. et al., 2016. Genetic influences on schizophrenia and subcortical brain volumes:

- large-scale proof of concept. *Nature Neuroscience*, 19(3), pp.420–431.
- Fushimi, Y. et al., 2007. Gray matter-white matter contrast on spin-echo T1-weighted images at 3 T and 1.5 T: a quantitative comparison study. *European Radiology*, 17(11), pp.2921–2925.
- Giedd, J.N. et al., 1999. Brain development during childhood and adolescence: a longitudinal MRI study. *Nature Neuroscience*, 2(10), pp.861–863.
- Glahn, D.C. et al., 2008. Meta-analysis of gray matter anomalies in schizophrenia: application of anatomic likelihood estimation and network analysis. *Biological Psychiatry*, 64(9), pp.774–781.
- Golzio, C. et al., 2015. A Potential Contributory Role for Ciliary Dysfunction in the 16p11.2 600 kb BP4-BP5 Pathology. *The American Journal of Human Genetics*, 96(5), pp.784–796.
- Golzio, C. et al., 2012. KCTD13 is a major driver of mirrored neuroanatomical phenotypes of the 16p11.2 copy number variant. *Nature*, 485(7398), pp.363–367.
- Goodkind, M. et al., 2015. Identification of a Common Neurobiological Substrate for Mental Illness. *JAMA Psychiatry*, 72(4), pp.305–23.
- Gothelf, D. et al., 2007. Abnormal cortical activation during response inhibition in 22q11.2 deletion syndrome. *Human Brain Mapping*, 28(6), pp.533–542.
- Green Snyder, L.A. et al., 2016. Autism Spectrum Disorder, Developmental and Psychiatric Features in 16p11.2 Duplication. *Journal of Autism and Developmental Disorders*, 46(8), pp.2734–2748.
- Guna, A., Butcher, N.J. & Bassett, A.S., 2015. Comparative mapping of the 22q11.2 deletion region and the potential of simple model organisms. *Journal of Neurodevelopmental Disorders*, 7(1), pp.1-16.
- Gurung, R. & Prata, D.P., 2015. What is the impact of genome-wide supported risk variants for schizophrenia and bipolar disorder on brain structure and function? A systematic review. *Psychological medicine*, 45(12), pp.2461–2480.
- Hanson, E. et al., 2015. The Cognitive and Behavioral Phenotype of the 16p11.2 Deletion in a Clinically Ascertained Population. *Biological Psychiatry*, 77(9), pp.785–793.
- Hardan, A.Y., Libove, R.A., Keshavan, M.S., Melhem, N.M. & Minshew, N.J., 2009. A preliminary longitudinal magnetic resonance imaging study of brain volume and cortical thickness in autism. *Biological Psychiatry*, 66(4), pp.320–326.
- Hashimoto, R. et al., 2015. Imaging Genetics and Psychiatric Disorders. *Current Molecular Medicine*, 15, pp.168–175.
- Hazlett, H.C. et al., 2017. Early brain development in infants at high risk for autism spectrum disorder. *Nature*, 542(7641), pp.348–351.

- Hazlett, H.C. et al., 2011. Early Brain Overgrowth in Autism Associated With an Increase in Cortical Surface Area Before Age 2 Years. *Archives of General Psychiatry*, 68(5), pp.467–76.
- Hazlett, H.C. et al., 2009. Teasing apart the heterogeneity of autism: Same behavior, different brains in toddlers with fragile X syndrome and autism. *Journal of Neurodevelopmental Disorders*, 1, pp.81–90.
- Haznedar, M.M. et al., 2006. Volumetric analysis and three-dimensional glucose metabolic mapping of the striatum and thalamus in patients with autism spectrum disorders. *American Journal of Psychiatry*, 163(7), pp.1252–1263.
- Herbert, M.R. et al., 2003. Dissociations of cerebral cortex, subcortical and cerebral white matter volumes in autistic boys. *Brain*, 126(5), pp.1182–1192.
- Hippolyte, L. et al., 2016. The Number of Genomic Copies at the 16p11.2 Locus Modulates Language, Verbal Memory, and Inhibition. *Biological Psychiatry*, 80(2), pp.129–139.
- Hollander, E. et al., 2005. Striatal volume on magnetic resonance imaging and repetitive behaviors in autism. *Biological Psychiatry*, 58(3), pp.226–232.
- Honea, R., Crow, T.J., Passingham, D. & Mackay, C.E., 2005. Regional Deficits in Brain Volume in Schizophrenia: A Meta-Analysis of Voxel-Based Morphometry Studies. *Am J Psychiatry*, 162(12), pp.2233–45.
- Horev, G. et al., 2011. Dosage-dependent phenotypes in models of 16p11.2 lesions found in autism. *PNAS*, 108(41), pp.17076–17081.
- Hsiao, E.Y. et al., 2013. The microbiota modulates gut physiology and behavioral abnormalities associated with autism. *Cell*, 155(7), pp.1451–1463.
- Huguet, G., Ey, E. & Bourgeron, T., 2013. The Genetic Landscapes of Autism Spectrum Disorders. *Annual Review of Genomics and Human Genetics*, 14(1), pp.191–213.
- Hulshoff Pol, H.E. & Kahn, R.S., 2007. What Happens After the First Episode? A Review of Progressive Brain Changes in Chronically Ill Patients With Schizophrenia. *Schizophrenia Bulletin*, 34(2), pp.354–366.
- Huttenlocher, P.R., 1990. Morphometric study of human cerebral cortex development. *Neuropsychologia*, 28(6), pp.517–527.
- Huttenlocher, P.R. & de Courten, C., 1987. The development of synapses in striate cortex of man. *Human neurobiology*, 6(1), pp.1–9.
- Huguet, G. et al, 2018. Measuring and estimating the effect sizes of copy number variants on general intelligence in community-based samples. *JAMA Psychiatry*, pp.e0039.
- Hyde, K.L. et al., 2010. Neuroanatomical differences in brain areas implicated in perceptual and other core features of autism revealed by cortical thickness analysis and voxel-based morphometry. *Human Brain Mapping*, 31(4), pp.556–566.

- Itsara, A. et al., 2009. Population Analysis of Large Copy Number Variants and Hotspots of Human Genetic Disease. *The American Journal of Human Genetics*, 84(2), pp.148–161.
- Jacquemont, S. et al., 2011. Mirror extreme BMI phenotypes associated with gene dosage at the chromosome 16p11.2 locus. *Nature*, 478(7367), pp.97–102.
- Jahanshad, N. et al., 2013. Multi-site genetic analysis of diffusion images and voxelwise heritability analysis: A pilot project of the ENIGMA–DTI working group. *NeuroImage*, 81, pp.455–469.
- Jalbrzikowski, M. et al., 2013. Structural abnormalities in cortical volume, thickness, and surface area in 22q11.2 microdeletion syndrome: Relationship with psychotic symptoms. *NeuroImage: Clinical*, 3, pp.405–415.
- Jiang, H. et al., 2015. Altered fecal microbiota composition in patients with major depressive disorder. *Brain, behavior, and immunity*, 48, pp.186–194.
- Kates, W.R. et al., 2011. Neuroanatomic Predictors to Prodromal Psychosis in Velocardiofacial Syndrome (22q11.2 Deletion Syndrome): A Longitudinal Study. *Biological Psychiatry*, 69(10), pp.945–952.
- Kates, W.R. et al., 2001. Regional cortical white matter reductions in velocardiofacial syndrome: a volumetric MRI analysis. *Biological Psychiatry*, 49(8), pp.677–684.
- Kelly, S. et al., 2017. Widespread white matter microstructural differences in schizophrenia across 4322 individuals: results from the ENIGMA Schizophrenia DTI Working Group. *Molecular Psychiatry*, pp.1–9.
- Kurth, F. et al., 2011. Diminished Gray Matter Within the Hypothalamus in Autism Disorder: A Potential Link to Hormonal Effects? *Biological Psychiatry*, 70(3), pp.278–282.
- Langen, M. et al., 2007. Caudate nucleus is enlarged in high-functioning medication-naive subjects with autism. *Biological Psychiatry*, 62(3), pp.262–266.
- Lau, J.C. et al., 2008. Longitudinal neuroanatomical changes determined by deformation-based morphometry in a mouse model of Alzheimer's disease. *NeuroImage*, 42(1), pp.19–27.
- Le Chatelier, E. et al., 2013. Richness of human gut microbiome correlates with metabolic markers. *Nature*, 500(7464), pp.541–546.
- Lee, P.H. et al., 2016. Partitioning heritability analysis reveals a shared genetic basis of brain anatomy and schizophrenia. *Molecular Psychiatry*, 21(12), pp.1680–1689.
- Lefebvre, A. et al., 2015. Neuroanatomical Diversity of Corpus Callosum and Brain Volume in Autism: Meta-analysis, Analysis of the Autism Brain Imaging Data Exchange Project, and Simulation. *Biological Psychiatry*, 78, pp.126–134.
- Levy, D. et al., 2011. Rare De Novo and Transmitted Copy-Number Variation in Autistic Spectrum Disorders. *Neuron*, 70(5), pp.886–897.

- Lewis, J.D. et al., June 2017. Thickness and contrast in 16p11.2 CNVs. Poster presented at OHBM- Organization for Human Brain Mapping, Vancouver.
- Lin, A. et al., 2017. Mapping 22q11.2 gene dosage effects on brain morphometry. *Journal of Neuroscience*, 37(26), pp.6183-6199.
- Lin, G.N. et al., 2015. Spatiotemporal 16p11.2 Protein Network Implicates Cortical Late Mid-Fetal Brain Development and KCTD13- Cul3-RhoA Pathway in Psychiatric Diseases. *Neuron*, 85(4), pp.742–754.
- Lupski, J.R., 2007. Structural Variation in the Human Genome. *The New England Journal of Medicine*, 356(11), pp.1169–1171.
- Lutti, A. et al., 2014. Using high-resolution quantitative mapping of R1 as an index of cortical myelination. *NeuroImage*, 93, pp.176–188.
- Maillard, A.M. et al., May 2017. Cognitive and head circumference differences in 16p11.2 CNV carriers with and without autism. Poster presented at IMFAR- International Meeting for Autism Research, San Francisco.
- Maillard, A.M. et al., 2015. 16p11.2 Locus modulates response to satiety before the onset of obesity. *International Journal of Obesity*, 40(5), pp.1–7.
- Maillard, A.M. et al., 2014. The 16p11.2 locus modulates brain structures common to autism, schizophrenia and obesity. *Molecular Psychiatry*, 20(1), pp.140–147.
- Malhotra, D. & Sebat, J., 2012. CNVs: Harbingers of a Rare Variant Revolution in Psychiatric Genetics. *Cell*, 148(6), pp.1223–1241.
- Marshall, C.R. et al., 2016. Contribution of copy number variants to schizophrenia from a genome-wide study of 41,321 subjects. *Nature Genetics*, 49(1), pp.27–35.
- Männik, K. et al., 2015. Copy Number Variations and Cognitive Phenotypes in Unselected Populations. *JAMA*, 313(20), pp.2044–11.
- Martin-Brevet, S. et al., 2018. Quantifying the effects of 16p11.2 copy number variants on brain structure: A multi-site 'genetic-first' study. *Accepted in Biological Psychiatry*.
- McCarthy, S.E. et al., 2009. Microduplications of 16p11.2 are associated with schizophrenia. *Nature Genetics*, 41(11), pp.1223–1227.
- Mellerup, E. et al., 2017. Combinations of genetic variants associated with bipolar disorder. *PloS ONE*, 12(12), pp.e0189739.
- Merikangas, A.K., Corvin, A.P. & Gallagher, L., 2009. Copy-number variants in neurodevelopmental disorders: promises and challenges. *Trends in Genetics*, 25(12), pp.536–544.
- Miller, D.T. et al., 2010. Consensus Statement: Chromosomal Microarray Is a First-Tier Clinical Diagnostic Test for Individuals with Developmental Disabilities or Congenital Anomalies.

- The American Journal of Human Genetics*, 86(5), pp.749–764.
- Moberget, T. et al., 2017. Cerebellar volume and cerebellocerebral structural covariance in schizophrenia: a multisite mega-analysis of 983 patients and 1349 healthy controls. *Molecular Psychiatry*, pp.1–9.
- Moreau, C. et al., October 2017. Altered brain connectivity in patients with 16p11.2 CNVs. Poster presented at WCPG – World Congress of Psychiatric Genetics, Orlando.
- Moreau, C. et al., June 2017. Altered subcortical diffusivity in 16p11.2 CNVs. Poster presented at OHBM- Organization for Human Brain Mapping, Vancouver.
- Moreno-De-Luca, A. et al., 2015. The Role of Parental Cognitive, Behavioral, and Motor Profiles in Clinical Variability in Individuals With Chromosome 16p11.2 Deletions. *JAMA Psychiatry*, 72(2), pp.119–126.
- Moreno-De-Luca, D. & Cubells, J.F., 2011. Copy Number Variants: A New Molecular Frontier in Clinical Psychiatry. *Current Psychiatry Reports*, 13(2), pp.129–137.
- Namkung, H., Kim, S.-H. & Sawa, A., 2017. The Insula: An Underestimated Brain Area in Clinical Neuroscience, Psychiatry, and Neurology. *Trends in Neurosciences*, 40(4), pp.200–207.
- Neufeld, K.-A.M. et al., 2011. Effects of intestinal microbiota on anxiety-like behavior. *Communicative & Integrative Biology*, 4(4), pp.492–494.
- Nordahl, C.W. et al., 2007. Cortical folding abnormalities in autism revealed by surface-based morphometry. *Journal of Neuroscience*, 27(43), pp.11725–11735.
- Owen, J.P. et al., 2014. Aberrant White Matter Microstructure in Children with 16p11.2 Deletions. *Journal of Neuroscience*, 34(18), pp.6214–6223.
- Paus, T. et al., 2001. Maturation of white matter in the human brain: A review of magnetic resonance studies. *Brain Research Bulletin*, 54(3), pp.255–266.
- Pontious, A. et al., 2008. Role of intermediate progenitor cells in cerebral cortex development. *Developmental neuroscience*, 30(1-3), pp.24–32.
- Portmann, T. et al., 2014. Behavioral Abnormalities and Circuit Defects in the Basal Ganglia of a Mouse Model of 16p11.2 Deletion Syndrome. *Cell Reports*, 7(4), pp.1077–1092.
- Pua, E.P.K., Bowden, S.C. & Seal, M.L., 2017. Autism spectrum disorders: Neuroimaging findings from systematic reviews. *Research in Autism Spectrum Disorders*, 34, pp.28–33.
- Pugliese, L. et al., 2009. The anatomy of extended limbic pathways in Asperger syndrome: a preliminary diffusion tensor imaging tractography study. *NeuroImage*, 47(2), pp.427–434.
- Qureshi, A.Y. et al., 2014. Opposing Brain Differences in 16p11.2 Deletion and Duplication Carriers. *Journal of Neuroscience*, 34(34), pp.11199–11211.
- Rakic, P., 1995. A small step for the cell, a giant leap for mankind: a hypothesis of neocortical

- expansion during evolution. *Trends in Neurosciences*, 18(9), pp.383–388.
- Rakic, P., 1988. Specification of cerebral cortical areas. *Science*, 241(4862), pp.170–176.
- Rakic, P. & Lombroso, P.J., 1998. Development of the cerebral cortex: I. Forming the cortical structure. *Journal of the American Academy of Child & Adolescent Psychiatry*, 37(1), pp.116–117.
- Rimol, L.M. et al., 2012. Cortical Volume, Surface Area, and Thickness in Schizophrenia and Bipolar Disorder. *Biological Psychiatry*, 71(6), pp.552–560.
- Sanders, S.J. et al., 2011. Multiple Recurrent De Novo CNVs, Including Duplications of the 7q11.23 Williams Syndrome Region, Are Strongly Associated with Autism. *Neuron*, 70(5), pp.863–885.
- Savignac, H.M. et al., 2015. Bifidobacteria modulate cognitive processes in an anxious mouse strain. *Behavioural Brain Research*, 287, pp.59–72.
- Schaer, M. et al., 2009. Deviant trajectories of cortical maturation in 22q11.2 deletion syndrome (22q11DS): A cross-sectional and longitudinal study. *Schizophrenia Research*, 115(2-3), pp.182–190.
- Scheperjans, F. et al., 2015. Gut microbiota are related to Parkinson's disease and clinical phenotype. *Movement disorders*, 30(3), pp.350–358.
- Schultz, R.T. et al., 2003. The role of the fusiform face area in social cognition: implications for the pathobiology of autism. *Philosophical Transactions of the Royal Society B: Biological Sciences*, 358(1430), pp.415–427.
- Schumann, C.M. et al., 2010. Longitudinal Magnetic Resonance Imaging Study of Cortical Development through Early Childhood in Autism. *Journal of Neuroscience*, 30(12), pp.4419–4427.
- Schumann, C.M. et al., 2004. The amygdala is enlarged in children but not adolescents with autism; the hippocampus is enlarged at all ages. *Journal of Neuroscience*, 24(28), pp.6392–6401.
- Sebat, J. et al., 2007. Strong association of de novo copy number mutations with autism. *Science*, 316(5823), pp.445–449.
- Shashi, V. et al., 2010. Evidence of gray matter reduction and dysfunction in chromosome 22q11.2 deletion syndrome. *Psychiatry Research: Neuroimaging*, 181(1), pp.1–8.
- Shepherd, A.M. et al., 2012. Systematic meta-review and quality assessment of the structural brain alterations in schizophrenia. *Neuroscience and biobehavioral reviews*, 36(4), pp.1342–1356.
- Simon, T.J. et al., 2005. Volumetric, connective, and morphologic changes in the brains of children with chromosome 22q11.2 deletion syndrome: an integrative study. *NeuroImage*, 25(1), pp.169–180.

- Sled, J.G., Zijdenbos, A.P. & Evans, A.C., 1998. A nonparametric method for automatic correction of intensity nonuniformity in MRI data. *IEEE transactions on medical imaging*, 17(1), pp.87–97.
- Smeland, O.B. et al., 2017. Genetic Overlap Between Schizophrenia and Volumes of Hippocampus, Putamen, and Intracranial Volume Indicates Shared Molecular Genetic Mechanisms. *Schizophrenia Bulletin*, 21(4), pp.1–11.
- Son, J.S. et al., 2015. Comparison of Fecal Microbiota in Children with Autism Spectrum Disorders and Neurotypical Siblings in the Simons Simplex Collection. *PLoS ONE*, 10(10), p.e0137725.
- Sønderby, I.E. et al., October 2017. Dose response of the 16p11.2 distal CNV on intracranial volume and structures of basal ganglia. Poster presented at WCPG – World Congress of Psychiatric Genetics, Orlando.
- Sowell, E.R. et al., 2004. Longitudinal mapping of cortical thickness and brain growth in normal children. *Journal of Neuroscience*, 24(38), pp.8223–8231.
- Stanfield, A.C. et al., 2008. Towards a neuroanatomy of autism: a systematic review and meta-analysis of structural magnetic resonance imaging studies. *Neuroimaging*, 23(4), pp.289–299.
- Stanisz, G.J. et al., 2005. T1, T2 relaxation and magnetization transfer in tissue at 3T. *Magnetic Resonance in Medicine*, 54(3), pp.507–512.
- Stefansson, H. et al., 2014. CNVs conferring risk of autism or schizophrenia affect cognition in controls. *Nature*, 505(7483), pp.361–366.
- Stein, J.L. et al., 2012. Identification of common variants associated with human hippocampal and intracranial volumes. *Nature Genetics*, 44(5), pp.552–561.
- Steinman, K.J. et al., 2016. 16p11.2 deletion and duplication: Characterizing neurologic phenotypes in a large clinically ascertained cohort. *American Journal of Medical Genetics Part A*, 170(11), pp.2943–2955.
- Stessman, H.A., Bernier, R. & Eichler, E.E., 2014. A Genotype-First Approach to Defining the Subtypes of a Complex Disease. *Cell*, 156(5), pp.872–877.
- Stilling, R.M., Dinan, T.G. & Cryan, J.F., 2013. Microbial genes, brain & behaviour - epigenetic regulation of the gut-brain axis. *Genes, Brain and Behavior*, 13(1), pp.69–86.
- Sullivan, P.F. et al., 2018. Psychiatric Genomics: An Update and an Agenda. *Am J Psychiatry*, 175, pp.15–27.
- Tamnes, C.K. et al., 2009. Brain Maturation in Adolescence and Young Adulthood: Regional Age-Related Changes in Cortical Thickness and White Matter Volume and Microstructure. *Cerebral Cortex*, 20(3), pp.534–548.
- The Simons VIP Consortium, 2012. Simons Variation in Individuals Project (Simons VIP): A

- Genetics-First Approach to Studying Autism Spectrum and Related Neurodevelopmental Disorders. *Neuron*, 73(6), pp.1063–1067.
- Thompson, P.M. et al., 2016. ENIGMA and the individual: Predicting factors that affect the brain in 35 countries worldwide. *NeuroImage*, 145, pp.389–408.
- Torres, F., Barbosa, M. & Maciel, P., 2016. Recurrent copy number variations as risk factors for neurodevelopmental disorders: critical overview and analysis of clinical implications. *Journal of Medical Genetics*, 53(2), pp.73–90.
- Travers, B.G. et al., 2012. Diffusion Tensor Imaging in Autism Spectrum Disorder: A Review. *Autism research*, 5(5), pp.289–313.
- van Amelsvoort, T. et al., 2004. Brain anatomy in adults with velocardiofacial syndrome with and without schizophrenia: preliminary results of a structural magnetic resonance imaging study. *Archives of General Psychiatry*, 61(11), pp.1085–1096.
- van Erp, T.G.M. et al., 2015. Subcortical brain volume abnormalities in 2028 individuals with schizophrenia and 2540 healthy controls via the ENIGMA consortium. 21(4), pp.547–553.
- van Rooij, D. et al., 2017. Cortical and Subcortical Brain Morphometry Differences Between Patients With Autism Spectrum Disorder and Healthy Individuals Across the Lifespan: Results From the ENIGMA ASD Working Group. *AJP in Advance*, pp.e17010100.
- Volkmar, F.R. et al., 2004. Autism and pervasive developmental disorders. *J Child Psychol Psychiatry*, 45, pp.135–170.
- Waiter, G.D. et al., 2005. Structural white matter deficits in high-functioning individuals with autistic spectrum disorder: a voxel-based investigation. *NeuroImage*, 24(2), pp.455–461.
- Wallace, G.L. et al., 2013. Increased gyrification, but comparable surface area in adolescents with autism spectrum disorders. *Brain*, 136(6), pp.1956–1967.
- Weiner, D.J. et al., 2017. Polygenic transmission disequilibrium confirms that common and rare variation act additively to create risk for autism spectrum disorders. *Nature Genetics*, 45, pp.86–50.
- Weiskopf, N., 2013. Quantitative multi-parameter mapping of R1, PD*, MT, and R2* at 3T: a multi-center validation. *Frontiers in neurosciences*, 7, pp.1–11.
- Weiss, L.A. et al., 2008. Association between Microdeletion and Microduplication at 16p11.2 and Autism. *The New England Journal of Medicine*, 356(7), pp.667–675.
- Willer, C.J. et al., 2009. Six new loci associated with body mass index highlight a neuronal influence on body weight regulation. *Nature Genetics*, 41(1), pp.25–34.
- Yang, M. et al., 2015. 16p11.2 Deletion mice display cognitive deficits in touchscreen learning and novelty recognition tasks. *Learning & Memory*, 22(12), pp.622–632.
- Zufferey, F. et al., 2012. A 600 kb deletion syndrome at 16p11.2 leads to energy imbalance

and neuropsychiatric disorders. *Journal of Medical Genetics*, 49(10), pp.660–668.

6. ARTICLE

Quantifying the effects of 16p11.2 copy number variants on brain structure: A multi-site 'genetic-first' study

Quantifying the Effects of 16p11.2 Copy Number Variants on Brain Structure: A Multisite Genetic-First Study

Sandra Martin-Brevet, Borja Rodríguez-Herreros, Jared A. Nielsen, Clara Moreau, Claudia Modenato, Anne M. Maillard, Aurélie Pain, Sonia Richetin, Aia E. Jønch, Abid Y. Qureshi, Nicole R. Zürcher, Philippe Conus, 16p11.2 European Consortium, Simons Variation in Individuals Project (VIP) Consortium, Wendy K. Chung, Elliott H. Sherr, John E. Spiro, Ferath Kherif, Jacques S. Beckmann, Nouchine Hadjikhani, Alexandre Reymond, Randy L. Buckner, Bogdan Draganski, and Sébastien Jacquemont

ABSTRACT

BACKGROUND: 16p11.2 breakpoint 4 to 5 copy number variants (CNVs) increase the risk for developing autism spectrum disorder, schizophrenia, and language and cognitive impairment. In this multisite study, we aimed to quantify the effect of 16p11.2 CNVs on brain structure.

METHODS: Using voxel- and surface-based brain morphometric methods, we analyzed structural magnetic resonance imaging collected at seven sites from 78 individuals with a deletion, 71 individuals with a duplication, and 212 individuals without a CNV.

RESULTS: Beyond the 16p11.2-related mirror effect on global brain morphometry, we observe regional mirror differences in the insula (deletion > control > duplication). Other regions are preferentially affected by either the deletion or the duplication: the calcarine cortex and transverse temporal gyrus (deletion > control; Cohen's $d > 1$), the superior and middle temporal gyri (deletion < control; Cohen's $d < -1$), and the caudate and hippocampus (control > duplication; $-0.5 > \text{Cohen's } d > -1$). Measures of cognition, language, and social responsiveness and the presence of psychiatric diagnoses do not influence these results.

CONCLUSIONS: The global and regional effects on brain morphometry due to 16p11.2 CNVs generalize across site, computational method, age, and sex. Effect sizes on neuroimaging and cognitive traits are comparable. Findings partially overlap with results of meta-analyses performed across psychiatric disorders. However, the lack of correlation between morphometric and clinical measures suggests that CNV-associated brain changes contribute to clinical manifestations but require additional factors for the development of the disorder. These findings highlight the power of genetic risk factors as a complement to studying groups defined by behavioral criteria.

Keywords: 16p11.2, Autism spectrum disorder, Copy number variant, Genetics, Imaging, Neurodevelopmental disorders

<https://doi.org/10.1016/j.biopsych.2018.02.1176>

Autism spectrum disorder (ASD) and related neurodevelopmental disorders are defined behaviorally and characterized by a significant clinical and etiologic heterogeneity. As a consequence, investigating ASD under the assumption of an underlying homogeneous condition has resulted in controversial findings in the field of neuroimaging (1). Increased brain growth early in development (2–4) and alterations of many regional brain volumes (5) have been implicated in ASD, but results have proven difficult to replicate (1,6–8).

To mitigate some of these issues, cohorts of individuals with shared genetic risk factors have been assembled to minimize the noise introduced by etiologic and biological heterogeneity (9). Such a “genetic-first” study design provides the opportunity to

investigate a given neurodevelopmental risk (and associated mechanism) shared by individuals who carry the same genetic etiology irrespective of the psychiatric diagnosis.

Copy number variants (CNVs) at the 16p11.2 (breakpoints 4–5, 29.6–30.2 Mb-hg19) (10) are among the most frequent risk factors for neurodevelopmental and psychiatric conditions. There is a similar 10-fold enrichment of deletions and duplications in ASD cohorts (11,12), and both CNVs have large effects on IQ (Z scores of 1.5 and 0.8, respectively) and Social Responsiveness Scale (SRS) (Z scores of 1 and 2, respectively) (10,13–15). However, there are phenotypic differences between both CNVs: the 10-fold enrichment in schizophrenia cohorts (16,17) is only observed for duplications, and only

SEE COMMENTARY ON PAGE 234

deletions affect measures of language by 1.5 Z scores (18). Previous studies demonstrated “mirror” effects of both CNVs on head circumference and body mass index (13,19). Neuroimaging studies reported gene-dosage effects on global brain metrics (20,21). However, large global effects and sample size limited the interpretation of the regional analyses, any estimate of effect size, and the generalizability of study results across different ascertainment.

In the current study, we aimed at quantifying the effects of 16p11.2 deletions and duplications on brain structure. We also examined the generalizability of our results across cohorts, scanning sites, sex, and a broad age range. Finally, we aimed at understanding the influence of clinical ascertainment. In particular, we asked whether language, social responsiveness, IQ, or the presence of psychiatric disorders may impact any of the findings. To this end, we analyzed structural magnetic resonance imaging (MRI) performed at seven sites from two international cohorts of 16p11.2 CNV carriers, familial control subjects, and unrelated control subjects. Voxel- and surface-based methods were performed in parallel on 361 participants, including 307 individuals not previously analyzed at the regional level, using whole-brain statistical methods.

METHODS AND MATERIALS

Participants

Data were acquired in two different cohorts in North America and Europe. Enrollment in the Simons Variation in Individuals Project (22) included referral by clinical genetic centers or web-based networks, or active online registration of families, while in the European 16p11.2 consortium the families were directly recruited by the referring physician.

Carriers were ascertained regardless of clinical diagnoses or age. The CNV carriers were either probands ($n = 76$) referred to the genetic clinic for the investigation of neurodevelopmental and psychiatric disorders, or their relatives (parents [$n = 49$], siblings [$n = 14$], and other relatives [$n = 10$]). Familial control subjects were relatives who do not carry a 16p11.2 CNV.

All families participated in a larger phenotyping project, as previously reported (10,13,20–22). Trained neuropsychologists performed all cognitive and behavioral assessments, including tests of overall cognitive functioning (nonverbal IQ [NVIQ]) (23–27) and phonological skills (standard score of the nonword repetition) (28,29). Participants also completed a broad screening measure of social impairment, the SRS (30). Experienced, licensed clinicians provided clinical DSM-5 diagnoses (31), using all information obtained during the research evaluation. NVIQ scores and psychiatric diagnoses were available for all participants. SRS total score was available for 77% of the participants (72 of 78 deletion carriers, 57 of 71 duplication carriers, and 149 of 212 control subjects), and phonological measures for 43% of the participants (56 of 78 deletion carriers, 19 of 71 duplication carriers, and 81 of 212 control subjects). Full description of cognitive and psychiatric assessment is available in the [Supplemental Methods and Materials](#).

We analyzed data from 78 16p11.2 (breakpoints 4–5) deletion carriers, 71 duplication carriers, 72 familial control subjects, and 140 unrelated control subjects, including data not previously analyzed at the regional level on 64 deletion carriers,

54 duplication carriers, 51 familial control subjects, and 138 unrelated control subjects. The latter were selected among volunteers from the general population who had neither a major DSM-5 diagnosis nor a relative with a neurodevelopmental disorder.

The study was approved by the institutional review boards of each consortium. Signed informed consent was obtained from the participants or legal representatives. Full description of participants is available in [Table 1](#), [Supplemental Table S1](#), and the [Supplemental Methods and Materials](#).

MRI Data Acquisition and Processing

The MRI data included T1-weighted (T1w) anatomical images acquired at seven sites using different 3T whole-body scanners: Philips Achieva (Philips Healthcare, Andover, MA) and Siemens Prisma Syngo and TIM Trio (Siemens Corp., Erlangen, Germany). Four sites used multiecho sequences for 264 participants (52 deletion carriers, 51 duplication carriers, 21 familial control subjects, and 140 unrelated control subjects), and three sites used single-echo sequences for 97 participants (26 deletion carriers, 20 duplication carriers, and 51 familial control subjects). Thirty-four scans were excluded from the analysis based on standardized visual inspection, which identified significant artifacts potentially compromising the accurate tissue classification and boundary detection (details in [Supplemental Methods and Materials](#)).

Surface-Based Morphometry. In FreeSurfer 4.5.0 (<http://surfer.nmr.mgh.harvard.edu>), each participant's T1w image was registered to a custom hybrid template consisting of 48 subjects (12 deletion children, 12 noncarrier children, 12 duplication adults, and 12 noncarrier adults) (21). Then, we used FreeSurfer's volumetric (32) and surface-based (33) algorithms with default settings. We estimated the total intracranial volume (eTIV) (34), global brain measures, cortical thickness, and surface area. The cortical thickness and surface area maps were resampled in fsaverage5 space and spatially smoothed with a Gaussian kernel of 8-mm full width at half maximum.

Voxel-Based Morphometry. In parallel we processed subjects' T1w data within the computational anatomy framework of SPM12 (<http://www.fil.ion.ac.uk/spm>). T1w images were classified in different brain tissue classes using the “unified segmentation” (35) and an enhanced set of brain tissue priors (36). Aiming at optimal spatial registration, we applied the diffeomorphic registration algorithm DARTEL (37) followed by a Gaussian spatial smoothing with 8-mm full width at half maximum. Of note, total intracranial volume computed by SPM is referred to as TIV.

Regions of interest were extracted using maximum probability tissue labels (<http://www.neuromorphometrics.com>) within SPM12 using data from the OASIS project (<http://www.oasis-brains.org>).

All MRI scanning parameters and processing are detailed in the [Supplemental Methods and Materials](#).

Data Analysis

Our whole-brain voxel-based morphometry (VBM) (38) analysis used a factorial design to test for gene dosage-related local

Table 1. Population Characteristics

	Deletion		Control		Duplication	
	EU (n = 25)	SVIP (n = 53)	EU (n = 83)	SVIP (n = 129)	EU (n = 23)	SVIP (n = 48)
Age, Years, Mean (SD), Range [Minimum–Maximum]	21.2 (1.4) [6.3–53.6 ^{a,b}]	13.8 (9.5) [6.7–48 ^c]	28.5 (12.6) [7.8–62.5 ^b]	24 (14.5) [6.1–63.4]	32.5 (13.3) [9.8–58.1]	30.1 (15.4) [6.3–63.1]
Male/Female, n	14/11	30/23	56/27	71/58	13/10	25/23
HC Z Score	n = 23	n = 52	n = 46	n = 27	n = 22	n = 48
Mean (SD)	0.28 (1.23) ^{a,b}	1.34 (1.2)	-0.21 (1.3) ^c	0.32 (1) ^c	-0.64 (1.9)	-1.08 (1.4)
NVIQ, Mean (SD)	81 (13) ^b	89 (14)	107 (16) ^c	103 (12) ^c	78 (18) ^b	89 (20)
SRS Raw Total Score	n = 20	n = 52	n = 25	n = 124	n = 11	n = 46
Mean (SD)	62 (32)	70 (37)	33 (17) ^c	19 (13) ^c	84 (40) ^c	57 (38)
Phonological Skills	n = 9	n = 47	n = 3	n = 78	n = 3	n = 16
Mean (SD)	4.8 (1.5)	5.5 (2.4)	12.3 (2.1)	8.4 (2.2) ^c	10.7 (1.5)	6.25 (2.2)

Phonology skills were evaluated in SVIP with the comprehensive test of phonological processing, nonword repetition subtest (29); and in Europe with the developmental neuropsychological assessment, nonword repetition task (28). Mean standard scores are shown. Low sample size did not allow statistics on phonological skills of the European (EU) cohort. HC, head circumference; NVIQ, nonverbal IQ; SRS, Social Responsiveness Scale; SVIP, Simons Variation in Individuals Project cohort.

^aSignificantly different between copy number variant carrier groups in the same cohort; analysis of covariance, post hoc comparison, $p < .05$ Bonferroni corrected.

^bSignificantly different from the same genetic group in the other cohort; analysis of covariance, post hoc comparison, $p < .05$ Bonferroni corrected.

^cSignificantly different from all the genetic groups in the same cohort; analysis of covariance, post hoc comparison, $p < .05$ Bonferroni corrected.

gray matter (GM) volume differences within the general linear model framework of SPM12 (39). SPM t maps were generated with a voxel-level threshold of $p < .05$ after familywise error correction for multiple comparisons over the whole GM volume using Gaussian random field theory (40). We generated Cohen's d maps from familywise error-corrected t scores to show the unbiased magnitude of the effects (Supplemental Methods and Materials).

Surface-based analyses tested regional differences in cortical thickness and surface area using linear models. For each vertex in the cerebral cortex surface mesh, we ran a multiple regression analysis. The vertexwise results were corrected for multiple comparisons at a false discovery rate of $q < .05$ (41,42) (Supplemental Methods and Materials).

The main effects of linear and quadratic expansions of age, sex, MRI site, and NVIQ were included as additional variables. The cubic expansion of age did not show any significant effect and was subsequently removed from all analyses. In an attempt to increase the power of our analyses we controlled for the effect of the seven scanning sites by introducing them as a random factor in a linear mixed model. This approach did not change the obtained results.

Z scores for global brain metrics were obtained in CNV carriers and familial control subjects using the adjusted measures from unrelated control subjects as the reference population.

Regional analyses were also corrected for the SPM estimate of TIV, the mean cortical thickness, or the total cortical surface area. In addition to the linear effect of gene dosage, we investigated the quadratic term to identify nonreciprocal effects of both CNVs. Post hoc analyses comparing deletion carriers and control subjects as well as duplication carriers and control subjects identified regions predominantly altered by each CNV.

We analyzed the interaction of the genetic groups with the regressors (age, sex, MRI site, NVIQ) as well as the MRI parameters (single-echo vs. multiecho) and three other clinical variables: SRS, phonological processing (nonword repetition), and psychiatric diagnoses. NVIQ did not show any significant effect and was removed from the analyses on the whole dataset. Dice index was computed to estimate the overlap between 16p11.2-related alterations and statistical maps obtained from a large cross-disorder neuroimaging meta-analysis (<http://anima.fz-juelich.de>) (43). We computed the rate of overlap between both maps. Finally, to motivate future hypotheses we relied on the Neurosynth database (<http://neurosynth.org>) to meta-analytically decode the functional association of the structural alterations observed in the gene dosage analyses of the 16p11.2 CNV carriers. All these analyses are detailed in the Supplemental Methods and Materials.

Linear models on global metrics and regions of interest were performed in R, version 3.2.5 (<http://www.r-project.org>; R Project for Statistical Computing, Vienna, Austria), and voxel- and surface-based analyses in MATLAB 2016b (The MathWorks, Inc., Natick, MA).

RESULTS

Demographics

We analyzed 78 deletion carriers, 71 duplication carriers, and 212 familial and unrelated control subjects (Table 1,

Supplemental Table S1), including new data on 138 individuals and data on 307 individuals not previously analyzed with whole-brain statistical methods. Age ranges from 6 to 63 years. Deletion carriers and control subjects from the Simons Variation in Individuals Project cohort are younger than the same groups in the European cohort, and deletion carriers overall are younger than the other groups. There is no significant difference in sex ratio across genetic groups and cohorts. Mean NVIQ is 81 and 89 in deletion carriers, and 78 and 89 in duplication carriers for the European and Simons Variation in Individuals Project cohorts, respectively. Ninety percent of the deletion carriers, 69% of the duplication carriers, and 25% of familial control subjects meet criteria for at least one psychiatric diagnosis. Twelve categories of diagnoses are recorded across the CNV carrier groups, including ASD in 13% of deletion carriers and 11% of duplication carriers (Table 2).

Global Brain Metrics

Head circumference Z scores (Table 1) and eTIV (Figure 1A) correlate negatively with the number of genomic copies of the 16p11.2 locus in both cohorts. Both GM and white matter total volumes contribute to this effect on eTIV (Figure 1B, C). The effect sizes on global brain metrics are up to 1 Z score for the deletion and approximately -0.4 Z score for the duplication (Supplemental Table S2). FreeSurfer and SPM estimates of

TIV, GM, and white matter are comparable across groups, cohorts, and MRI parameters (Supplemental Figure S1). Gene dosage preferentially affects cortical surface area and not thickness (Figure 1E, F). Of note, age-related thinning of cortical thickness is not significantly different between genetic groups (Supplemental Figure S2).

Regional Brain Differences Related to the 16p11.2 CNVs

In both cohorts, the whole-brain VBM analysis shows a negative relationship between the number of genomic copies at the 16p11.2 locus and the volume of several brain regions. Alterations with an effect size >1 Cohen's d (detected with a conservative power of 74.4% for family-wise error-corrected $p < .05$) include the bilateral anterior and posterior insula, transverse temporal gyrus, and calcarine cortex (Figure 2A, Supplemental Table S3). Regions with smaller volumes in deletion carriers compared with control subjects and duplication carriers include the bilateral precentral gyrus and middle and superior temporal gyri. Altered regions with smaller effect sizes are detailed in Supplemental Table S3.

There is a high degree of overlap between VBM findings with large effects and regional cortical surface area alterations, namely the insula, transverse temporal gyrus, and calcarine cortex (negative gene dosage), as well as the precentral gyrus

Table 2. DSM-5 Diagnoses

	Deletion		Familial Control Subjects		Duplication	
	EU (n = 25)	SVIP (n = 53)	EU (n = 45)	SVIP (n = 27)	EU (n = 23)	SVIP (n = 48)
Neurodevelopmental Disorders	3	5	–	–	4	6
Intellectual Disability						
Communication disorder	16	53	–	2	–	3
Autism spectrum disorder	–	10	–	1	2	6
Attention-deficit/hyperactivity disorder	2	12	2	4	1	7
Specific learning disorder	1	14	1	–	4	4
Motor disorder, tic disorder	–	26	–	1	1	9
Schizophrenia Spectrum and Other Psychotic Disorders	–	–	–	–	1	–
Bipolar and Related Disorders	–	–	–	–	1	–
Depressive Disorders	2	3	7	1	5	9
Anxiety Disorders	2	7	–	3	9	13
Obsessive-Compulsive and Related Disorders	1	1	–	–	1	2
Trauma and Stressor-Related Disorders	1	–	–	–	–	2
Elimination Disorders	5	14	–	2	1	2
Disruptive, Impulse-Control, and Conduct Disorders	1	5	–	–	–	–
Substance-Related and Addictive Disorders	3	–	–	–	1	–
Feeding and Eating Disorders	–	–	2	–	–	–
Other Conditions That May Be a Focus of Clinical Attention	–	9	–	–	–	9

From the DSM-5 (31).

A total of 20 of 25 European (EU) cohort deletion carriers (80%) had at least one psychiatric diagnosis: 11 had one diagnosis and 9 had several diagnoses (between two and five); 17 of 23 EU cohort duplication carriers (74%) had at least one psychiatric diagnosis: 7 had one diagnosis and 10 had several diagnoses (two or three); 9 of 45 familial control subjects (20%) had at least one psychiatric diagnosis: 6 had one diagnosis and 3 had two diagnoses. In the Simons Variation in Individuals Project (SVIP) dataset, 50 of 53 deletion carriers (94.3%) had at least one psychiatric diagnosis: 6 had one diagnosis and 44 had several diagnoses (between two and eight); 32 of 48 SVIP duplication carriers (66.6%) had at least one psychiatric diagnosis: 10 had one diagnosis and 22 had several diagnoses (between two and five); 9 of 27 familial control subjects (33%) had at least one psychiatric diagnosis: 4 had one diagnosis and 5 had two diagnoses. In both cohorts, unrelated control subjects without psychiatric diagnosis were recruited.

Effects of 16p11.2 Copy Number Variants on Neuroanatomy

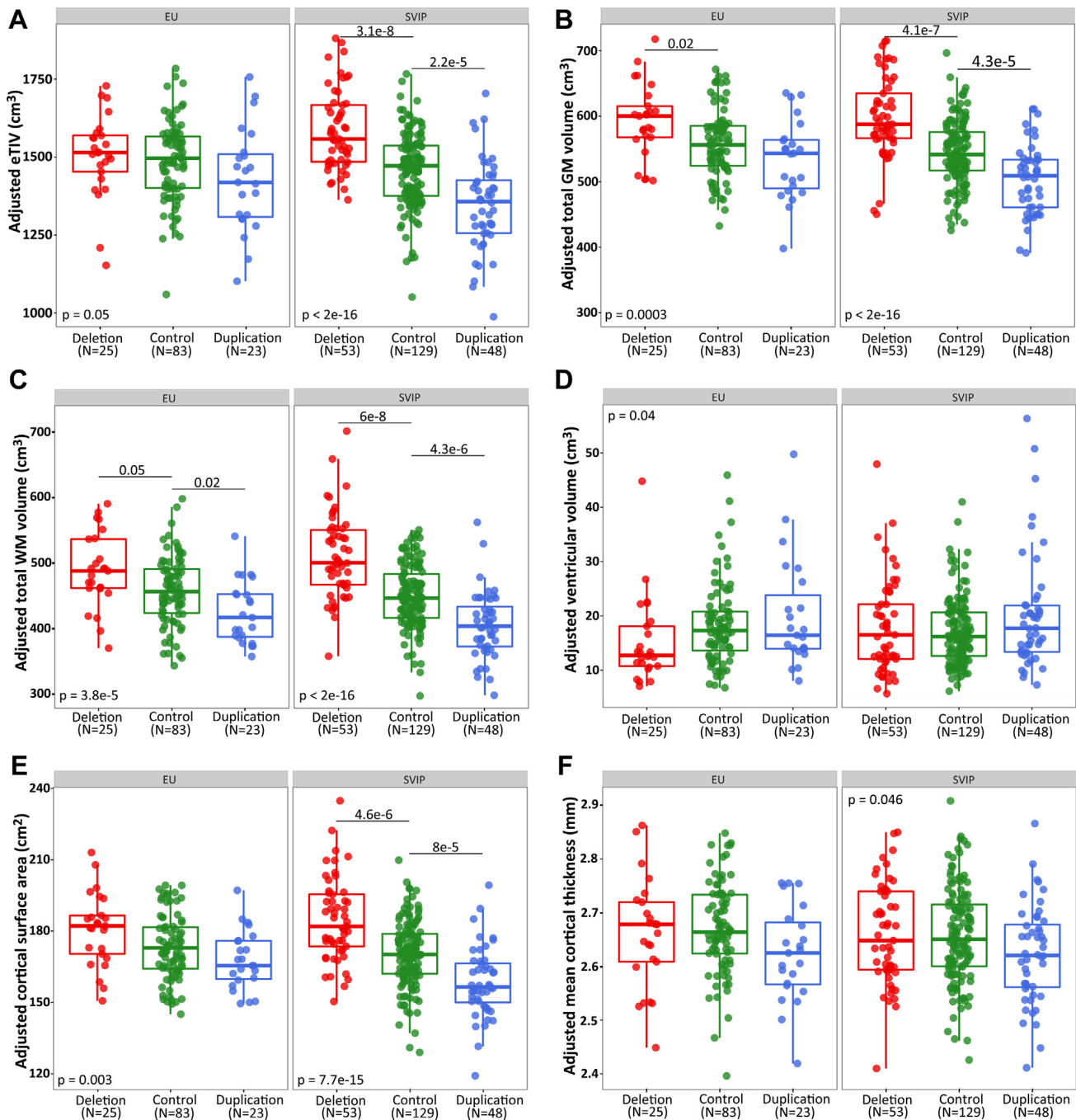


Figure 1. Effects of gene dosage on global brain measures in the European (EU) and Simons Variation in Individuals Project (SVIP) cohorts. Boxplots of (A) estimated total intracranial volume (eTIV), (B) gray matter (GM) volume, (C) white matter (WM) volume, (D) ventricular volume, (E) cortical surface area, and (F) mean cortical thickness in each genetic group separately for the EU and SVIP cohorts. Gene dosage effect is estimated with a linear model using the number of 16p11.2 genomic copies (1, 2, or 3), and including linear and quadratic expansions of age, sex, nonverbal IQ, and magnetic resonance imaging site as fixed covariates. In each box, the bold line corresponds to the median. The bottom and top of the box show the 25th (quartile 1 [Q1]) and 75th (quartile 3 [Q3]) percentiles, respectively. The upper whisker ends at the largest observed data value within the span from Q3 to $Q3 + 1.5 \times \text{interquartile range}$ ($Q3 - Q1$), and lower whisker ends at the smallest observed data value within the span for $Q1$ to $Q1 - (1.5 \times \text{interquartile range})$. Circles that exceed whiskers are outliers. Post hoc comparisons show Bonferroni-corrected p values.

and superior and middle temporal gyri (positive gene dosage). Regions with smaller effect size and no overlap are shown in Figure 3; Supplemental Figure S3A, C; and Supplemental

Table S4. Cortical thickness, on the other hand, shows little overlap with the VBM results (Figure 3; Supplemental Figure S3B, D; and Supplemental Table S5).

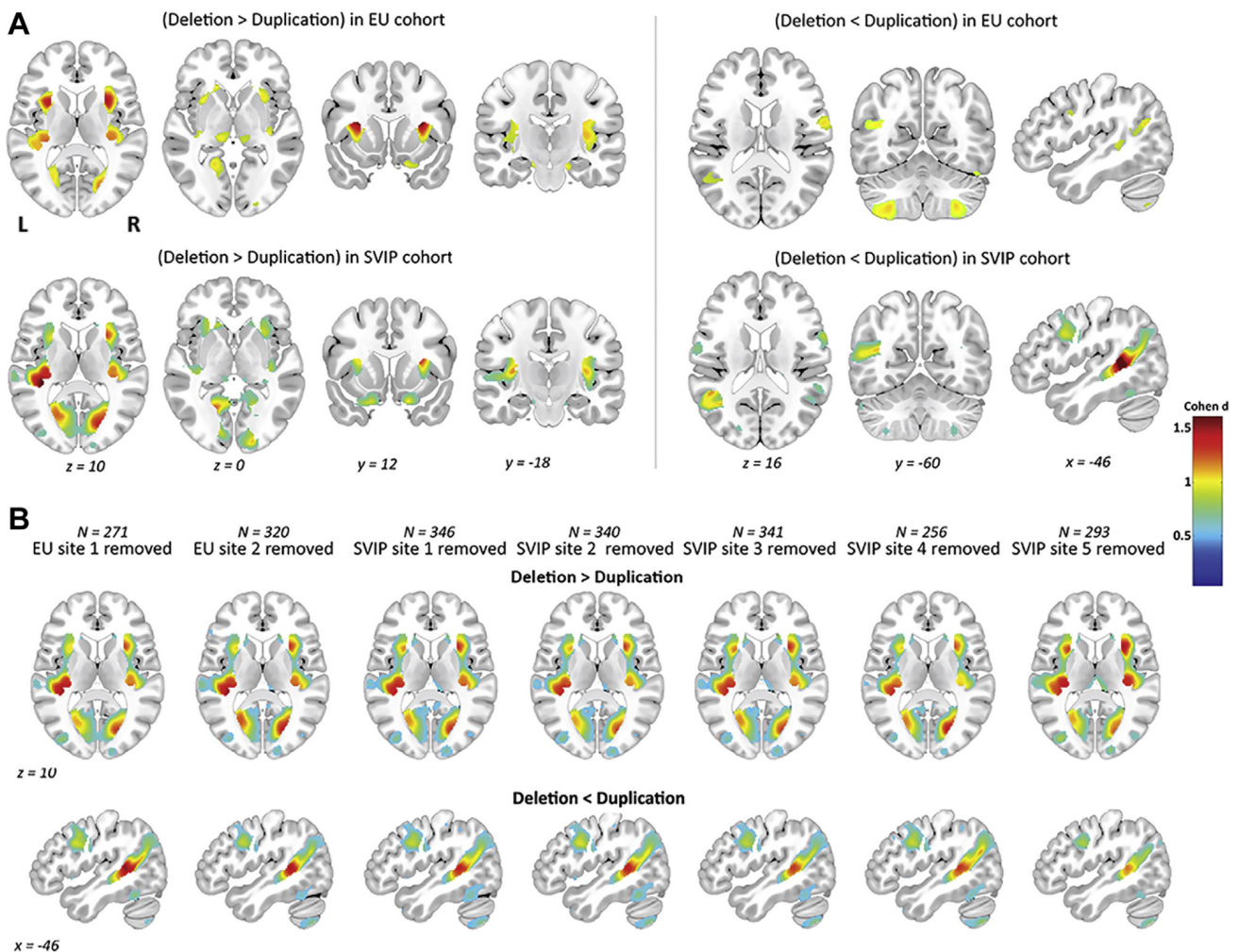


Figure 2. Effects of gene dosage on regional gray matter volume in the Europe (EU) and Simons Variation in Individuals Project (SVIP) cohorts. **(A)** Left panels (deletion > duplication) show voxel-based whole-brain maps, with the volumes of regions showing a negative relationship with the number of 16p11.2 genomic copies. Right panels (deletion < duplication) present the volumes of regions showing a positive relationship with the number of 16p11.2 genomic copies. **(B)** Negative and positive gene dosage effects on gray matter volume following a leave-one-out approach by systematically removing one of the magnetic resonance imaging sites. All the analyses are controlled for linear and quadratic expansions of age, sex, magnetic resonance imaging site, total intracranial volume, and nonverbal IQ. Results significant at a threshold of $p < .05$ familywise error corrected for multiple comparisons are displayed in standard Montreal Neurological Institute space. Color bars represent Cohen's *d*. L, left; R, right.

These regional results are not influenced by subjects' age, sex, cohort, MRI site, or MRI protocol (multiecho vs. single-echo): None of the variables shows an interaction with genetic groups (Figure 2B, Supplemental Figures S4 and S5A). In particular, a subgroup of participants who underwent both multi- and single-echo protocols presents the same alterations (Supplemental Figure S5B). NVIQ does not show any main effect on regional brain structure and was removed as a covariate for the subsequent analyses. Given the above observations, we pooled all data.

Relationship Between Total Brain Volume and Regional Differences

We examined the contribution of global differences to regional alterations. There was no relationship between global metrics and any of the aforementioned large effect regional findings,

even after adding GM volume as a covariate in the VBM analyses. We then tested for correlations between eTIV and the raw or adjusted volumes of some significant regions (Supplemental Figure S6). This demonstrates that small, average, or large brains contribute equally to the regional effects of 16p11.2 CNVs.

Mirror Effects Versus Differential Contribution of CNVs to Regional Differences

To differentiate reciprocal from nonreciprocal effects driven by either the deletion or the duplication carriers, we compared the linear and quadratic effects of gene dosage. The nonreciprocal effects of the 16p11.2 deletion and duplication identified by the quadratic term are detailed in Supplemental Figure S7. Post hoc analyses show that the deletion preferentially impacts the volume and surface area of the calcarine cortex and the

Effects of 16p11.2 Copy Number Variants on Neuroanatomy

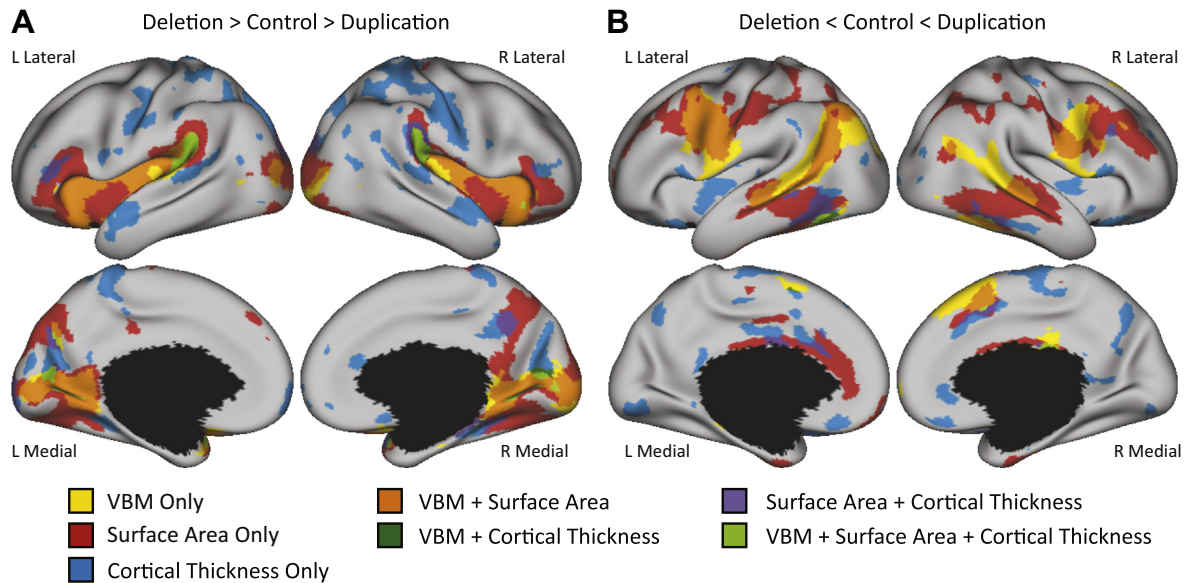


Figure 3. Overlap between voxel-based and surface-based results for cortical alterations associated with gene dosage. The relationship between gene dosage and the morphometric features was compared in the pooled sample ($n = 361$). The voxel-based and surface-based statistical maps are thresholded at the multiple comparisons–corrected p value and then projected on the cortical surface mesh. Regions with effect size ≥ 1 Cohen’s d and overlapping between voxel-based and surface-based analyses are **(A)** the bilateral insula, transverse temporal gyrus, calcarine cortex and **(B)** the precentral, superior and middle temporal gyri. L, left; R, right; VBM, voxel-based morphometry.

transverse temporal gyrus (deletion $>$ control) and the superior and middle temporal gyri (deletion $<$ control), with absolute effect size $> |1|$ Cohen’s d . The duplication carriers do not show any neuroanatomical differences with effect size $> |1|$ Cohen’s d . We observe GM volume changes in the caudate

and hippocampus with Cohen’s d between $[0.5]$ and $[1]$ (duplication $<$ control) (Figure 4B, Supplemental Table S6). Differences with smaller effect sizes or identified only by one of the analytical methods such as alterations in the cerebellum, precentral gyrus, and cingulate are detailed in the

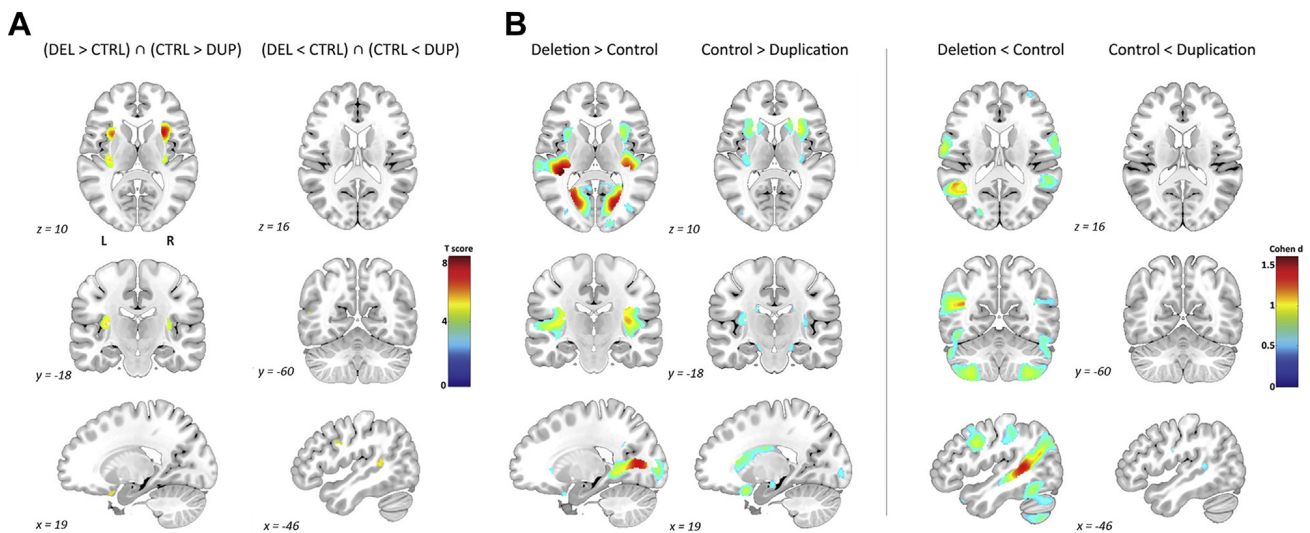


Figure 4. Differential and overlapping contribution of deletion and duplication to the regional gray matter volume differences. **(A)** Results of voxel-based whole-brain maps from the conjunction analysis of both negative (deletion $>$ control AND control $>$ duplication) and positive (deletion $<$ control AND control $<$ duplication) gene dosage. The main mirror pattern is the insula. **(B)** Results of voxel-based whole-brain maps showing the effect size in regions with larger volume in deletion carriers compared with control subjects (deletion $>$ control), in control subjects compared with duplication carriers (control $>$ duplication), in regions with smaller volume in deletion carriers compared with control subjects (deletion $<$ control), and in control subjects compared with duplication carriers (control $<$ duplication). Results significant at a voxel-level threshold of $p < .05$ familywise error corrected for multiple comparisons are displayed in standard Montreal Neurological Institute space. Color bars represent t scores for panel **(A)** and Cohen’s d for panel **(B)**. CTRL, control individuals; DEL, deletion carriers; DUP, duplication carriers; L, left; R, right.

Supplemental Table S6 and Supplemental Figures S8A–D and S9C–F.

The reciprocal mirror effects of the 16p11.2 deletion and duplication are restricted to the bilateral insula. The post hoc conjunction analysis shows that the deletion is associated with an increase of the volume and surface area of the insula, and the duplication is associated with a decrease of this region (Figure 4A, Supplemental Table S6). We do not observe reciprocal effects of gene dosage for cortical thickness measurements (Supplemental Figure S9A, B).

Relationship With Psychiatric Diagnosis and Cognitive Traits

Because the 16p11.2 locus is associated with more than one psychiatric diagnosis, we quantified the overlap of our findings with a large, cross-disorder neuroimaging meta-analysis [<http://anima.fz-juelich.de> (43)]. We observe that the 16p11.2-related VBM map overlaps 33% of the meta-analytic map (Dice index): 46% for the cluster including the left insula, 28% for the right insula, and none for the dorsal anterior cingulate cortex.

We used Neurosynth to meta-analytically decode the psychological terms most closely associated with the main anatomical clusters identified in the VBM analysis. Supplemental Table S7 illustrates the domains most associated with each cluster. The transverse, superior, and middle temporal gyri (regions predominantly affected in deletion carriers) show top associations with language, phonology, and auditory terms. The anterior insula and caudate (alterations found in duplication carriers) are associated with terms such as reward, pain, and executive function (Supplemental Figure S10). Recognizing such inverse inferences can provide hypotheses for future studies but are unable to support strong conclusions.

However, the measures of NVIQ, SRS, and phonological processing measured in participants do not show main effects or interact with the gene dosage effects. The presence of low general intelligence (NVIQ), language impairment (measured by phonological processing), or poor social skills (SRS), or the presence and number of comorbid psychiatric diagnoses, does not change any of the neuroanatomical findings associated with the 16p11.2 deletion or duplication.

Ascertainment and Additional Factors Contributing to Changes in Brain Structure

We tested whether ascertaining carriers for neurodevelopmental symptoms could bias our results. Because clinical ascertainment may enrich as well for additional neurodevelopmental factors present in CNV carriers and their families, we investigated potential brain alterations in the family members who do not carry a 16p11.2 CNV. Comparing control subjects from deletion families ($n = 51$) and unrelated control subjects shows changes in volume and thickness with medium effect size (>0.5 Cohen's d) of the left posterior insula and right lingual gyrus; changes of volume also include the putamen and hippocampus (Figure 5, Supplemental Figure S14E). No effect was found for the cortical surface area (Supplemental Figure S13E).

However, comparing deletion or duplication carriers with familial or unrelated control subjects does not change any of the global (Supplemental Table S2 and Supplemental Figure S11) or regional findings reported above (Supplemental Figures S12, S13A–D, and S14A–D).

DISCUSSION

This large, multisite dataset combines new and previously published data to expand our understanding of the neuroanatomical differences associated with 16p11.2 deletions and

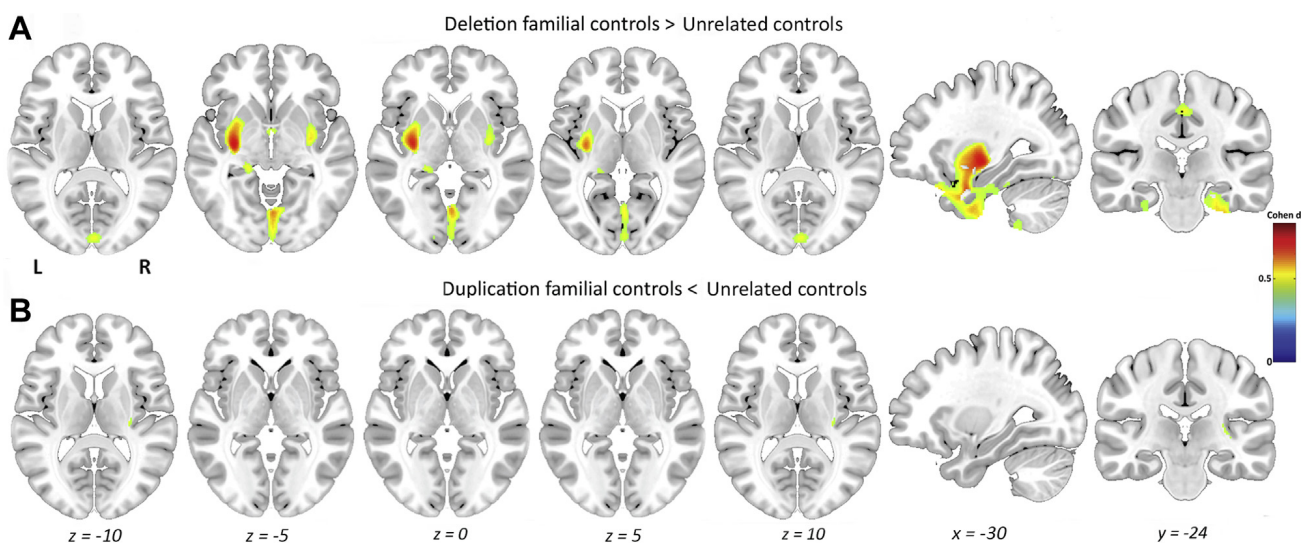


Figure 5. Contribution of familial control subjects to the regional gene dosage-dependent gray matter volume differences. Results of voxel-based whole-brain maps showing (A) regions with larger volume in control subjects from deletion families ($n = 51$) compared with unrelated control subjects ($n = 140$); and (B) regions with smaller volume in control subjects from duplication families ($n = 21$) compared with unrelated control subjects ($n = 140$). Results significant at a voxel-level threshold of $p < .05$ familywise error corrected for multiple comparisons are displayed in standard Montreal Neurological Institute space. Color bars represent effect size (Cohen's d). L, left; R, right.

duplications. The effect of the reciprocal CNVs on brain structure is generalizable across heterogeneously ascertained cohorts and remains significant beyond differences in MRI scanners, imaging protocols, analysis with two complementary computational methods, sex, age, and presence and number of comorbid psychiatric diagnoses. We extend previous neuroimaging studies by characterizing the reciprocal and differential effect of deletions and duplications on brain structure. While 16p11.2 deletions and duplications impact reciprocally bilateral insula [a gateway for sensory interoception, self-recognition, and emotional awareness (44)], differences in other brain areas are predominantly associated with either CNV.

Recent publications have questioned the reliability of neuroimaging studies that are prone to both type I and II errors (45). Our results provide robust estimates for CNV effect sizes on brain structure. Our sample size is adequate to detect the large effects associated with both CNVs, greatly reducing the probability of spurious findings. In imaging genetics, it has often been assumed that genetic variants may have larger effects on imaging phenotypes than on clinical traits or psychiatric risk (45). Our study shows, however, that the effect size of CNVs on brain structure is similar to their effect previously published for cognitive and behavioral traits (13,18). The effect of the deletion is approximately twice that of the duplication for global and regional brain volumes as well as clinical traits (such as IQ loss) (13).

The brain regions showing gene dosage effects are implicated in phonology, language, reward, and executive function networks. These are diverse functions that are each complex and heterogeneous. Nonetheless, the associations raise hypotheses for future studies. Similarly, the spatial overlap between our findings and the meta-analytical results performed across all Axis I psychiatric diagnoses from the DSM-IV-TR (43) may provide clues to pathological patterns underlying the risk for psychiatric diagnoses conferred by 16p11.2 CNVs.

The effects of CNVs on brain structure are not changed by ascertainment for either neurodevelopmental or psychiatric symptoms. Differences in IQ, language ability, or social responsiveness or the presence and number of psychiatric diagnoses do not influence any of the findings. We have previously reported a similar observation for cognition showing that the 16p11.2 deletion is associated with a decrease in IQ of 25 points regardless of whether carriers have intellectual disabilities or intelligence in the normal range (13).

This observation is consistent with an additive model underlying psychiatric disorders (46). Under this assumption, brain alterations associated with CNVs contribute to, but do not necessarily correlate with, a psychiatric diagnosis because additional brain alterations or other factors are required for the onset of the disorder. This is in agreement with studies demonstrating that GM changes in the superior temporal gyrus, insula, and cingulate are observed in individuals both diagnosed with psychosis and at high risk for developing psychosis (47).

Contrasting familial and unrelated control subjects reveals regional differences partially overlapping with the 16p11.2 gene dosage alterations. Of note, these alterations involve cortical thickness as opposed to CNV-related cortical surface

changes. This may suggest the presence of additional factors in these families ascertained in the neurodevelopmental clinic. Assortative mating in families (in particular when the CNV is inherited) may also contribute to an increase of risk factors (48).

We are not implying that our findings are specific to the 16p11.2 locus. Differences in global and local GM volumes as well as surface and thickness have been observed in similar regions in 22q11.2 deletion carriers, another large-effect-size genetic risk factor for psychiatric conditions (49–51). They are also reminiscent of decreased regional volumes in brain areas associated with emotion and face processing demonstrated in individuals with a 7q11.23 deletion (52,53). It is still unclear whether these shared alterations in brain structure relate to similar changes in tissue properties and underlying molecular mechanisms, but they may suggest neuroanatomical convergence across different genetic risk factors. This is illustrated by a study of several genetically modified mouse models of ASD and intellectual disability showing that their regional neuroanatomical alterations can be grouped in three different clusters (6).

Limitations

The broad age range of our dataset (6–63 years of age) is a potential limitation. However, we did not find any interaction between age and effects of gene dosage. The global and regional alterations remain unchanged in age-specific subgroups, with the caveat of a significant decrease in power (Supplemental Figures S2 and S4A). The developmental onset of global and regional differences in 16p11.2 CNV carriers remains unknown, but the insula, striatum, and thalamus are also altered in a 7-day-old 16p11.2 deletion mouse model (54,55), suggesting an early developmental effect. However, specific anatomical effects are difficult to interpret between humans and mouse models. The multisite data represents another limitation and can introduce false-positive findings. However, investigating the impact of sites using main as well as random effects did not identify any biases introduced by the different scanners: this means that the effect of the CNV may be more important than the noise introduced by the multiple MRI sites. Finally, the missing clinical data may limit our power to detect correlations between the brain morphometric measurements and the cognitive and clinical data.

The strong results of this multisite genetic-first neuroimaging study provide a robust characterization of 16p11.2 deletion and duplication effects on neuroanatomy. The deletion and duplication of the same genetic interval may affect brain regions in opposing ways, but other structures are preferentially altered by one of the two CNVs. The morphometric effect sizes are comparable to those previously recorded on cognitive traits. Results are generalizable across sites, computational methods, age, sex, and ascertainment for psychiatric or neurodevelopmental disorders. This suggests that these brain alterations are related to the risk conferred by the CNVs rather than the clinical manifestations observed in carriers. This highlights the relevance of studying genetic risk factors as a complement to groups

defined on the basis of behavioral criteria. Future longitudinal studies are required to establish the onset of these alterations.

ACKNOWLEDGMENTS AND DISCLOSURES

This work was supported by Simons Foundation Grant Nos. SFARI219193 (to RLB) and SFARI274424 (to AR); a Bursary Professor fellowship of the Swiss National Science Foundation (SNSF) (to SJ); SNSF Grant No. 31003A160203 (to AR); SNSF Sinergia Grant No. CRSII33-133044 (to AR); SNSF National Centre of Competence in Research Synapsy and project Grant No. 32003B_159780 (to BD); Foundation Parkinson Switzerland and Foundation Synapsis (to BD); European Union Seventh Framework Programme (FP7/2015-2018) Grant No. 604102 (Human Brain Project) (to BD); the Roger De Spoelberch and Partridge Foundations; a Canada Research Chair in neurodevelopmental disorders (to SJ), and a chair from the Jeanne et Jean Louis Levesque Foundation (to SJ). This research was enabled by support provided by Calcul Quebec (<http://www.calculquebec.ca>) and Compute Canada (<http://www.computeCanada.ca>).

We thank all of the families at the participating Simons Variation in Individuals Project (VIP) sites, as well as the Simons VIP Consortium. We appreciate obtaining access to imaging and phenotypic data on SFARI Base. Approved researchers can obtain the Simons VIP population dataset described in this study by applying at <https://base.sfari.org>. Statistical support was provided by data scientist Steven Worthington, at the Institute for Quantitative Social Science, Harvard University. We are grateful to all families who participated in the 16p11.2 European Consortium.

The authors report no biomedical financial interests or potential conflicts of interest.

ARTICLE INFORMATION

From the Service of Medical Genetics (SM-B, BR-H, CMod, AMM, AP, SR, JSB, SJ), Laboratoire de Recherche en Neuroimagerie (SM-B, CMod, FK, BD), Département des neurosciences cliniques, Centre Cantonal Autisme (AMM, AP), Service of General Psychiatry (PC), Department of Psychiatry, Centre Hospitalier Universitaire Vaudois and University of Lausanne; and Center for Integrative Genomics (AR), University of Lausanne, Lausanne, Switzerland; CHU Sainte-Justine Research Center (BR-H, CMor, AEJ, SJ), Université de Montréal, Montréal, Quebec, Canada; Department of Psychology (JAN, RLB) and Center for Brain Science (JAN, AYQ, RLB) Harvard University, Cambridge; and Department of Psychiatry (JAN, RLB), Massachusetts General Hospital; and Athinoula A. Martinos Center for Biomedical Imaging (NRZ, NH, RLB), Department of Radiology, Massachusetts General Hospital, Harvard Medical School, Boston, Massachusetts; Department of Clinical Genetics (AEJ), Odense University Hospital; and Human Genetics (AEJ), Department of Clinical Research, University of Southern Denmark, Odense, Denmark; Department of Neurology (AYQ), University of Kansas Medical Center, Kansas City, KS; Simons Foundation (WKC, JES); and Departments of Pediatrics and Medicine (WKC), Columbia University, New York, New York; Department of Neurology (EHS), Department of Pediatrics, and Weill Institute for Neurosciences, University of California, San Francisco, California; Gillberg Neuropsychiatry Centre (NH), University of Gothenburg, Gothenburg, Sweden; and the Department of Neurology, Max Planck Institute for Human Cognitive and Brain Sciences (BD), Leipzig, Germany.

Contributors to the Simons VIP Consortium include the following: Hanalore Alupay, BS, Benjamin Aaronson, BS, Sean Ackerman, MD, Katy Ankenman, MSW, Ayesha Anwar, BA, Constance Atwell, PhD, Alexandra Bowe, BA, Arthur L. Beaudet, MD, Marta Benedetti, PhD, Jessica Berg, MS, Jeffrey Berman, PhD, Leandra N. Berry, PhD, Audrey L. Bibb, BS, Lisa Blaskey, PhD, Jonathan Brennan, PhD, Christie M. Brewton, MS, Randy Buckner, PhD, Polina Bukshpun, BA, Jordan Burko, BA, Phil Cali, EdS, Bettina Cerban, BA, Yishin Chang, MS, Maxwell Cheong, BE, MS, Vivian Chow, BA, Zili Chu, PhD, Darina Chudnovskaya, BS, Lauren Cornew, PhD, Corby Dale, PhD, John Dell, BS, Allison G. Dempsey, PhD, Trent Deschamps, BS, Rachel Earl, BA, James Edgar, PhD, Jenna Elgin, BS, Jennifer Endre Olson, PsyD, Yolanda L. Evans, MA, Anne Findlay, MA,

Gerald D Fischbach, MD, Charlie Fisk, BS, Briana Fregeau, BA, Bill Gaetz, PhD, Leah Gaetz, MSW, BSW, BA, Silvia Garza, BA, Jennifer Gerds, PhD, Orit Glenn, MD, Sarah E Gobuty, MS, CGC, Rachel Golembki, BS, Marion Greenup, MPH, MEd, Kory Heiken, BA, Katherine Hines, BA, Leighton Hinkley, PhD, Frank I. Jackson, BS, Julian Jenkins III, PhD, Rita J. Jeremy, PhD, Kelly Johnson, PhD, Stephen M. Kanne, PhD, Sudha Kessler, MD, Sarah Y. Khan, BA, Matthew Ku, BS, Emily Kuschner, PhD, Anna L. Laakman, MEd, Peter Lam, BS, Morgan W. Lasala, BA, Hana Lee, MPH, Kevin LaGuerre, MS, Susan Levy, MD, Alyss Lian Cavanagh, MA, Ashlie V. Llorens, BS, Katherine Loftus Campe, MEd, Tracy L. Luks, PhD, Elysa J. Marco, MD, Stephen Martin, BS, Alastair J. Martin, PhD, Gabriela Marzano, HS, Christina Masson, BFA, Kathleen E. McGovern, BS, Rebecca McNally Keehn, PhD, David T. Miller, MD, PhD, Fiona K. Miller, PhD, Timothy J. Moss, MD, PhD, Rebecca Murray, BA, Srikanth S. Nagarajan, PhD, Kerri P. Nowell, MA, Julia Owen, PhD, Andrea M. Paal, MS, Alan Packer, PhD, Patricia Z. Page, MS, Brianna M. Paul, PhD, Alana Peters, BS, Danica Peterson, MPH, Annapurna Poduri, PhD, Nicholas J. Pojman, BS, Ken Porche, MS, Monica B. Proud, MD, Saba Qasmieh, BA, Melissa B. Ramocki, MD, PhD, Beau Reilly, PhD, Timothy P. L. Roberts, PhD, Dennis Shaw, MD, Tuhin Sinha, PhD, Bethanny Smith-Packard, MS, CGC, Anne Snow Gallagher, PhD, Vivek Swarnakar, PhD, Tony Thieu, BA, MS, Christina Triantafallou, PhD, Roger Vaughan, PhD, Mari Wakahiro, MSW, Arianne Wallace, PhD, Tracey Ward, BS, Julia Wenegrat, MA, and Anne Wolken, BS.

Members of the European 16p11.2 Consortium include the following: Addor Marie-Claude, Service de génétique médicale, Centre Hospitalier Universitaire Vaudois, Lausanne University, Switzerland; Andrieux Joris, Institut de Génétique Médicale, CHRU de Lille, Hôpital Jeanne de Flandre, France; Arveiler Benoît, Service de génétique médicale, CHU de Bordeaux-GH Pellegrin, France; Baujat Geneviève, Service de Génétique Médicale, CHU Paris - Hôpital Necker-Enfants Malades, France; Sloan-Béna Frédérique, Service de médecine génétique, Hôpitaux Universitaires de Genève - HUG, Switzerland; Belfiore Marco, Service de génétique médicale, Centre Hospitalier Universitaire Vaudois, Lausanne University, Switzerland; Bonneau Dominique, Service de génétique médicale, CHU d'Angers, France; Bouquillon Sonia, Institut de Génétique Médicale, Hôpital Jeanne de Flandre, Lille, France; Boute Odile, Hôpital Jeanne de Flandre, CHRU de Lille, Lille, France; Brusco Alfredo, Genetica Medica, Dipartimento di Scienze Mediche, Università di Torino, Italy; Busa Tiffany, Département de génétique médicale, CHU de Marseille, Hôpital de la Timone, France; Caberg Jean-Hubert, Centre de génétique humaine, CHU de Liège, Belgique; Campion Dominique, Service de psychiatrie, Centre hospitalier de Rouvray, Sotteville lès Rouen, France; Colombert Vanessa, Service de génétique médicale, Centre Hospitalier Bretagne Atlantique CH Chubert- Vannes, France; Cordier Marie-Pierre, Service de génétique clinique, CHU de Lyon, Hospices Civils de Lyon, France; David Albert, Service de Génétique Médicale, CHU de Nantes, Hôtel Dieu, France; Debray François-Guillaume, Service de Génétique Humaine, CHU Sart Tilman - Liège, Belgique; Delrue Marie-Ange, Service de génétique médicale, CHU de Bordeaux, Hôpital Pellegrin, France; Doco-Fenzy Martine, Service de Génétique et Biologie de la Reproduction, CHU de Reims, Hôpital Maison Blanche, France; Dunkhase-Heinl Ulrike, Department of Pediatrics, Aabenraa Hospital, Sonderjylland, Denmark; Edery Patrick, Service de génétique clinique, CHU de Lyon, Hospices Civils de Lyon, France; Fagerberg Christina, Department of Clinical Genetics, Odense University Hospital, Denmark; Favre Laurence, Centre de génétique, Hôpital d'Enfants, CHU Dijon Bourgogne - Hôpital François Mitterrand, France; Forzano Francesca, Ambulatorio di Genetica Medica, Ospedal Galliera di Genova, Italy and Clinical Genetics Department, 7th Floor Borough Wing, Guy's Hospital, Guy's & St Thomas' NHS Foundation Trust, Great Maze Pond, London SE1 9RT, UK; Genevieve David, Département de Génétique Médicale, Maladies Rares et Médecine Personnalisée, service de génétique clinique, Université Montpellier, Unité Inserm U1183, CHU Montpellier, Montpellier, France; Gérard Marion, Service de Génétique, CHU de Caen, Hôpital Clémenceau, France; Giachino Daniela, Genetica Medica, Dipartimento di Scienze Cliniche e Biologiche, Università di Torino, Italy; Guichet Agnès, Service de génétique, CHU d'Angers, France; Guillin Olivier, Service de psychiatrie, Centre hospitalier du Rouvray, Sotteville lès Rouen, France; Héron Delphine, Service de Génétique clinique, CHU Paris-GH La Pitié Salpêtrière-Charles Foix - Hôpital Pitié-Salpêtrière, France; Isidor Bertrand, Service de

Effects of 16p11.2 Copy Number Variants on Neuroanatomy

Génétique Médicale, CHU de Nantes, Hôtel Dieu, France; Jacqueline Aurélie, Service de Génétique clinique, CHU Paris-GH La Pitié Salpêtrière-Charles Foix - Hôpital Pitié-Salpêtrière, France; Jaillard Sylvie, Service de Génétique Moléculaire et Génomique – Pôle biologie, CHU de Rennes, Hôpital Pontchaillou, France; Journel Hubert, Service de génétique médicale, Centre Hospitalier Bretagne Atlantique CH Chubert- Vannes, France; Keren Boris, Centre de Génétique Moléculaire et Chromosomique, CHU Paris-GH La Pitié Salpêtrière-Charles Foix - Hôpital Pitié-Salpêtrière, France; Lacombe Didier, Service de génétique médicale, CHU de Bordeaux-GH Pellegrin, France; Lebon Sébastien, Pediatric Neurology Unit, Department of Pediatrics, Lausanne University Hospital, Lausanne, Switzerland; Le Caignec Cédric, Service de Génétique Médicale - Institut de Biologie, CHU de Nantes, France; Lemaître Marie-Pierre, Service de Neuropédiatrie, Centre Hospitalier Régional Universitaire de Lille, France; Lespinasse James, Service génétique médicale et oncogénétique, Hotel Dieu, Chambéry, France; Mathieu-Dramart Michèle, Service de Génétique Clinique, CHU Amiens Picardie, France; Mercier Sandra, Service de Génétique Médicale, CHU de Nantes, Hôtel Dieu, France; Mignot Cyril, Service de Génétique clinique, CHU Paris-GH La Pitié Salpêtrière-Charles Foix - Hôpital Pitié-Salpêtrière, France; Missirian Chantal, Département de génétique médicale, CHU de Marseille, Hôpital de la Timone, France; Petit Florence, Service de génétique clinique Guy Fontaine, Hôpital Jeanne de Flandre, CHRU de Lille, France; Pilekær Sørensen Kristina, Department of Clinical Genetics, Odense University Hospital, Denmark; Pinson Lucile, Département de Génétique Médicale, Maladies Rares et Médecine Personnalisée, service de génétique clinique, Université Montpellier, Unité Inserm U1183, CHU Montpellier, Montpellier, France; Plessis Ghislaine, Service de Génétique, CHU de Caen, Hôpital Clémenceau, France; Prieur Fabienne, Service de génétique clinique, CHU de Saint-Etienne - Hôpital Nord, France; Rooryck-Thambo Caroline, Laboratoire de génétique moléculaire, CHU de Bordeaux-GH Pellegrin, France; Rossi Massimiliano, Service de génétique clinique, CHU de Lyon, Hospices Civils de Lyon, France; Sanlaville Damien, Laboratoire de Cytogénétique Constitutionnelle, CHU de Lyon, Hospices Civils de Lyon, France; Schlott Kristiansen Britta, Department of Clinical Genetics, Odense University Hospital, Denmark; Schluth-Bolard Caroline, Laboratoire de Cytogénétique Constitutionnelle, CHU de Lyon, Hospices Civils de Lyon, France; Till Marianne, Service de génétique clinique, CHU de Lyon, Hospices Civils de Lyon, France; Van Haelst Mieke, Department of Genetics, University Medical Center Utrecht, Holland; Van Maldergem Lionel, Centre de Génétique humaine, CHRU de Besançon - Hôpital Saint-Jacques, France.

SM-B, BR-H, and JAN contributed equally to this work as joint first authors. BD and SJ contributed equally to this work as joint senior authors.

Address correspondence to Sébastien Jacquemont, M.D., Service of Medical Genetics, Lausanne University Hospital and University of Lausanne, CH-1015 Lausanne, Switzerland; and Department of Pediatrics, Division of Medical Genetics, Centre Hospitalier Universitaire Sainte-Justine Research Center, Montreal, QC H3T 1C5, Canada; E-mail: sebastien.jacquemont@umontreal.ca.

Received Oct 18, 2017; revised Feb 1, 2018; accepted Feb 24, 2018.

Supplementary material cited in this article is available online at <https://doi.org/10.1016/j.biopsych.2018.02.1176>.

REFERENCES

- Pua EPK, Bowden SC, Seal ML (2017): Autism spectrum disorders: Neuroimaging findings from systematic reviews. *Res Autism Spectr Disord* 34:28–33.
- Sparks BF, Friedman SD, Shaw DW, Aylward EH, Echelard D, Artru AA, *et al.* (2002): Brain structural abnormalities in young children with autism spectrum disorder. *Neurology* 59:184–192.
- Courchesne E, Pierce K, Schumann CM, Redcay E, Buckwalter JA, Kennedy DP, Morgan J (2007): Mapping early brain development in autism. *Neuron* 56:399–413.
- Hazlett HC, Gu H, Munsell BC, Kim SH, Styner M, Wolff JJ, *et al.* (2017): Early brain development in infants at high risk for autism spectrum disorder. *Nature* 542:348–351.
- Stanfield AC, McIntosh AM, Spencer MD, Philip R, Gaur S, Lawrie SM (2008): Towards a neuroanatomy of autism: A systematic review and meta-analysis of structural magnetic resonance imaging studies. *Eur Psychiatry* 23:289–299.
- Ellegood J, Anagnostou E, Babineau BA, Crawley JN, Lin L, Genestine M, *et al.* (2014): Clustering autism: using neuroanatomical differences in 26 mouse models to gain insight into the heterogeneity. *Mol Psychiatry* 20:118–125.
- Amaral DG (2011): The promise and the pitfalls of autism research: An introductory note for new autism researchers. *Brain Res* 1380:3–9.
- Amaral DG, Schumann CM, Nordahl CW (2008): Neuroanatomy of autism. *Trends Neurosci* 31:137–145.
- Franke B, Ripke S, Anttila V, Hibar DP, van Hulzen KJE, Smoller JW, *et al.* (2016): Genetic influences on schizophrenia and subcortical brain volumes: Large-scale proof of concept. *Nat Neurosci* 19:420–431.
- Zufferey F, Sherr EH, Beckmann ND, Hanson E, Maillard AM, Hippolyte L, *et al.* (2012): A 600 kb deletion syndrome at 16p11.2 leads to energy imbalance and neuropsychiatric disorders. *J Med Genet* 49:660–668.
- Weiss LA, Shen Y, Korn JM, Arking DE, Miller DT, Fossdal R, *et al.* (2008): Association between microdeletion and microduplication at 16p11.2 and autism. *N Engl J Med* 358:667–675.
- Sanders SJ, He X, Willsey AJ, Ercan-Sencicek AG, Samocha KE, Cicek AE, *et al.* (2015): Insights into autism spectrum disorder genomic architecture and biology from 71 risk loci. *Neuron* 87:1215–1233.
- D'Angelo D, Lebon S, Chen Q, Martin-Brevet S, Snyder LG, Hippolyte L, *et al.* (2016): Defining the effect of the 16p11.2 duplication on cognition, behavior, and medical comorbidities. *JAMA Psychiatry* 73:20–11.
- Hanson E, Bernier R, Porche K, Jackson FI, Goin-Kochel RP, Snyder LG, *et al.* (2015): The Cognitive and behavioral phenotype of the 16p11.2 deletion in a clinically ascertained population. *Biol Psychiatry* 77:785–793.
- Moreno-De-Luca A, Evans DW, Boomer KB, Hanson E, Bernier R, Goin-Kochel RP, *et al.* (2015): The role of parental cognitive, behavioral, and motor profiles in clinical variability in individuals with chromosome 16p11.2 deletions. *JAMA Psychiatry* 72:119–8.
- McCarthy SE, Makarov V, Kirov G, Addington AM, McClellan J, Yoon S, *et al.* (2009): Microduplications of 16p11.2 are associated with schizophrenia. *Nat Genet* 41:1223–1227.
- Marshall CR, Howrigan DP, Merico D, Thiruvahindrapuram B, Wu W, Greer DS, *et al.* (2016): Contribution of copy number variants to schizophrenia from a genome-wide study of 41,321 subjects. *Nat Genet* 49:27–35.
- Hippolyte L, Maillard AM, Rodriguez-Herreros B, Pain A, Martin-Brevet S, Ferrari C, *et al.* (2016): The number of genomic copies at the 16p11.2 locus modulates language, verbal memory, and inhibition. *Biol Psychiatry* 80:129–139.
- Jacquemont S, Raymond A, Zufferey F, Harewood L, Walters RG, Kutalik Z, *et al.* (2011): Mirror extreme BMI phenotypes associated with gene dosage at the chromosome 16p11.2 locus. *Nature* 478:97–102.
- Maillard AM, Ruef A, Pizzagalli F, Migliavacca E, Hippolyte L, Adaszewski S, *et al.* (2014): The 16p11.2 locus modulates brain structures common to autism, schizophrenia and obesity. *Mol Psychiatry* 20:140–147.
- Qureshi AY, Mueller S, Snyder AZ, Mukherjee P, Berman JI, Roberts TPL, *et al.* (2014): Opposing brain differences in 16p11.2 deletion and duplication carriers. *J Neurosci* 34:11199–11211.
- Simons VIP Consortium (2012): Simons Variation in Individuals Project (Simons VIP): A genetics-first approach to studying autism spectrum and related neurodevelopmental disorders. *Neuron* 73:1063–1067.
- Wechsler D (2004): WPPSI-III Echelle d'intelligence pour la période pré-scolaire et primaire: Troisième édition. Paris: ECPA, Les Editions du Centre de Psychologie Appliquée.
- Wechsler D (2005): WISC-IV Echelle d'intelligence de Wechsler pour enfants: WISC-IV. Paris: ECPA, Les Editions du Centre de Psychologie Appliquée.
- Wechsler D (2008): WAIS III Echelle d'intelligence pour adultes. Paris: ECPA, Les Editions du Centre de Psychologie Appliquée.

26. Wechsler D (1999): Wechsler Abbreviated Scale of Intelligence. San Antonio, TX: The Psychological Corporation.
27. Elliott CD (2006): Differential Abilities Scale–2nd Edition (DAS-II). San Antonio, TX: The Psychological Corporation.
28. Korkman M, Kemp SL, Kirk U (2008): Nepsy, Bilan Neuropsychologique de l'enfant: Manuel. Paris: ECPA, les Éditions du Centre de Psychologie Appliquée.
29. Wagner RK, Torgesen JK, Rashotte CA (1999): Comprehensive Test of Phonological Processes (CTOPP). Austin, TX: Pro-Ed.
30. Constantino JN (2002): The Social Responsiveness Scale. Los Angeles: Western Psychological Services.
31. American Psychiatric Association (2013): Diagnostic and Statistical Manual of Mental Disorders, 5th ed. Washington, DC: American Psychiatric Association.
32. Fischl B, Salat DH, Busa E, Albert M, Dieterich M, Haselgrove C, *et al.* (2002): Whole brain segmentation: Neurotechnique automated labeling of neuroanatomical structures in the human brain. *Neuron* 33:341–355.
33. Fischl B, Dale AM (2000): Measuring the thickness of the human cerebral cortex from magnetic resonance images. *Proc Natl Acad Sci U S A* 97:11050–11055.
34. Buckner RL, Head D, Parker J, Fotenos AF, Marcus D, Morris JC, Snyder AZ (2004): A unified approach for morphometric and functional data analysis in young, old, and demented adults using automated atlas-based head size normalization: Reliability and validation against manual measurement of total intracranial volume. *Neuroimage* 23:724–738.
35. Ashburner J, Friston KJ (2005): Unified segmentation. *Neuroimage* 26:839–851.
36. Lorio S, Fresard S, Adaszewski S, Kherif F, Chowdhury R, Frackowiak RS, *et al.* (2016): New tissue priors for improved automated classification of subcortical brain structures on MRI. *Neuroimage* 130:157–166.
37. Ashburner J (2007): A fast diffeomorphic image registration algorithm. *Neuroimage* 38:95–113.
38. Ashburner J, Friston KJ (2000): Voxel-based morphometry—The methods. *Neuroimage* 11:805–821.
39. Friston KJ, Holmes AP, Worsley KJ, Poline JP, Frith CD, Frackowiak RSJ (1994): Statistical parametric maps in functional imaging: A general linear approach. *Hum Brain Mapp* 2:189–210.
40. Worsley KJ (2005): An improved theoretical P value for SPMs based on discrete local maxima. *Neuroimage* 28:1056–1062.
41. Genovese CR, Lazar NA, Nichols T (2002): Thresholding of statistical maps in functional neuroimaging using the false discovery rate. *Neuroimage* 15:870–878.
42. Toro R, Perron M, Pike B, Richer L, Veillette S, Pausova Z, Paus T (2008): Brain size and folding of the human cerebral cortex. *Cereb Cortex* 18:2352–2357.
43. Goodkind M, Eickhoff SB, Oathes DJ, Jiang Y, Chang A, Jones-Hagata LB, *et al.* (2015): Identification of a common neurobiological substrate for mental illness. *JAMA Psychiatry* 72:305–323.
44. Namkung H, Kim S-H, Sawa A (2017): The insula: An underestimated brain area in clinical neuroscience, psychiatry, and neurology. *Trends Neurosci* 40:200–207.
45. Carter CS, Bearden CE, Bullmore ET, Geschwind DH, Glahn DC, Gur RE, *et al.* (2017): Enhancing the informativeness and replicability of imaging genomics studies. *Biol Psychiatry* 82:157–164.
46. Weiner DJ, Wigdor EM, Ripke S, Walters RK, Kosmicki JA, Grove J, *et al.* (2017): Polygenic transmission disequilibrium confirms that common and rare variation act additively to create risk for autism spectrum disorders. *Nat Genet* 45: 86–90.
47. Fusar-Poli P, Radua J, McGuire P, Borgwardt S (2012): Neuroanatomical maps of psychosis onset: Voxel-wise meta-analysis of antipsychotic-naïve VBM studies. *Schizophr Bull* 38:1297–1307.
48. Nordsletten AE, Larsson H, Crowley JJ, Almqvist C, Lichtenstein P, Mataix-Cols D (2016): Patterns of nonrandom mating within and across 11 major psychiatric disorders. *JAMA Psychiatry* 73: 354–2.
49. Chow EWC, Ho A, Wei C, Voormolen EHJ, Crawley AP, Bassett AS (2011): Association of schizophrenia in 22q11.2 deletion syndrome and gray matter volumetric deficits in the superior temporal gyrus. *Am J Psychiatry* 168:522–529.
50. Jalbrzikowski M, Jonas R, Senturk D, Patel A, Chow C, Green MF, Bearden CE (2013): Structural abnormalities in cortical volume, thickness, and surface area in 22q11.2 microdeletion syndrome: Relationship with psychotic symptoms. *Neuroimage Clin* 3:405–415.
51. Schmitt JE, Vandekar S, Yi J, Calkins ME, Ruparel K, Roalf DR, *et al.* (2015): Aberrant cortical morphometry in the 22q11.2 deletion syndrome. *Biol Psychiatry* 78:135–143.
52. Meyer-Lindenberg A, Mervis CB, Berman KF (2006): Neural mechanisms in Williams syndrome: A unique window to genetic influences on cognition and behaviour. *Nat Rev Neurosci* 7:380–393.
53. Reiss AL (2004): An experiment of nature: Brain anatomy parallels cognition and behavior in Williams syndrome. *J Neurosci* 24:5009–5015.
54. Portmann T, Yang M, Mao R, Panagiotakos G, Ellegood J, Dolen G, *et al.* (2014): Behavioral abnormalities and circuit defects in the basal ganglia of a mouse model of 16p11.2 deletion syndrome. *Cell Rep* 7:1077–1092.
55. Ellegood J, Crawley JN (2015): Behavioral and neuroanatomical phenotypes in mouse models of autism. *Neurotherapeutics* 12:521–533.

Quantifying the Effects of 16p11.2 Copy Number Variants on Brain Structure: A Multi-site ‘Genetic-First’ Study

Supplemental Information

Supplemental Methods & Materials

Participants

Participants below 6 years old were excluded. Participants with lower intelligence quotient (IQ) and severe externalized behavior and anxiety were unable to undergo the scanning procedure.

Thirty-four scans were excluded from the analysis based on standardized visual inspection which detected the following image artefacts: incomplete head coverage, ghosting, inhomogeneities, and susceptibility artefacts. We scored each individual image for the abovementioned artefacts using a scale from 1 to 4 (1=extensive, 4=non-existent). Images scoring 3 or 4 in the scale were not used in the analyses. We applied a second level of inspection after the first step of the pre-processing in order to check if the tissue segmentation succeed or failed. If failed, the segmentation was done again.

Psychiatric and cognitive assessments

We pooled IQ assessments using the Wechsler intelligence scales, Wechsler Abbreviated Scale of Intelligence or Differential Abilities Scale (1-5). We used nonverbal IQ (NVIQ) standardized to a mean (standard deviation) of 100 (15), and four IQ subtests: block design, matrices, vocabulary and verbal similarities. Phonological skills were evaluated in the American cohort with the comprehensive test of phonological processing – non-word Repetition subtest (6) and in the European cohort with the developmental neuropsychological assessment - nonword repetition task

(7). Parents completed the social responsiveness scale, SRS (8)– an extensively validated quantitative measure of characterizing traits and symptoms of the autistic syndrome– about their offspring 4-18 years old. The SRS-Adult version was completed for each parent by a spouse or partner. Raw scores were used to provide greater differentiation of scores at the lower and higher end of the scales.

Experienced, licensed clinicians provided clinical DSM-V diagnoses (9), using all information obtained during the research evaluation. In Europe, participants underwent a Diagnostic Interview for Genetic Studies (DIGS) (10) in case of suspicion of a psychiatric diagnosis, and an Autism Diagnostic Interview (ADI-R) (11) in case of suspicion of autism. In North America, the Autism Diagnostic Observation Schedule (ADOS) (12), ADI-R, Vineland-II (13) and Social Communication Questionnaire (14) were systematically performed. Unrelated controls with any major DSM-V diagnosis or with a family member diagnosed with neurodevelopmental disorders or genetic abnormalities were excluded. Data have been collected on the entire dataset for NVIQ and the number of psychiatric diagnosis. Numbers for the other measures are detailed in **Table 1** and **Supplemental Table S1**.

MRI data acquisition and processing

16p11.2 European Consortium. MRI data of the EU participants were acquired on two 3T whole-body scanners: 14 carriers of a 16p11.2 deletion and 17 duplication carriers, together with 59 controls (21 familial and 38 unrelated controls) were examined on a Magnetom TIM Trio (Siemens Healthcare, Erlangen, Germany), using a 12-channel RF receive head coil and RF body transmit coil. New data from 17 carriers (11 deletions, 6 duplications) and 24 familial controls were scanned on a Magnetom Prisma Syngo (Siemens Healthcare, Erlangen, Germany) using a

64-channel RF receive head coil and RF body transmit coil. T1-weighted (T1w) anatomical images acquired with the TIM Trio scanner used a Multi-Echo Magnetization Prepared RApid Gradient Echo sequence (ME-MPRAGE: 176 slices; 256×256 matrix; echo time (TE): TE1 = 1.64 ms, TE2 = 3.5 ms, TE3 = 5.36 ms, TE4 = 7.22 ms; repetition time (TR): 2530 ms; flip angle 7°). On the Prisma Syngo scanner, T1w images were acquired using a single-echo MPRAGE sequence (176 slices; 256×256 matrix; TE = 2.39 ms; TR = 2000 ms; flip angle 9°).

Simons VIP study. Data were acquired using multi and single-echo sequences. Overall, 174 participants (38 deletion carriers, 34 duplication carriers and 102 unrelated controls) underwent the research MRI protocol at two imaging core sites on matched 3T Magnetom TIM Trio MRI scanners (Siemens Healthcare, Erlangen, Germany), using the vendor-supplied 32-channel phased-array radio-frequency head coils. Sixty-eight participants were scanned at University of California sites (UC) and 106 at the Children Hospital of Philadelphia (CHOP). Structural MRI data included multi-echo T1w ME-MPRAGE using the following parameters: 176 slices, 256×256 matrix, TR = 2530 ms, TI = 1200 ms, TE = 1.64 ms, and flip angle 7°. Clinical MRI images (single-echo) obtained at the phenotyping core sites were also analyzed. A sample of 15 deletion and 14 duplication carriers, together with 27 familial controls were scanned at University of Washington Medical Center, Baylor University Medical Center and Boston Children's Hospital on two matched 3T Philips Achieva (Philips Healthcare, United States of America) and one unmatched Magnetom TIM Trio scanner (Siemens Healthcare, Erlangen, Germany), respectively. T1w images were acquired using single-echo MPRAGE sequence and the following parameters: 160 slices; 256×256 matrix; TE = 2.98 ms; TR = 2300 ms; flip angle 9°.

All multi-echo images were averaged following a Root-Mean Square (RMS) averaging method. For each voxel, RMS calculates the mean of the intensities between the magnitude images of all echo times as follows:

$$RMS_{average} = \sqrt{I(TE1)^2 + I(TE2)^2 + I(TE3)^2 + I(TE4)^2}$$

Surface-based processing. The FreeSurfer's automated volumetric algorithm allowed to estimate the global measures of brain structure such as cortical gray and white matter volumes (GM and WM respectively) (15) and the ventricular volumes. Cortical GM volume was then decomposed by FreeSurfer's automated surface-based algorithms into its two orthogonal components: cortical thickness and surface area (16). This algorithm estimated the white matter/gray matter and gray matter/pial matter boundaries and constructed tessellated meshes, representing the cortical surfaces. The cortical thickness of all vertices in the cerebral cortex was then calculated from the white matter and pial surfaces. The total surface area for each individual was calculated by summing the area of the triangles that formed the tessellated mesh of the cortex. The local cortical surface area measurements were calculated by summing the area of the triangles immediately surrounding a vertex.

Voxel-based processing. The SPM12 algorithm (Wellcome Trust Centre for Neuroimaging, London, UK, www.fil.ion.ac.uk/spm), running under MATLAB 9.0 (Mathworks, Sherborn, MA, USA), followed the automated tissue classification in the "unified segmentation" framework (17), using an enhanced set of brain tissue priors for increased accuracy for subcortical structures (18). The resulting tissue probability maps were transformed non-linearly to standard MNI space using the diffeomorphic inter-subject registration algorithm (DARTEL) (19). Grey matter probability maps were scaled with the corresponding Jacobian determinants to preserve the initial total amount

of signal intensity followed by an isotropic Gaussian smoothing kernel of 8 mm full-width-at-half-maximum (FWHM) (20; 21).

Data analysis

Z-scores for Head Circumference (HC) were estimated based on age- and sex-normed orbitofrontal HC measurements obtained using Swiss anthropometric normative data as a reference population (22; 23).

Voxel-brain morphometry (VBM) analysis. An explicit masking of GM was used to ensure inclusion of the same number of voxels in all analyses. The mask was created by averaging smoothed (FWHM of 3 mm isotropic) Jacobian-modulated tissue probability maps in MNI space across all subjects.

For visualization purposes, final brain maps were generated using BSPMVIEW MATLAB toolbox (<http://doi.org/10.5281/zenodo.59461>), and highlighted GM regions were identified and labelled by mapping the Neuromorphometrics human brain atlas (Neuromorphometrics Inc., <http://neuromorphometrics.com>). SPM T-maps were converted to Cohen d maps with CAT12 toolbox (<http://dbm.neuro.uni-jena.de/cat12/>).

Surface-based analysis. We used the Desikan-Killiany atlas (24) to label brain regions. All vertices in the fsaverage5 space were included in the analyses, except those that were part of the corpus callosum or medial wall, or those labeled as “unknown”. We visualized the results with the Connectome Workbench on the Human Connectome Project’s 32k vertex standard inflated mesh (25).

Analyses on the covariates. We estimated the influence of several covariates on the regional pattern of gene-dosage dependency in the VBM analyses. For the influence of MRI sites, we

performed a ‘leave-one-out’ approach. We systematically removed one of the MRI sites from the statistical design to determine whether any of the sites were preferentially driving the effect. We also controlled for the effect of the 7 scanning “sites” including them as a random term in a linear mixed model.

Furthermore, we interacted the genetic groups with different covariates, especially the age, the sex (male and female), the MRI parameters (single- vs multi-echo). We divided the dataset in 3 age bins to analyze the effect of the broad age range on the results: individuals below or equal to 12 years of age (40 deletion carriers, 12 duplication carriers and 36 controls); individuals between 12 and 21 years of age (22 deletion carriers, 11 duplication carriers and 68 controls); individuals above 21 years of age (16 deletion carriers, 48 duplication carriers and 108 controls). We also compared the results on a subset of 31 deletion carriers and 33 duplication carriers who underwent both single- and multi-echo protocols. Finally, we used two distinct methods to explore the contribution of the global GM volume to the regional brain differences between genetic groups. The local covariation approach (26) consisted in including the total GM volume of each participant as an additional covariate in the statistical design. Secondly, some regional volumes extracted with Neuromorphometric toolbox were plotted against the eTIV measures to determine whether the regional gene dosage-dependent differences were present across the full range of eTIV distribution.

Meta-analytic functional decoding analysis. We used the NeuroSynth database (<http://neurosynth.org>), which contains activation coordinates for 5809 fMRI studies. The Neurosynth platform provides a quantitative inference about potential cognitive functions linked to patterns of activation. The database contains automatically generated meta-analysis maps for several thousand psychological terms and topics (27). Statistical inference is calculated using a

chi-square test to generate P value maps (28). Contrast maps for each term were computed by comparing studies that loaded highly on that term to all other studies where that term did not load. A correlation analysis was performed between each term and the peak of each anatomical cluster associated with the 16p11.2 alterations. The resulting coefficients were ranked to find the most associated psychological terms.

Table S1. Population characteristics of familial controls and unrelated controls

	Controls of deletion families			Unrelated controls			Controls of duplication families		
	EU	SVIP	N	EU	SVIP	N	EU	SVIP	N
N	30	21	38	38	102	15	15	6	6
Age (years)									
Mean (SD)	34.8 (14) ^b	15.2 (11)	21.4 (7.7) ^a	26.5 (14.7) ^a	34.1 (12) ^b	13.6 (4.9)	12.3 – 52.1	7.3 – 20.3	7.3 – 20.3
range (min-max)	7.8 – 62.5	6.1 – 46.1	9 – 43	7.3 – 63.4	12.3 – 52.1	7.3 – 20.3			
Sex (M/F)	15/15	11/10	32/6	57/45	9/6	3/3			
HC z-scores									
Mean (SD)	N=	N=	N=	-	N=	N=	0.29 (1.5)	0.23 (1.4)	
	-0.41 (1.25)	0.35 (0.9) ^b	0.86 (1.15) ^a						
NVIQ									
Mean (SD)	104 (16)	107 (11)	112 (13) ^b	102 (13)	102 (18)	111 (10)			
SRS - Raw Total score									
Mean (SD)	N=19	N=21	N=0	N=98	N=6	N=5	41 (19) ^c	23 (25)	
	30 (17) ^b	18 (12)		19 (12) ^b					
Phonological skills - Standard Scores									
Mean (SD)	N=3	N=19	N=0	N=54	N=0	N=5	N=0	N=5	
	12 (2)	7 (2)		9 (2)		8 (0.5)			

The three control groups were matched for age, sex, handedness, and Non-Verbal IQ in the SVIP study. Phonology skills were evaluated in North America with the comprehensive test of phonological processing, non-word repetition subtest (6), and in Europe with the developmental neuropsychological assessment, non-word repetition task (7).

^a Significantly different between familial and unrelated groups in the same cohort; ANCOVA, post-hoc comparison, $p < 0.05$ Bonferroni corrected.

^b Significantly different from the same control group in the other cohort; ANCOVA, post-hoc comparison, $p < 0.05$ Bonferroni corrected.

^c Significantly different from the same genetic group in the other cohort; ANCOVA, post-hoc comparison, $p < 0.05$ Bonferroni corrected.

N, sample size; *SD*, standard deviation; *M*, male; *F*, female; *HC*, Head Circumference; *NVIQ*, non-verbal intellectual quotient; *SRS*, social responsiveness scale; *EU* cohort, European cohort; *SVIP* cohort, American cohort.

Table S2. Effect sizes (Z-scores) on global brain metrics when comparing carriers to their familial controls

	eTIV	GM volume	WM volume	Ventricular volume	Cortical surface area	Mean cortical thickness
Deletion vs Controls of deletion families	0.94*	0.89*	0.98*	-0.15	0.61*	-0.04
Duplication vs Controls of duplication families	-0.07	-0.39	-0.42	0.04	-0.27	-0.38

* *p* value < 0.001*eTIV*, estimated total intracranial volume; *GM*, grey matter; *WM*, white matter

Table S3. Voxel-based results in EU and SVIP cohorts separately: Coordinates of regional gene dosage-dependent differences in gray matter volume

	EU cohort					SVIP cohort					
	Side	Cluster Size	X	Y	Z	t-score	Cluster Size	X	Y	Z	t-score
Anterior insula, putamen, frontal operculum	R	2773*	32	12	15	8.72	4686*	30	15	14	9.58
Only SVIP** [†] : Orbital part of inferior frontal gyrus	L	951	-28	10	15	8.66	5482*	-36	-34	10	11.7
R. posterior and medial orbital gyrus, L. temporale pole	R	158	18	10	-24	5.31	4686*	30	15	14	9.58
Only SVIP** [†] : L. subcallosal area	L	134	-40	21	-21	5.75	975	-18	12	-26	6.74
Only EU** [†] : L. posterior orbital gyrus											
Posterior insula, transverse temporal gyrus, parietal and central operculum, L. planum polare and temporale	R	2773*	32	12	15	8.72	4686*	30	15	14	9.58
Only SVIP** [†] : L. superior temporal gyrus, L. supramarginal gyrus, R. planum polare and temporale	L	1787	-33	-33	22	6.95	5482*	-36	-34	10	11.7
Calcarine cortex, L. precuneus, L. lingual gyrus, L. posterior cingulate gyrus	R	551	22	-72	10	6.25	8244 R/L	21	-74	12	10.1
Only SVIP** [†] : cuneus, R. precuneus, R. lingual gyrus, R. posterior cingulate gyrus	L	1068	-20	-54	2	5.8	97	-16	-57	27	5.61
Thalamus											
Only EU** [†] : ventral DC, brainstem	L	383	-12	-26	-3	5.67	90	-8	-32	3	5.63
R. Parahippocampal gyrus, Hippocampus, ventral DC	R	163	14	-27	-2	5.04	101	9	-32	4	5.82
Only SVIP** [†] : L. amygdala, L. Parahippocampal gyrus	R	210	15	-14	-21	5.96	35	15	-13.5	-21	4.97
Middle and inferior occipital	L	98	-14	-16	-18	5.46	90	-14	-14	-18	5.14
Caudate nucleus	L	-	-	-	-	-	182	-38	-84	6	5.44
	R	-	-	-	-	-	115	18	26	0	5.38

Deletion < Duplication	EU cohort						SVIP cohort					
	Side	Cluster Size	X	Y	Z	t-score	Cluster Size	X	Y	Z	t-score	
Cerebellum exterior	L	2111	-34	-68	-58	6.17	236	-40.5	-69	-55.5	4.87	
	R	1659	30	-62	-52	5.76	493	28	-66	-57	5.35	
Precentral and postcentral gyri	L	516	-58	2	40	6.41	2506	-48	8	33	6.96	
	R	400	60	-2	16	5.75	2763	60	10	3	7.28	
Only SVIP**: middle frontal gyrus, opercular part of inferior frontal gyrus, R. frontal and central operculum												
L. angular gyrus, superior and middle temporal gyri	L	486	-44	-63	22	5.9	3810	-46	-44	9	12.7	
	R	356	-54	-38	4	5.61	1203	44	-39	8	7.31	
Inferior temporal gyrus, fusiform gyrus	R	94	48	-57	-22	5.35	269	39	-46	-14	5.66	
	L	-	-	-	-	-	150	-44	-52	-20	5.47	
Superior frontal gyrus, superior frontal gyrus medial segment, Supplementary motor cortex	R	-	-	-	-	-	1563	9	15	52	7.01	
	L	-	-	-	-	-	110	-21	-27	-12	5.92	
Hippocampus, parahippocampal gyrus, ventral DC												
Caudate nucleus	R	-	-	-	-	-	76	4	12	2	5.52	
	L	-	-	-	-	-	-	-	-	-	-	

EU cohort, European cohort; SVIP cohort, American cohort; R, Right; L, Left.

* Same cluster described in several lines in the table

** Only SVIP / Only EU: when the regions are found only in one of the cohort

Table S4. Surface-based results in EU and SVIP cohorts separately: Coordinates of regional gene dosage-dependent differences in cortical surface area

		EU cohort					SVIP cohort					
	Side	Cluster Size (mm ²)	X	Y	Z	t-score	Cluster Size (mm ²)	X	Y	Z	t-score	
Insula, Lateral orbitofrontal cortex,		L	3639	-30	20	4	8.34	6574	-31	13	12	6.81
Pars opercularis, Pars orbitalis,		R	2066	36	-14	-4	5.96	2908	30	23	3	7.77
Pars triangularis, Superior			192	40	-30	11	4.08	823	44	-33	10	4.16
temporal gyrus, Supramarginal			265	36	27	-18	3.76	121	26	46	-10	2.87
gyrus, Transverse temporal			185	22	12	-19	4.08	82	28	21	-22	3.41
cortex, L. Rostral middle frontal							73	61	-7	0	3.23	
gyrus												
Only EU**: R. precentral												
Only SVIP**: Postcentral gyrus, L.												
Precentral gyrus, Temporal pole												
L. Inferior parietal cortex, Superior		L	1646	-22	-93	4	4.97	5986	-26	-96	11	7.40
parietal cortex, Lateral occipital			788	-6	-72	42	4.18	580	-18	-75	28	2.90
cortex, Isthmus of cingulate			898	-10	-67	3	7.06	-	-	-	-	-
cortex, Lingual gyrus,			53	-28	-79	-7	2.84	-	-	-	-	-
Pericalcarine cortex, Precuneus		R	920	25	-69	6	4.99	4062	15	-74	7	5.91
cortex, Cuneus cortex, L.			814	25	-92	19	19	1944	21	-96	17	5.83
Fusiform gyrus, R.			466	6	-58	49	3.84	107	7	-70	44	2.74
Parahippocampal gyrus			295	29	-64	-14	4.06					
Only SVIP**: R. Fusiform gyrus			97	20	-41	-10	3.41					
			320	37	-89	-12	3.63					
			630	14	-91	5	5					
Superior frontal gyrus		L	-	-	-	-	-	426	-6	42	41	3.52
Medial orbitofrontal cortex		L	-	-	-	-	-	138	-6	36	-20	3.22
Posterior cingulate cortex		L	-	-	-	-	-	57	-5	-30	36	2.78

Deletion < Duplication		EU cohort						SVIP cohort					
		Side	Cluster Size (mm2)	X	Y	Z	t-score	Cluster Size (mm2)	X	Y	Z	t-score	
Caudal middle frontal gyrus, Pars opercularis, Postcentral gyrus, Precentral gyrus, Superior parietal cortex, L. Supramarginal gyrus, R. Rostral middle frontal gyrus		L	2515 95	-50 -22	-16 -76	34 32	-5.66 -3.08	3830 209	-34 -26	3 -41	30 52	-5.04 -3.26	
Only EU**: R. supramarginal gyrus, R. Rostral middle frontal gyrus		R	462 418 608	36 54 46	17 -5 -26	30 20 38	-3.77 -5.77 -4.60	3156 96 174	56 28 42	-11 -37 2	31 52 47	-6.61 -3.36 -3.13	
Only SVIP**: L. Rostral middle frontal gyrus, R. Superior frontal gyrus			82 68 60	55 20 18	-40 -47 -58	44 61 63	-3.38 -3.09 -3.01	362 558 4932	32 35 -44	12 -15 -40	51 53 -19	-3.27 -4.64 -5.63	
L. Fusiform gyrus, Inferior-Middle-Superior temporal gyri, L. Inferior and superior parietal cortex, L. Banks of the superior temporal sulcus		L	503 409 151 162 154 109	-45 -56 -41 -55 -38 -36	-58 -26 -10 -45 -59 -74	-7 -13 -35 -12 20 43	-3.74 -4.12 -3.07 -3.06 -3.54 -3.59	229 884 -	-56 -29 -	-26 1 -	-3 -39 -	4.05 -3.74 -	
Only SVIP**: Entorhinal cortex, Parahippocampal gyrus, R. Banks of the superior temporal sulcus, R. Fusiform gyrus, R. inferior parietal cortex		R	86 54 619 468 116	-27 -56 54 61 53	-64 -44 -56 -17 -26	30 -3 -18 -15 -1	-3.00 -3.06 -3.60 -4.08 -3.27	3341 389 1224 201 449	- 59 41 34 38 28	- -46 -26 -62 -62 -6	- -18 -21 46 18 -34	- -5.52 -3.53 -4.60 -3.83 -4.25	
L. Caudal and rostral anterior cingulate cortex, L. Posterior cingulate cortex		L	121 23	-4 -7	15 39	24 12	-3.39 -2.71	697 30	-6 -6	35 -13	13 30	-4.14 -2.76	
Only SVIP**: Superior frontal gyrus		R	-	-	-	-	-	299	11	12	51	-4.12	
Lateral and medial orbitofrontal cortex		L	137	-5	58	-20	-4.01	99	-12	41	-23	-2.91	
Only EU**: Frontal pole													
Isthmus of cingulate cortex, Precuneus cortex		L	-	-	-	-	-	293	-15	-46	32	-3.82	

*EU cohort, European cohort; SVIP cohort, American cohort; R, Right; L, Left.
Clusters above 50 have mm² or bilateral clusters are reported and, for reading purposes, clusters with same names of regions are merged.
** Only SVIP / Only EU: when the regions are included only in one of the cohort*

Table S5. Surface-based results in EU and SVIP cohorts separately: Coordinates of regional gene dosage-dependent differences in cortical thickness

		EU cohort					SVIP cohort				
Side	Cluster Size (mm ²)	X	Y	Z	t-score	Cluster Size (mm ²)	X	Y	Z	t-score	
Cuneus cortex, Pericalcarine cortex, Precuneus cortex	L 570 R 727	-9 12	-70 -69	14 18	5.30 5.27	718 734	-19 18	-73 -67	18 15	6.39 5.84	
Superior temporal gyrus, Insula, Supramarginal gyrus, Transverse temporal cortex, R. Temporal pole,	L 503 98 - -	-39 -42 - -	-37 8 - -	10 -27 - -	6.18 4.72 - -	610 349 184 620	-48 -61 -43 -57	-37 -38 4 2	10 6 -25 -8	8.52 6.18 6.45 4.25	
Only SVIP**: Banks of the superior temporal sulcus, Middle temporal gyrus	R 499 90 243	41 39 42	-36 -25 10	15 1 -27	4.66 4.77 6.76	1371 962 198	62 41 43	-32 -13 6	3 -13 -26	5.86 6.39 7.25	
Postcentral gyrus, L. Paracentral lobule, L. Precuneus cortex, Superior parietal cortex	L 378 243 -	-16 -44 -	-43 -22 -	68 38 -	4.32 5.36 -	583 88 242	-16 -14 -33	-44 -47 -37	73 59 54	4.95 3.99 3.97	
Only SVIP**: Precentral gyrus, R. Paracentral lobule, R. Precuneus cortex	R 86 693	29 60	-45 -9	61 32	3.78 4.52	1434 1099	19 42	-22 -32 -19	38 65 35	6.89 6.00 7.11	
Only EU**: R. Supramarginal gyrus	250	39	-15	33	5.47	-	-	-	-	-	
Lateral occipital cortex, Superior and Inferior parietal cortex	L 302 191 102 - 64 112 77 79	-28 -34 -17 - 34 14 15 49	-78 -55 -67 - -48 -51 -71 -52	14 34 46 - 38 68 53 26	3.91 4.70 3.61 - 3.62 4.31 3.77 3.85	169 152 204 349 104 103 222 -	-20 -27 -22 -18 36 22 23 -	-93 -56 -83 -101 -46 -70 -85 -	15 41 35 -8 52 39 16 -	4.08 4.75 4.67 4.89 3.48 3.22 3.82 -	

		EU cohort						SVIP cohort					
		Side	Cluster Size (mm ²)	X	Y	Z	t-score	Cluster Size (mm ²)	X	Y	Z	t-score	
Fusiform gyrus, Lingual gyrus, Parahippocampal gyrus		L	137	-31	-39	-12	4.48	63	-32	-45	-7	3.45	
		R	475	30	-35	-14	6.38	224	36	-46	-9	5.03	
Pars triangularis		L	30	-44	34	7	3.07	116	-43	33	9	3.36	
Only SVIP**: L. Rostral middle frontal gyrus		R	-	-	-	-	-	107	47	34	6	3.47	
Frontal pole, Superior frontal gyrus		L	-	-	-	-	-	193	-6	61	-14	3.64	
Isthmus of cingulate cortex, Precuneus cortex		R	-	-	-	-	-	229	12	-55	37	5.35	
Caudal and rostral anterior cingulate cortex		R	-	-	-	-	-	136	7	31	17	4.04	
Lateral orbitofrontal cortex		R	-	-	-	-	-	59	30	26	-7	3.69	
Deletion < Duplication		EU cohort						SVIP cohort					
Side	Cluster Size (mm ²)	X	Y	Z	t-score	Cluster Size (mm ²)	X	Y	Z	t-score			
Inferior temporal gyrus, R.		L	538	-52	-60	-9	-5.23	1507	-50	-51	-15	-6.14	
Fusiform gyrus		R	50	38	-19	-28	-3.46	54	35	-10	-37	-3.27	
Only SVIP**: Lateral occipital cortex, L. Fusiform gyrus		L	93	57	-44	-23	-3.20	178	51	-50	-17	-4.13	
Lingual gyrus		L	275	-16	-81	-12	-4.17	613	-12	-82	-12	-5.30	
		R	251	11	-85	-13	-3.74	115	16	-87	-14	-3.28	
Insula		L	207	-37	-5	3	-4.56	113	-34	-29	8	-4.20	
Only SVIP**: L. Transverse temporal cortex		R	203	37	5	5	-4.26	38	38	-6	2	-2.95	

Deletion < Duplication		EU cohort						SVIP cohort					
		Side	Cluster Size (mm ²)	X	Y	Z	t-score	Cluster Size (mm ²)	X	Y	Z	t-score	
Pars opercularis		L	200	-46	14	4	-4.37	52	-51	14	5	-3.47	
Only EU**: R. Postcentral gyrus, R. Precentral gyrus		R	220	50	10	1	-5.21	254	53	14	5	-5.69	
Only SVIP**: R. Pars triangularis													
Lateral and R. Medial orbitofrontal cortex		L	128	-15	23	-17	-3.91	124	-16	12	-15	-5.08	
Only SVIP**: R. Insula			185	-19	42	-16	-4.17	165	-29	20	-19	-5.27	
Only EU**: L. Medial orbitofrontal cortex		R	154	6	37	-21	-4.50	71	5	40	-23	-4.70	
			35	15	38	-25	-3.12	108	17	36	-21	-3.45	
			119	24	40	-11	-3.51	343	30	21	-19	-4.90	
Paracentral lobule, Precentral gyrus, Superior frontal gyrus		L	53	-11	-16	69	-3.51	268	-6	-21	71	-3.33	
			325	6	-16	59	-4.17	227	6	-17	69	-4.39	
			78	-52	1	5	-4.21	63	-29	-15	64	-3.53	
		R						138	-9	7	55	-4.15	
			68	5	-25	72	-3.45	227	6	-17	69	-4.39	
			96	12	29	32	-4.05	178	12	21	38	-4.66	
			56	20	-8	59	-3.33	93	60	3	18	-4.07	
Inferior parietal cortex, Lateral occipital cortex		R	384	37	-81	29	-3.94	-	-	-	-	-	
		L	67	-42	-83	5	-3.71	-	-	-	-	-	
Banks of the superior temporal sulcus, R. Middle temporal gyrus		L	13	-48	-35	-2	-3.22	34	-54	-44	-2	-3.25	
Only EU**: L. Middle temporal gyrus		R	77	-63	-35	-12	-3.64	-	-	-	-	-	
								50	52	-36	-7	-3.11	
Caudal anterior cingulate cortex		L	87	-4	18	22	-3.66	381	-6	14	33	-4.53	
Only SVIP**: Posterior cingulate cortex, Superior frontal gyrus								195	-4	-19	39	-4.10	

Deletion < Duplication		EU cohort						SVIP cohort					
		Side	Cluster Size (mm ²)	X	Y	Z	t-score	Cluster Size (mm ²)	X	Y	Z	t-score	
Isthmus of cingulate cortex,	L	-	-	-	-	-	-	93	-19	-47	-5	-3.43	
Lingual gyrus, Parahippocampal gyrus								84	-8	-44	25	-3.77	
Rostral anterior cingulate cortex	R	-	-	-	-	-	-	156	6	32	-5	-4.38	
Precuneus cortex, Superior parietal cortex	L	-	-	-	-	-	-	316	-6	-72	40	-5.38	
	R	204	5	-67	40	-5.80	438	6	-69	32	-5.18		
Postcentral gyrus, L.	L	-	-	-	-	-	-	83	-59	-48	31	-3.32	
Supramarginal gyrus	R	-	-	-	-	-	-	67	53	-18	19	-3.63	
Caudal middle frontal gyrus	L	-	-	-	-	-	-	51	-28	-1	47	-3.57	
	R	86	30	23	46	-3.58							
Rostral middle frontal gyrus	R	125	32	41	22	-3.57	-	-	-	-	-	-	

EU cohort, European cohort; SVIP cohort, American cohort; R, Right; L, Left.

Clusters above 50 have mm² or clusters in both cohorts are reported and, for reading purposes, clusters with same names of regions are merged.

** Only SVIP / Only EU: when the regions are included only in one of the cohort

Table S6. Voxel-based results in the pooled EU and SVIP cohorts: Coordinates of the differential and overlapping contribution of deletion and duplication to the regional gene dosage-dependent differences in gray matter volume

	Side	Cluster Size	X	Y	Z	t-score
Deletion > Control						
Anterior and Posterior insula, transverse temporal gyrus, frontal – parietal - central operculum, planum temporale and polare, L. superior temporal, R. posterior and medial orbital gyri	L	5025	-33	-34	22	13.92
	R	4159	38	-30	12	11.39
		56	18	10	-26	5.54
Calcarine cortex, lingual gyrus, posterior cingulate, precuneus, R. occipital pole, R. occipital fusiform gyrus	R	4403	22	-70	12	12.42
	L	3131	-26	-66	10	11.72
Caudate	L	152	-16	26	-4	7.50
	R	58	16	27	-3	5.44
Superior parietal lobule, angular gyrus	L	130	-30	-57	33	6.87
Inferior and middle occipital gyrus	R	252	40	-78	6	5.98
Brainstem, cerebellum exterior	R	172	3	-44	-48	5.91
Thalamus proper	L	177	-8	-32	4	5.16
	R	4403*	22	-70	12	12.42
Control > Duplication						
Anterior and posterior Insula, frontal – central - parietal operculum, caudate, putamen, triangular part of inferior frontal gyrus, L. transverse temporal gyrus	R	2604	28	15	12	9.01
	L	3011	-27	12	14	7.66
Medial and posterior orbital gyri, subcallosal area, L. gyrus rectus, L. temporal pole	R	825	20	15	-22	7.78
	L	1480	-18	14	-24	6.75
Hippocampus, ventral DC, L. amygdala	R	183	32	-33	2	6.84
	L	115	16	-15	-15	5.79
	L	97	-15	-15	-15	5.69
Inferior and middle occipital gyri	L	192	-36	-86	6	5.22

	Side	Cluster Size	X	Y	Z	t-score
Control > Duplication						
Calcarine cortex, occipital pole	R	133	18	-94	-2	5.19
Thalamus proper	R	50	9	-30	4	5.02
Deletion > Control \cap Control > Duplication						
Anterior and posterior insula, transverse temporal gyrus, planum polare, frontal-central-parietal operculum	R	1012	30	14	14	8.64
	L	969	-28	12	15	7.35
Calcarine cortex, lingual gyrus and occipital pole	R	132	18	-94	-2	5.19
Caudate	L	73	-20	22	0	5.25
Medial and posterior orbital gyri	R	45	18	10	-26	5.54
Thalamus proper	R	42	9	-30	4	5.02
Deletion < Control						
Superior and middle temporal gyri, angular gyrus, L. middle occipital, L. supramarginal	L	6538	-50	-44	8	12.29
	R	3290	45	-34	0	9.66
Cerebellum exterior	L	4716	-30	-64	-57	8.05
	R	6443	30	-64	-56	8.03
		152	20	-34	-45	6.02
Precentral gyrus, postcentral gyrus central and R. frontal operculum, middle frontal gyrus, opercular part of inferior frontal gyrus, L. supramarginal	L	6455	-63	-4	14	7.93
	R	3131	62	3	12	6.91
Fusiform gyrus, inferior temporal gyrus, occipital gyrus, cerebellum exterior	L	1612	-44	-54	-16	7.63
R/L Middle cingulate gyrus, R/L Supplementary motor cortex, superior frontal gyrus and R. medial segment of superior frontal gyrus	R/L	6593	9	26	56	7.23
Temporale pole	R	526	39	20	-42	6.12
		123	21	16	-39	5.18
	L	346	-38	21	-39	5.78
Gyrus rectus, medial orbital gyrus, frontal pole	R	571	4	60	-26	5.88

	Side	Cluster Size	X	Y	Z	t-score
Deletion < Control						
Frontal pole	R	463	10	68	3	5.59
Caudate, Accubems area	R	121	8	10	-2	5.79
Medial segment of precentral gyrus	R	191	3	-28	69	5.18
Control < Duplication						
Precentral gyrus, L. postcentral gyrus, R. opercular part of inferior frontal gyrus	L	92	-50	-3	24	5.64
Superior temporal gyrus	R	89	62	9	4	5.45
Superior temporal gyrus	L	65	-44	-44	9	5.60
Deletion < Control \cap Control < Duplication						
Superior temporal gyrus	L	65	-44	-44	9	5.60
Precentral gyrus, R. opercular part of inferior frontal gyrus	R	86	62	9	4	5.45
	L	32	-52	-2	24	5.26

* Same cluster described in several lines in the table

Table S7. Top functional associations with the gene dosage dependent regional volumetric alterations.

	TTG	Calcarine	STG/MTG	Anterior insula	Caudate
Auditory	0.64	0.02	0.41	0.01	-0.04
Visual	-0.04	0.4	0.09	-0.02	-0.09
Multisensory	0.29	0.02	0.12	0	-0.02
Music	0.44	0.01	0.22	0.01	-0.02
Emotional	-0.04	-0.07	-0.03	-0.07	0
Fear	-0.04	-0.05	-0.06	-0.02	0
Affective	-0.02	-0.03	-0.03	0.01	0.02
Anxiety	-0.02	-0.03	-0.04	-0.01	0
Inhibition	-0.02	0	0	0.03	0.01
Execution	-0.04	0.01	-0.02	0.25	0.01
Pain	0.16	0.01	-0.04	0.31	0.16
Sensorimotor	0.18	0.01	-0.05	0.16	-0.01
Language	0.28	0.07	0.61	0.01	-0.01
Phonological	0.26	0.09	0.46	0.1	0
Semantic	0.09	0.02	0.46	-0.05	-0.04
Speech	0.58	0.03	0.44	0.02	-0.04
Reward	0.04	-0.01	-0.08	0.15	0.24

The numbers represent the meta-analytic coactivation (r) scores of the cognitive domains most associated with the main neuroanatomical clusters identified in the gene dosage analyses. *TTG*, *transverse temporal gyrus*; *STG*, *superior temporal gyrus*; *MTG*, *middle temporal gyrus*.

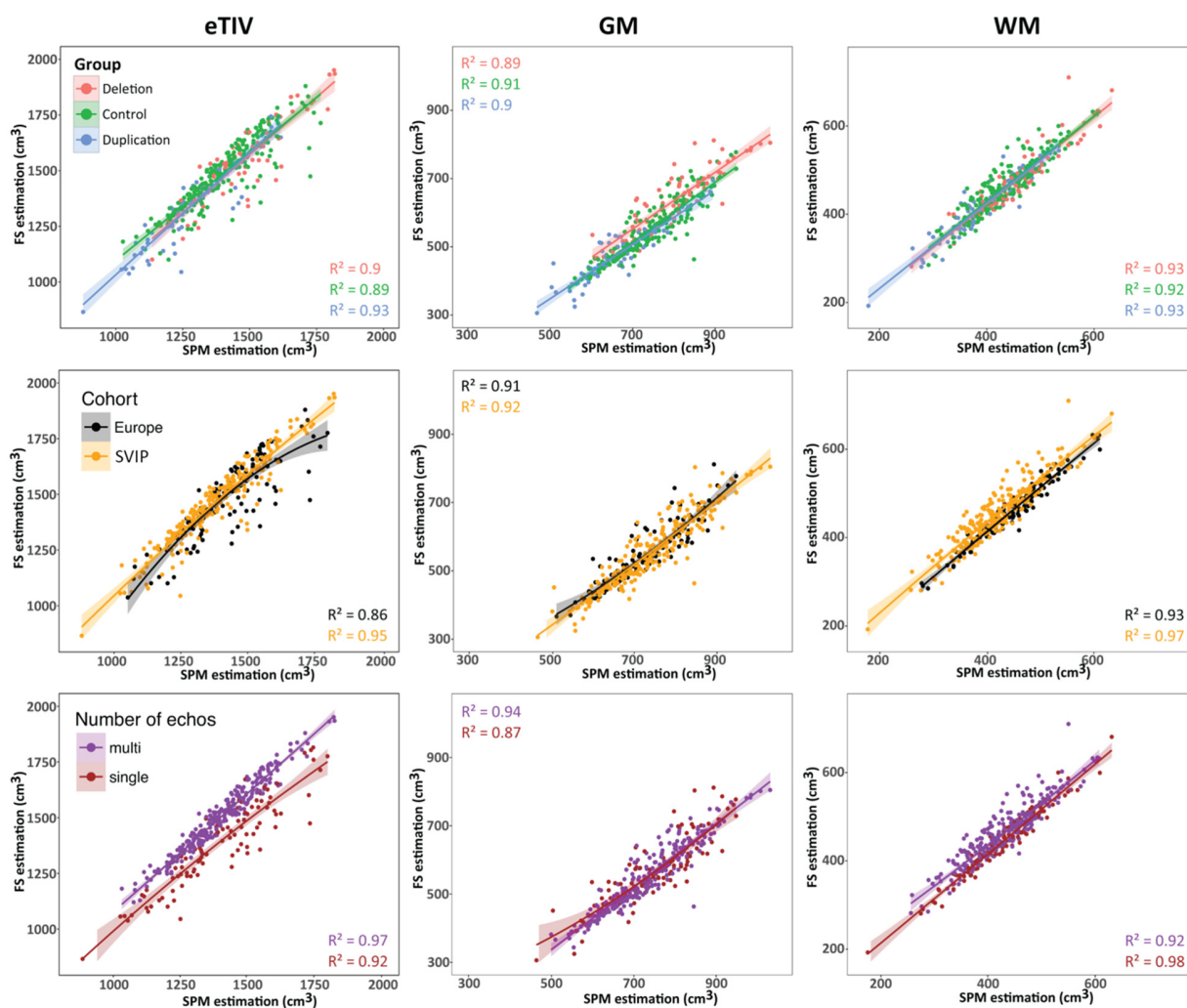


Figure S1. Correlation between the estimation of total intracranial volume, gray matter and white matter volumes computed with FreeSurfer and implemented in SPM

Correlation between the estimation of the brain volumes in cubic centimeter, computed with FreeSurfer and implemented in SPM, for each genetic group (1st row), for each cohort (2nd row), and for both multi and single echos as MRI parameters (3rd row). *eTIV*, estimated total intracranial volume; *GM*, gray matter; *WM*, white matter; *SVIP*, Simons VIP; *FS*, FreeSurfer.

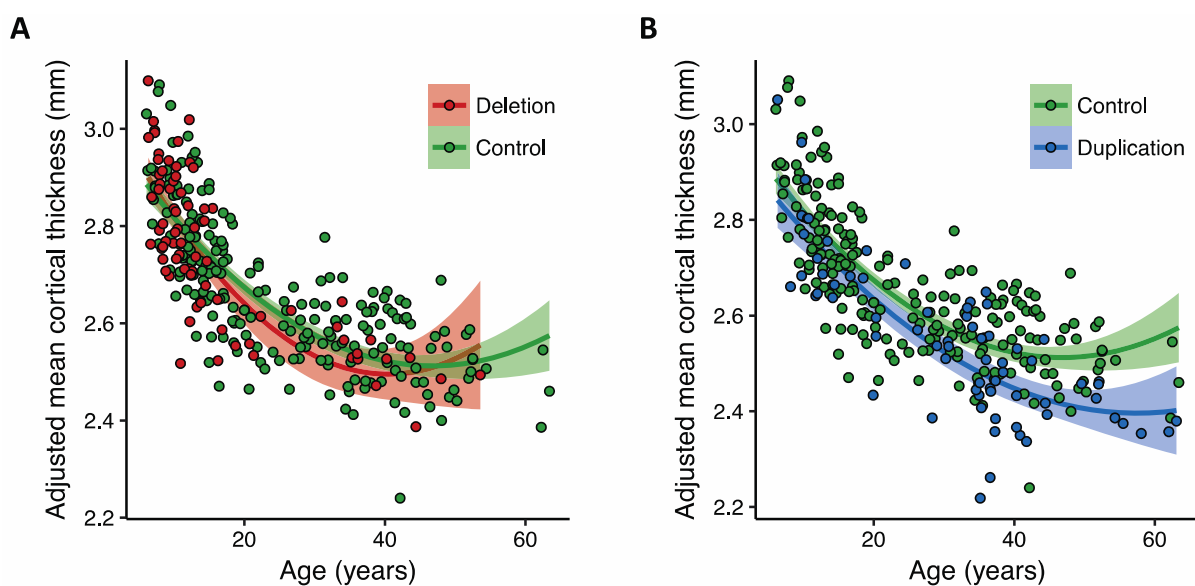


Figure S2. Developmental trajectory of mean cortical thickness per genetic group

Relationship between age and mean cortical thickness in the control (**A** and **B**), deletion (**A**), and duplication (**B**) groups. The mean cortical thickness measurements were corrected for sex, NVIQ, and cohort. The fit lines (red = deletion group, green = control group, and blue = duplication group) and 95% confidence intervals are included for the regressions between mean cortical thickness and age (i.e., both age and age² terms). The group differences in developmental trajectory were modeled with mean cortical thickness as the dependent variable and group, age, age², group X age, and group X age² as the independent variables. The relationship between age and mean cortical thickness did not differ between the three groups. We ran the multiple regression analyses after re-centering the age variable to the mean age (24.7 years) and one standard deviation above (39.1 years) and below the mean age (10.3 years). The duplication carriers' cerebral cortex was thinner than the age-matched control participants at 39.1 years ($t = -3.47$, $p = 0.0006$) but not 24.7 years ($t = -1.43$, $p = 0.15$) or 10.3 years ($t = -0.89$, $p = 0.37$). The deletion carriers' mean cortical thickness did not differ from the control participants' mean cortical thickness at any point in development.

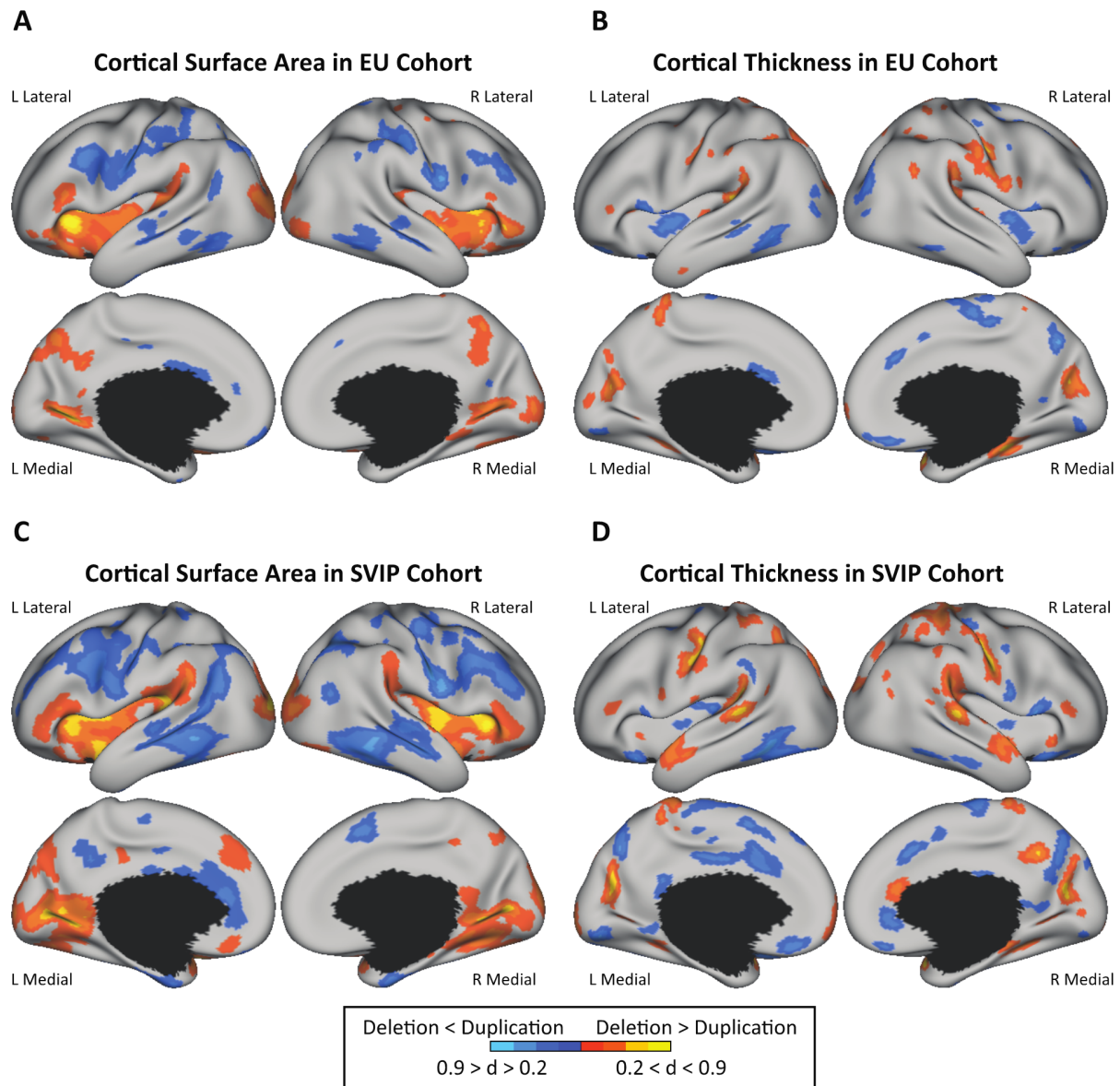


Figure S3. Effects of gene dosage on regional cortical thickness and cortical surface area in EU and SVIP cohorts

For every vertex in the cerebral cortex, the relationship between either cortical thickness or cortical surface area and the number of 16p11.2 genomic copies was estimated for the EU (**A** and **B**) and SVIP (**C** and **D**) cohorts, after controlling for age, age², sex, MRI site, NVIQ, and either mean cortical thickness or total cortical surface area. The cool colors depict a positive relationship (i.e., Deletion < Duplication), and the warm colors depict a negative relationship (i.e., Deletion > Duplication) between cortical metrics and the number of 16p11.2 genomic copies. The results are corrected for multiple comparisons at a false discovery rate of $q < 0.05$. Color bars represent Cohen *d*. *EU*, European; *SVIP*, Simons VIP; *L*, left; *R*, Right.

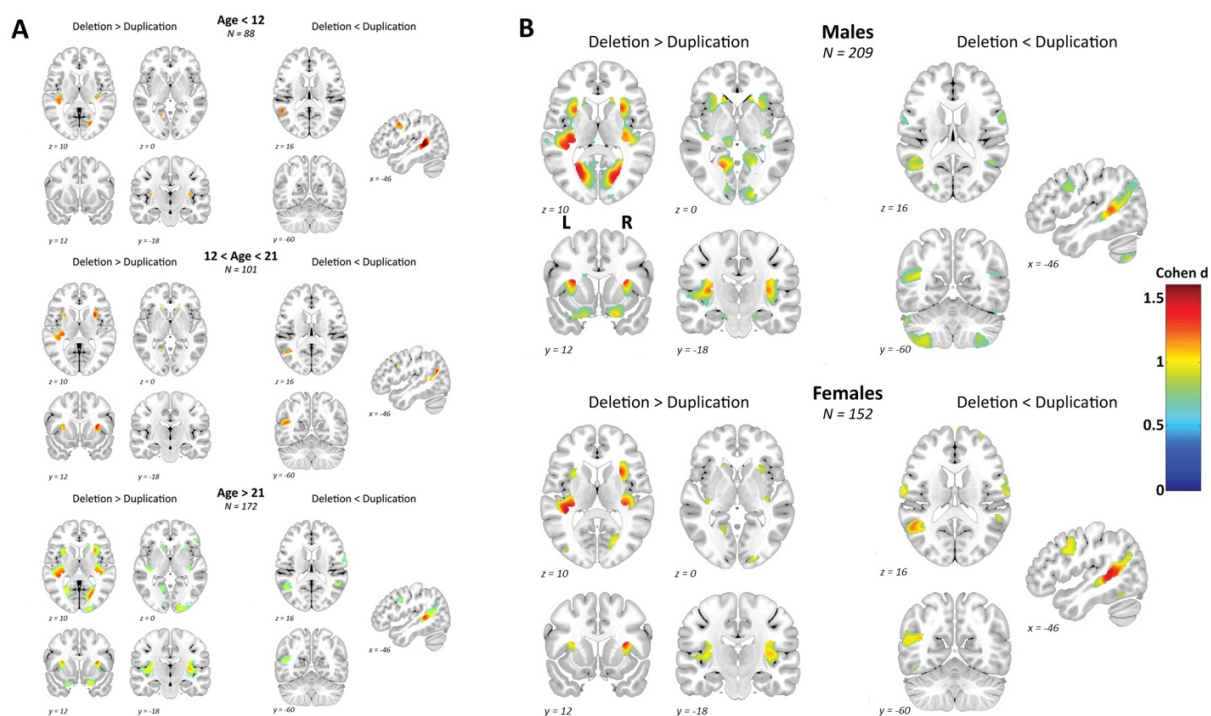


Figure S4. Effects of gene dosage on regional gray matter volume according to age category and sex

Effects of gene dosage on regional gray matter volume separately in children, adolescents and adults (A), and in males and females (B). Results of voxel-based whole-brain maps with volume of regions showing negative (Deletion>Duplication) and positive (Deletion<Duplication) relationship with the number of 16p11.2 genomic copies, after controlling for age, age², sex, cohort, total intracranial volume and non-verbal IQ. Results significant at a threshold of $p < 0.05$ family-wise error corrected for multiple comparisons are displayed in standard Montreal Neurological Institute (MNI) space. Color bars represent Cohen d. *L, left; R, Right.*

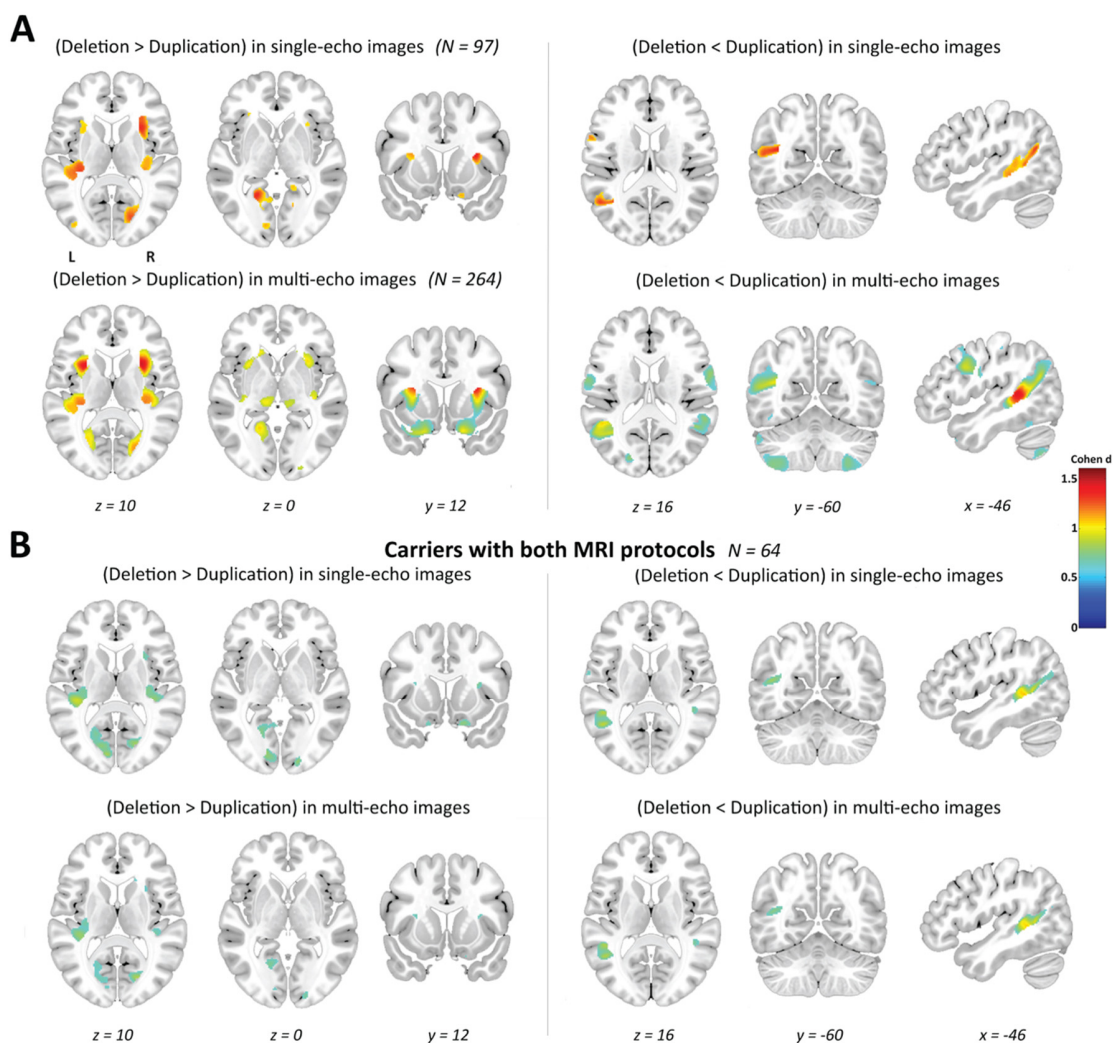


Figure S5. Effects of gene dosage on regional gray matter volume according to MRI parameters

A. Left panels (Deletion > Duplication) show voxel-based whole-brain maps with volume of regions showing a negative relationship with the number of 16p11.2 genomic copies, for single-echo and multi-echo images, after controlling for age, age², sex, cohort, TIV and NVIQ. Right panels (Deletion < Duplication) present positive relationship with the number of 16p11.2 genomic copies. **B.** Same analyses on a subset of carriers (31 deletion, 33 duplication carriers) that underwent both single- and multi-echo protocols. Results significant at a threshold of $p < 0.05$ family-wise error corrected for multiple comparisons are displayed in standard Montreal Neurological Institute (MNI) space. Color bars represent Cohen d . *L, left; R, Right.*

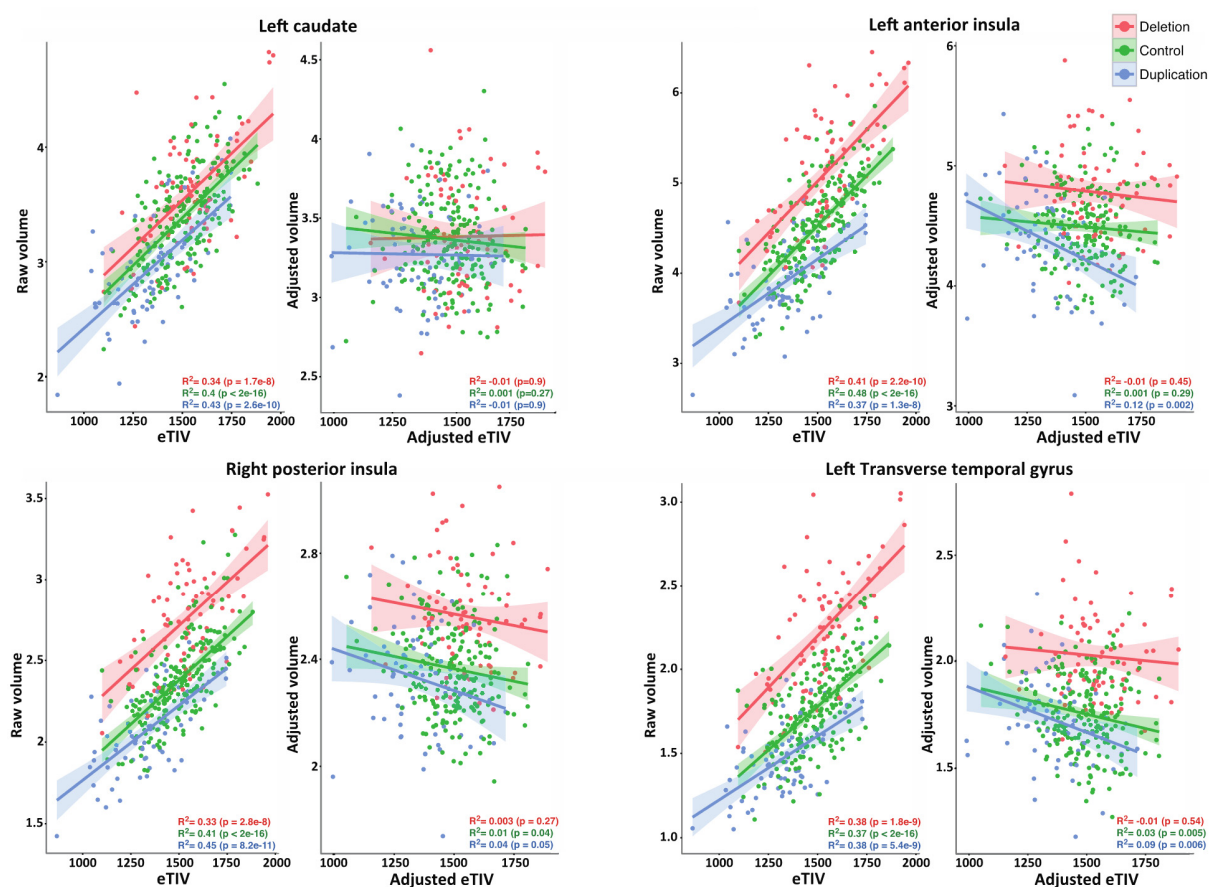


Figure S6. Relationship between global and regional differences associated with 16p11.2 deletion and duplication

Correlation of the raw and adjusted volumes (in cm³) in a group of regions obtained from the local brain gene dosage Deletion>Duplication, with respectively the unadjusted and adjusted eTIV. Adjusted volumes are estimated in a linear model including age, age², sex and cohort as fixed covariates. Calcarine cortex, hippocampus and superior/middle temporal gyri present the same pattern. The bold line represents the linear regressions between the region of interest and the eTIV. *eTIV*, estimated total intracranial volume.

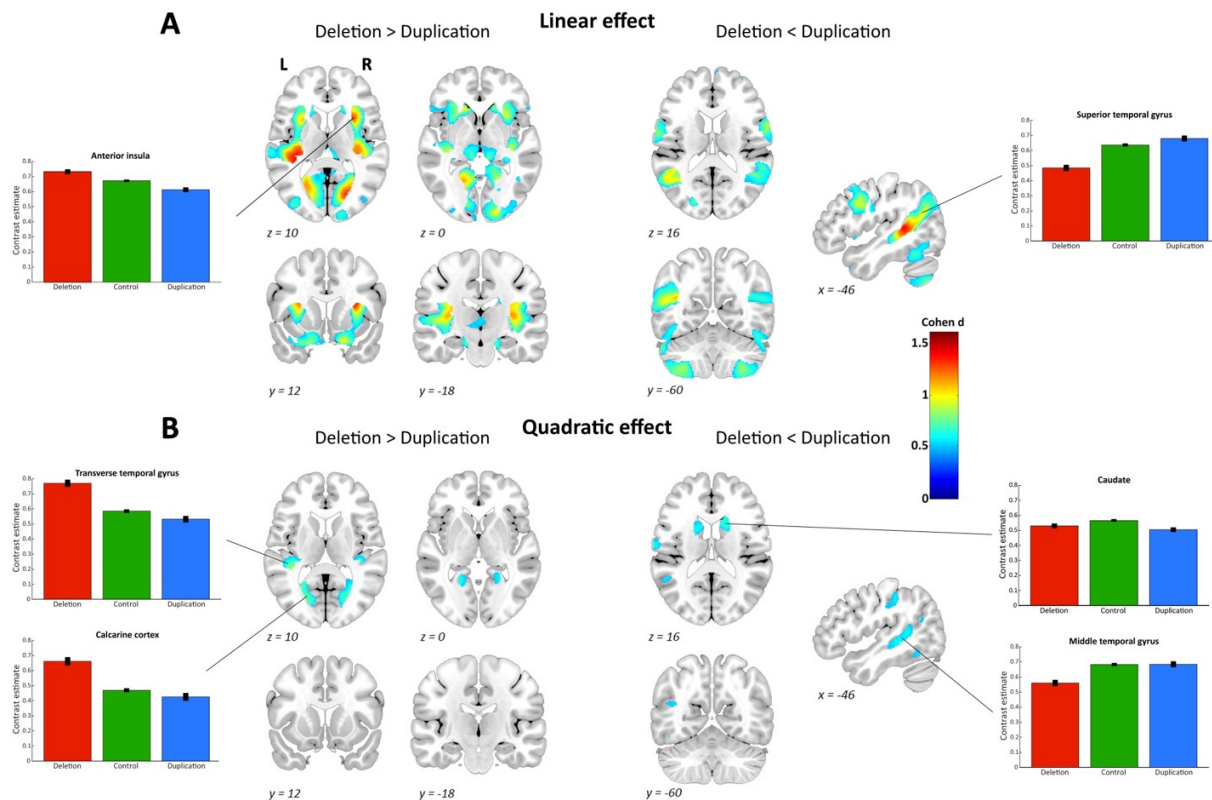


Figure S7. Linear and quadratic effect of gene dosage on regional gray matter volume

Linear (A) and quadratic (B) effects of gene dosage on regional gray matter volume. Results of voxel-based whole-brain maps with volume of regions showing negative (Deletion>Duplication) and positive (Deletion<Duplication) relationship with the number of 16p11.2 genomic copies, after controlling for age, age2, sex, cohort, total intracranial volume and non-verbal IQ. Results significant at a threshold of $p < 0.05$ family-wise error corrected for multiple comparisons are displayed in standard Montreal Neurological Institute (MNI) space. Each bar plot represents the contrast estimate of a peak voxel in a brain regions showing significant linear effects (eg. insula) or in regions showing alterations predominantly associated with the deletion (superior, transverse and middle temporal gyri, calcarine cortex) or the duplication (caudate). Color bars represent Cohen d. L, left; R, Right.

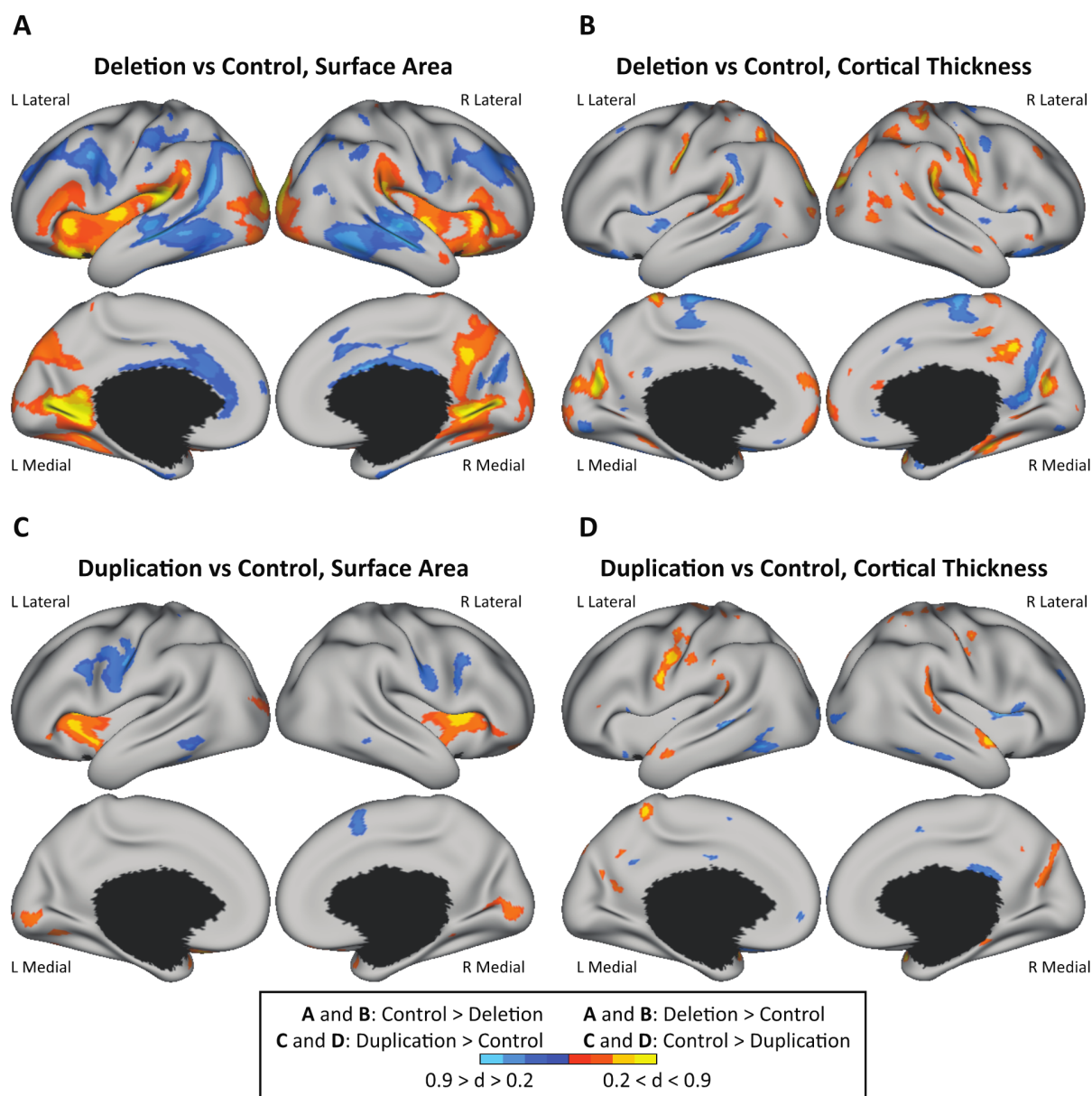


Figure S8. Differential and overlapping contribution of deletion and duplication to the regional gene dosage-dependent differences on cortical thickness and cortical surface area

For every vertex in the cerebral cortex, the relationship between the number of 16p11.2 genomic copies and either surface area or cortical thickness was estimated for deletion carriers compared to controls (respectively **A** and **B**) and for duplication carriers compared to controls (respectively **C** and **D**) after controlling for age, age², sex, cohort and either mean cortical thickness or total cortical surface area. The cool colors depict a positive relationship (i.e., Control>Deletion or Duplication>Control), and the warm colors depict a negative relationship (i.e., Control<Deletion or Duplication<Control) between either cortical thickness or surface area and the number of 16p11.2 genomic copies. The results are corrected for multiple comparisons at a false discovery rate of $q < 0.05$. Color bars represent Cohen *d*. *L*, left; *R*, Right.

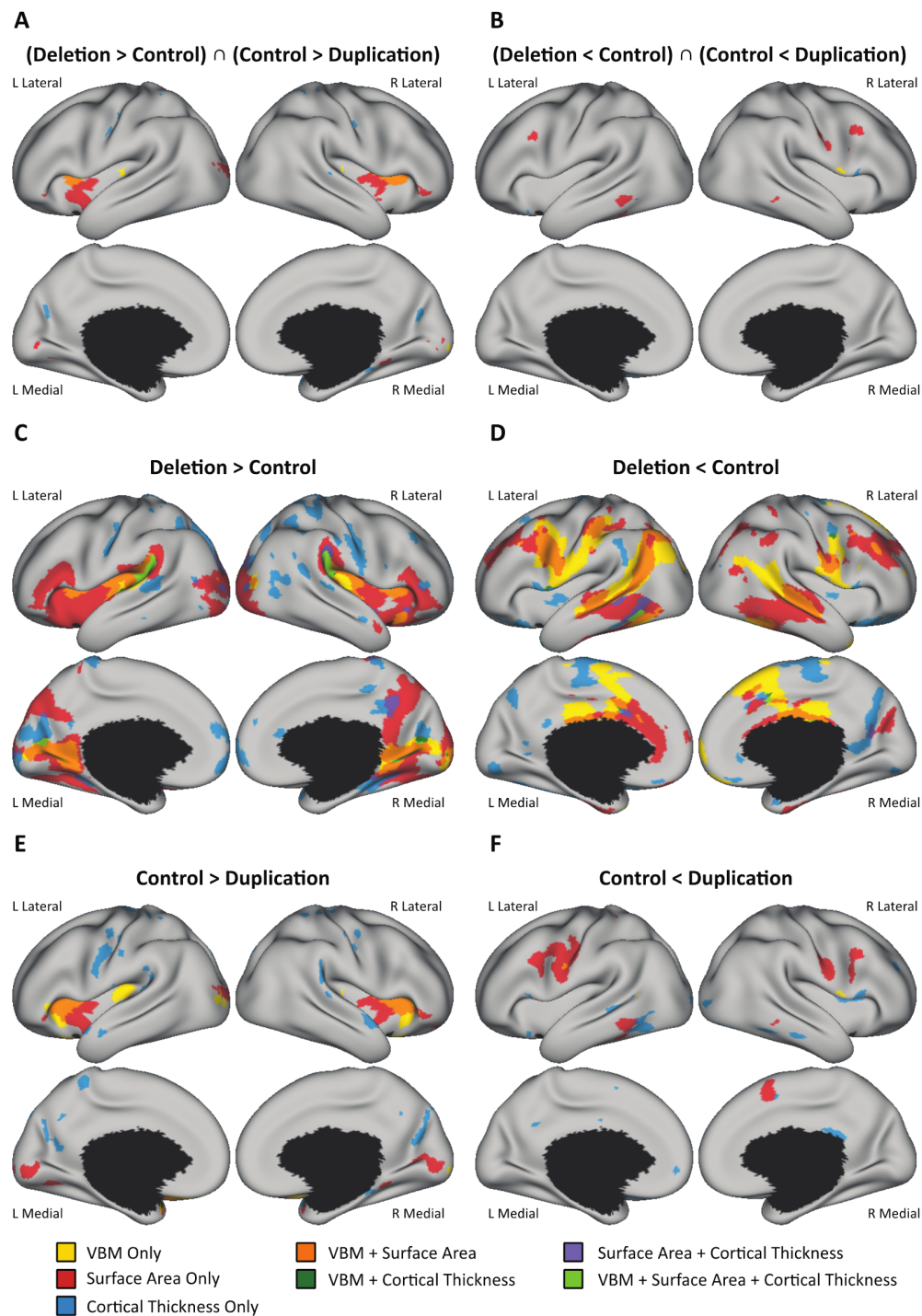


Figure S9. Overlap between voxel-based and surface-based results for cortical alterations specific to deletion and duplication

Significant voxel-based results (Family wise error correction, $p < 0.05$) are projected on the significant surface-based maps (False discovery rate, $q < 0.05$) for deletion carriers compared to controls (**C,D**), for duplication carriers compared to controls (**E,F**) and for the conjunction analysis between the 3 genetic groups (**A,B**). *L*, left; *R*, Right.

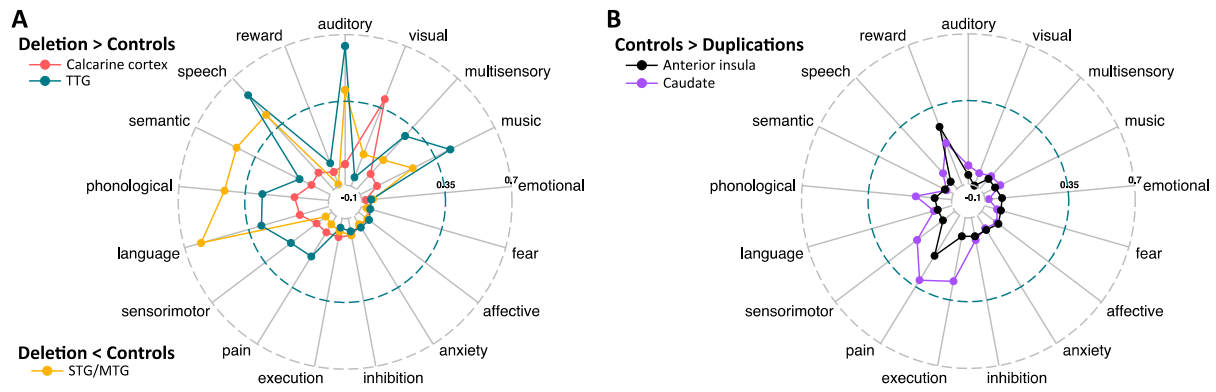


Figure S10. Functional associations of the deletion and duplication regional gene dosage-dependent differences in volume

Radar plot displaying functional associations between meta-analytic coactivation and (A) deletion- and (B) duplication-related structural brain alterations. Correlation values are shown between peaks within each anatomical cluster and the top 17 psychological terms used in publications using Neurosynth platform. *TTG*, *transverse temporal gyrus*; *STG*, *superior temporal gyrus*; *MTG*, *middle temporal gyrus*.

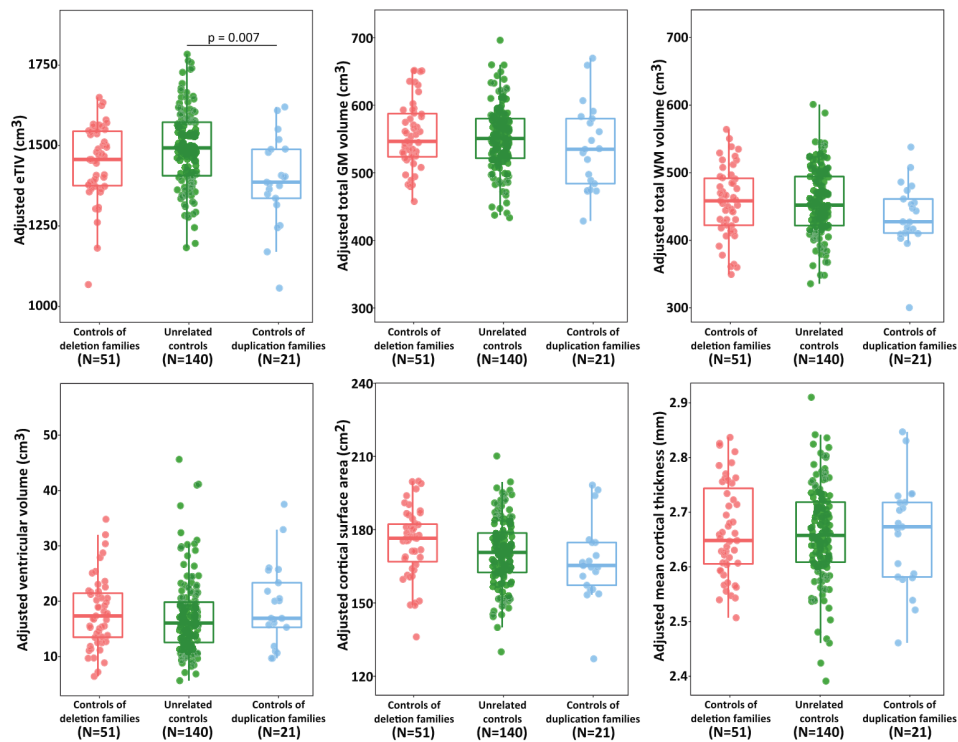


Figure S11. Global brain measures in familial controls and unrelated controls

Boxplots of eTIV, GM, WM and ventricular volumes, cortical surface area and mean cortical thickness in each control group. Regression is estimated with a linear model using an ordinal variable including controls of deletion families = 1, unrelated controls = 2, and control of duplication families = 3. Linear and quadratic expansions of age, sex, non-verbal IQ and MRI site are fixed covariates. In each box, the bold line corresponds to the median. The bottom and top of the box show the 25th (quartile 1 [Q1]) and the 75th (quartile 3 [Q3]) percentile, respectively. The upper whisker ends at highest observed data value within the span from Q3 to Q3+1.5 times the interquartile range (Q3–Q1), and lower whisker ends at lowest observed data value within the span for Q1 to Q1 - (1.5 * interquartile range). Circles that exceed whiskers are outliers. eTIV, estimated total intracranial volume; GM, gray matter; WM, white matter; EU, European; SVIP, Simons VIP.

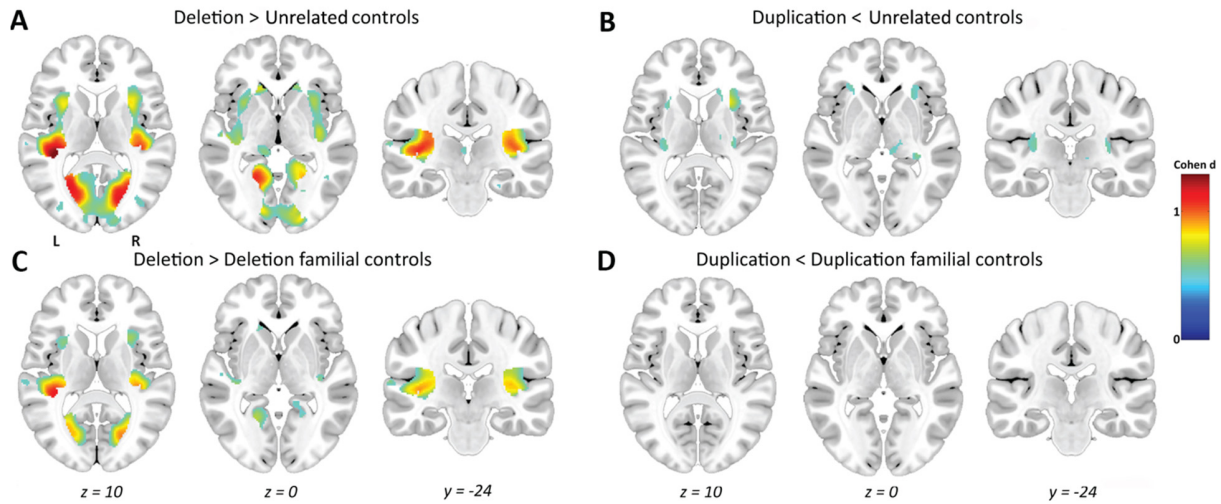


Figure S12. Grey matter volume differences between CNV carriers and the two different control groups (familial controls and unrelated controls)

A,C. Results of voxel-based whole-brain maps showing regions which volume is higher in deletion carriers compared to controls without any deletion-carrying family members (Deletion > Unrelated controls), in deletion carriers compared to controls with a deletion-carrying family member (Deletion > Deletion familial controls). **B,D.** Results of voxel-based whole-brain maps showing regions which volume is lower in duplication carriers compared to controls without any duplication-carrying family members (Duplication < Unrelated controls), in duplication carriers compared to controls with a duplication-carrying family member (Duplication < Duplication familial controls). Results significant at a voxel level at threshold of $p < 0.05$ family-wise error corrected for multiple comparisons are displayed in standard MNI space. Color bars represent Cohen *d*. *L*, left; *R*, Right.

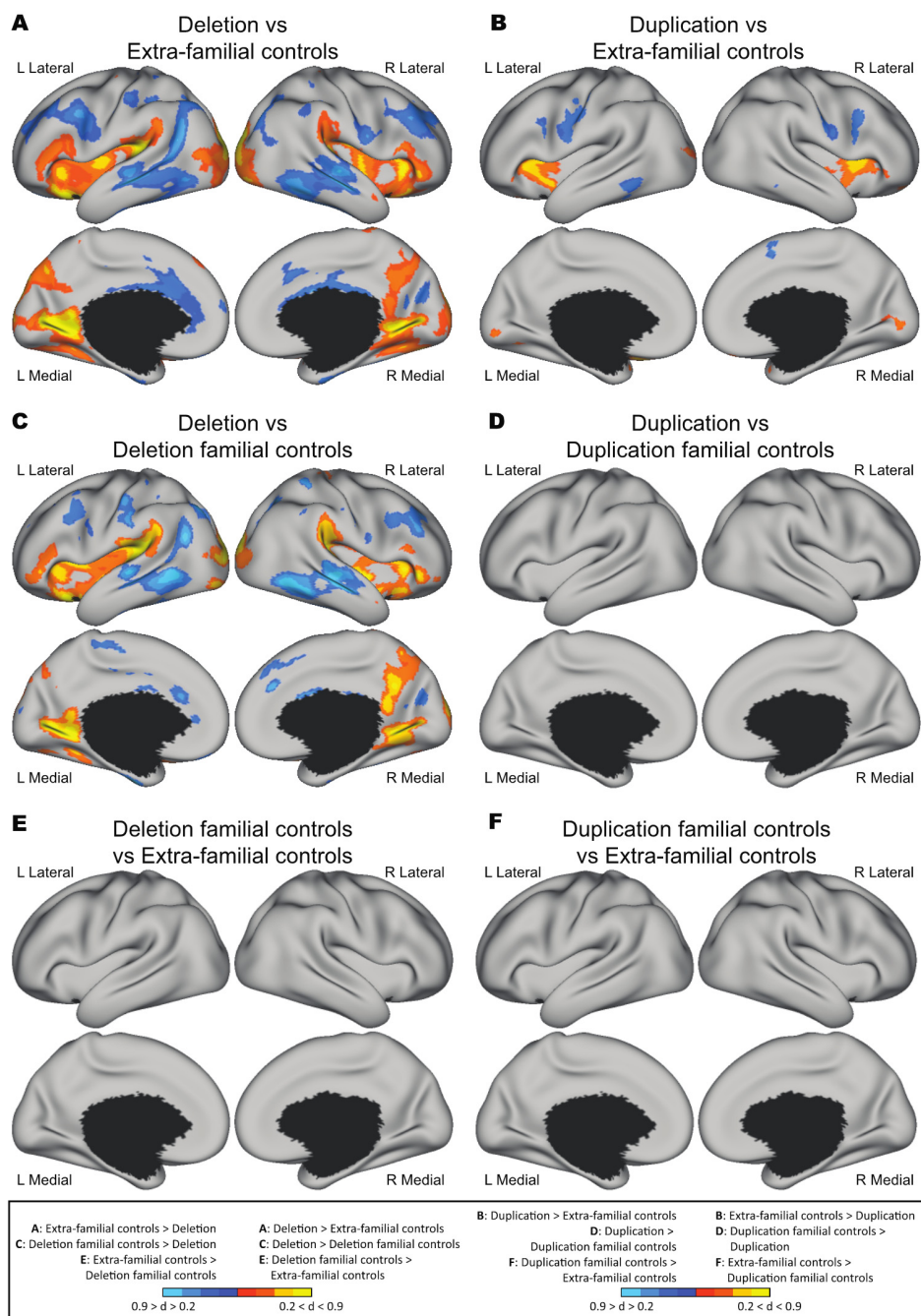


Figure S13. Contribution of CNV carriers and familial controls to the regional gene dosage-dependent differences in cortical surface area

A, C, and E. Cortical surface area comparisons between the deletion carriers, controls with a deletion-carrying family member (i.e., deletion familial controls), and controls without any deletion-carrying family members (i.e., Unrelated controls). **B, D, and F.** Cortical surface area comparisons between the duplication carriers, controls with a duplication-carrying family member (i.e., duplication familial controls), and controls without any duplication-carrying family members (i.e., Unrelated controls). Warm and cold colors represent negative and positive gene dosage throughout the figure. All comparisons controlled for age, age², sex, cohort and total cortical surface area. All results are corrected for multiple comparisons at a false discovery rate of $q < 0.05$. Color bars represent Cohen d . *L, left; R, Right.*

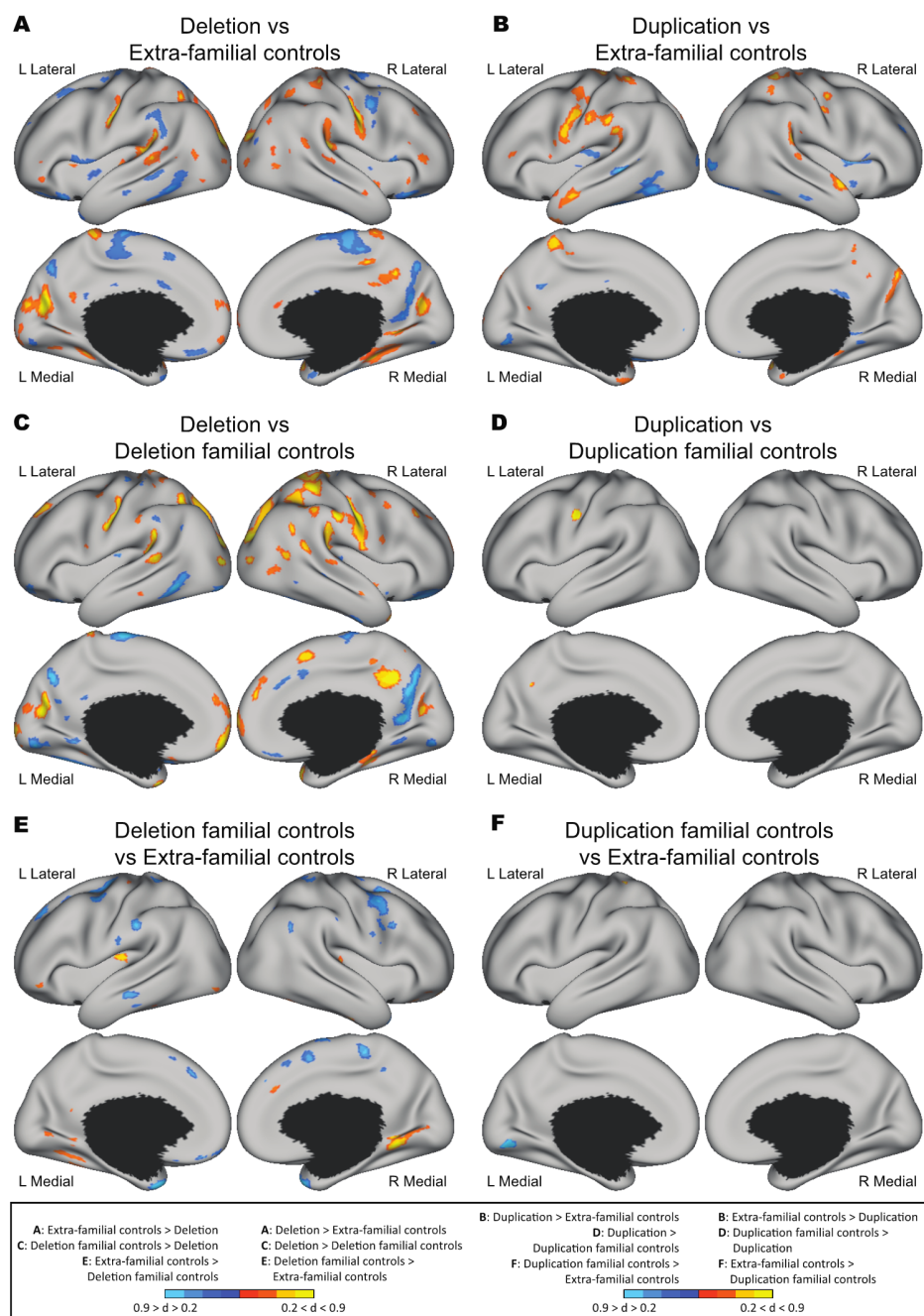


Figure S14. Contribution of CNV carriers and familial controls to the regional gene dosage-dependent differences in cortical thickness

A, C, and E. Cortical thickness comparisons between the deletion carriers, controls with a deletion-carrying family member (i.e., deletion familial controls), and controls without any deletion-carrying family members (i.e., Unrelated controls). **B, D, and F.** Cortical thickness comparisons between the duplication carriers, controls with a duplication-carrying family member (i.e., duplication familial controls), and controls without any duplication-carrying family members (i.e., Unrelated controls). Warm and cold colors represent negative and positive gene dosage throughout the figure. All comparisons controlled for age, age², sex, cohort and mean cortical thickness. All results are corrected for multiple comparisons at a false discovery rate of $q < 0.05$. Color bars represent Cohen *d*. *L, left; R, Right.*

Supplemental References

1. Wechsler D (2004): WPPSI-III Echelle d'intelligence pour la période pré-scolaire et primaire: Troisième édition. *Paris: ECPA, Les Editions du Centre de Psychologie Appliquée.*
2. Wechsler D (2005): WISC-IV Échelle d'intelligence de Wechsler pour enfants: WISC-IV. *Paris: ECPA, Les Editions du Centre de Psychologie Appliquée.*
3. Wechsler D (2008): WAIS III Echelle d'intelligence pour adultes. *Paris: ECPA, Les Editions du Centre de Psychologie Appliquée.*
4. Wechsler D (1999): Wechsler abbreviated scale of intelligence. *San Antonio, TX: The Psychological Corporation.*
5. Elliott CD (2006): Differential Abilities Scale—2nd Edition (DAS-II). *San Antonio, TX: The Psychological Corporation.*
6. Wagner RK, Torgesen JK, Rashotte CA (1999): Comprehensive test of phonological processes (CTOPP). *Austin, TX: Pro-Ed.*
7. Korkman M, Kemp SL, Kirk U (2008): Nepsy, Bilan Neuro- psychologique de l'enfant: Manuel. *Paris: ECPA, les Éditions du Centre de Psychologie Appliquée.*
8. Constantino JN (2002): The Social Responsiveness Scale. *Los Angeles: Western Psychological Services.*
9. Association Psychiatric Association (2013): Diagnostic and statistical manual of mental disorders (DSM-5®). *Washington, DC: American Psychiatric Association.*
10. Preisig M, Fenton BT, Matthey M-L, Berney A, Ferrero F (1999): Diagnostic interview for genetic studies (DIGS): inter-rater and test-retest reliability of the French version. *European archives of psychiatry and clinical neuroscience.* 249: 174–179.
11. Lord C, Rutter M, Le Couteur A (1994): Autism Diagnostic Interview-Revised: a revised version of a diagnostic interview for caregivers of individuals with possible pervasive developmental disorders. *J Autism Dev Disord.* 24: 659–685.
12. Lord C, Risi S, Lambrecht L, Cook EH, Leventhal BL, DiLavore PC, *et al.* (2000): The Autism Diagnostic Observation Schedule—Generic: A standard measure of social and communication deficits associated with the spectrum of autism. *J Autism Dev Disord.* 30: 205–223.
13. Sparrow SS, Cicchetti DV, Balla DA (2005): Vineland adaptive behavior scales (2nd ed.). *Circle Pines: Pearson Assessments.*
14. Rutter, M., Bailey, A., & Lord, C. (2003): Social Communication Questionnaire (SCQ). *Torrance, CA: Western Psychological Services.*
15. Fischl B, Salat DH, Busa E, Albert M, Dieterich M, Haselgrove C, *et al.* (2002): Whole Brain Segmentation: Neurotechnique Automated Labeling of Neuroanatomical Structures in the Human Brain. *Neuron.* 33: 341-355.
16. Fischl B, Dale AM (2000): Measuring the thickness of the human cerebral cortex from magnetic resonance images. *PNAS.* 97: 11050-11055.

17. Ashburner J, Friston KJ (2005): Unified segmentation. *NeuroImage*. 26: 839–851.
18. Lorio S, Fresard S, Adaszewski S, Kherif F, Chowdhury R, Frackowiak RS, *et al.* (2016): New tissue priors for improved automated classification of subcortical brain structures on MRI. *NeuroImage*. 130: 157–166.
19. Ashburner J (2007): A fast diffeomorphic image registration algorithm. *NeuroImage*. 38: 95–113.
20. Jones D, Symms M, Cercignani M, Howard R (2005): The effect of filter size on VBM analyses of DT-MRI data. *NeuroImage*. 26: 546–554.
21. Salmond CH, Ashburner J, Vargha-Khadem F, Connelly A, Gadian DG, Friston KJ (2002): Distributional Assumptions in Voxel-Based Morphometry. *NeuroImage*. 17: 1027–1030.
22. Prader A, Largo RH, Molinari L, Issler C (1989): Physical growth of Swiss children from birth to 20 years of age. First Zurich longitudinal study of growth and development. *Helv Paediatr Acta Suppl*. 52: 1–125.
23. Largo R, Jenni OG (2005): Jahre Forschung in den Zürcher Longitudinalstudien: Was haben wir daraus gelernt. *Bayern AF Tagungsband „Forschung für die Praxis I–Wie funktioniert (kindliche) Entwicklung“ München: Arbeitsstelle Frühförderung Bayern*. 50: 47–56.
24. Desikan RS, Ségonne F, Fischl B, Quinn BT, Dickerson BC, Blacker D, *et al.* (2006): An automated labeling system for subdividing the human cerebral cortex on MRI scans into gyral based regions of interest. *NeuroImage*. 31: 968–980.
25. Marcus DS (2011): Informatics and data mining tools and strategies for the Human Connectome Project. *Frontiers in Neuroinformatics*. 5: 1–12.
26. Peelle JE, Cusack R, Henson RNA (2012): Adjusting for global effects in voxel-based morphometry: Gray matter decline in normal aging. *NeuroImage*. 60: 1503–1516.
27. Poldrack RA, Kalar D, Barman B, Mumford JA, Yarkoni T (2011): Topic mapping: a literature-wide analysis of mind-brain relationships. Program No. 841.24. 2011, Neuroscience Meeting Planner; 2011 Nov 12--16; Washington (DC): Society for Neuroscience.
28. Yarkoni T, Poldrack RA, Nichols TE, Van Essen DC, Wager TD (2011): Large-scale automated synthesis of human functional neuroimaging data. *Nat Methods*. 8: 665–670.